

5-1-2008

## First and Second Law Analysis of Organic Rankine Cycle

Chandramohan Somayaji

Follow this and additional works at: <https://scholarsjunction.msstate.edu/td>

---

### Recommended Citation

Somayaji, Chandramohan, "First and Second Law Analysis of Organic Rankine Cycle" (2008). *Theses and Dissertations*. 2297.

<https://scholarsjunction.msstate.edu/td/2297>

This Dissertation - Open Access is brought to you for free and open access by the Theses and Dissertations at Scholars Junction. It has been accepted for inclusion in Theses and Dissertations by an authorized administrator of Scholars Junction. For more information, please contact [scholcomm@msstate.libanswers.com](mailto:scholcomm@msstate.libanswers.com).

FIRST AND SECOND LAW ANALYSIS OF ORGANIC RANKINE CYCLE

By

CHANDRAMOHAN SOMAYAJI

A Dissertation  
Submitted to the Faculty of  
Mississippi State University  
in Partial Fulfillment of the Requirements  
for the Degree of Doctor of Philosophy  
in Mechanical Engineering  
in the Department of Mechanical Engineering

Mississippi State, Mississippi

May 2008

Copyright by  
Chandramohan Somayaji  
2008

FIRST AND SECOND LAW ANALYSIS OF ORGANIC RANKINE CYCLE

By

Chandramohan Somayaji

Approved:

---

Pedro J. Mago  
Assistant Professor  
Mechanical Engineering  
(Major Professor)

---

Louay M. Chamra  
Professor and Acting Head  
Mechanical Engineering  
(Committee Member)

---

W. Glenn Steele  
Professor and Interim Dean  
Bagley College of Engineering  
(Committee Member)

---

B. K. Hodge  
Professor  
Mechanical Engineering  
(Committee Member)

---

S. R. Daniewicz  
Professor  
Mechanical Engineering  
(Graduate Program Coordinator)

---

Roger King  
Associate Dean  
for Research and Graduate Studies  
of the Bagley College of Engineering

Name: Chandramohan Somayaji

Date of degree: May 2, 2008

Institution: Mississippi State University

Major Field: Mechanical Engineering

Major Professor: Dr. Pedro J. Mago

Title of Study: FIRST AND SECOND LAW ANALYSIS OF ORGANIC RANKINE  
CYCLE

Pages in Study: 112

Candidate for Degree of Doctor of Philosophy

Many industrial processes have low-temperature waste heat sources that cannot be efficiently recovered. Low grade waste heat has generally been discarded by industry and has become an environmental concern because of thermal pollution. This has led to the lookout for technologies which not only reduce the burden on the non-renewable sources of energy but also take steps toward a cleaner environment.

One approach which is found to be highly effective in addressing the above mentioned issues is the Organic Rankine Cycle (ORC), which can make use of low-temperature waste heat to generate electric power. Similar in principle to the conventional cycle, ORC is found to be superior performance-wise because of the organic working fluids used in the cycle.

The focus of this study is to examine the ORC using different types of organic fluids and cycle configurations. These organic working fluids were selected to evaluate

the effect of the fluid boiling point temperature and the fluid classification on the performance of ORCs. The results are compared with those of water under similar conditions. In order to improve the cycle performance, modified ORCs are also investigated. Regenerative ORCs are analyzed and compared with the basic ORC in order to determine the configuration that presents the best thermal efficiency with minimum irreversibility. The evaluation for both configurations is performed using a combined first and second law analysis by varying certain system operating parameters at various reference temperatures and pressures. A unique approach known as topological method is also used to analyze the system from the exergy point of view. Effects of various components are studied using the exergy-wheel diagram.

The results show that ORCs using R113 as working fluid have the best thermal efficiency, while those using Propane demonstrate the worse efficiency. In addition, results from these analyses demonstrate that regenerative ORCs produce higher efficiencies compared to the basic ORC. Furthermore, the regenerative ORC requires less waste heat to produce the same electric power with a lower irreversibility.

**Key words:** Organic Rankine Cycle, Thermal efficiency, Irreversibility, Second-law analysis

## DEDICATION

To my Mom, Dad, and Brothers

## ACKNOWLEDGEMENTS

I would like to thank my parents and brothers for giving me the moral support needed to complete the PhD. I would also like to thank my major advisor Dr. Pedro J. Mago and committee member Dr. Louay M. Chamra whose support, both financially and technically, has been immense. I would also like to thank Dr. Glenn W. Steele and Dr. B. Keith Hodge, professors of Mechanical Engineering Department for their invaluable suggestions. Finally I would like to thank the Department of Mechanical Engineering for giving me the opportunity to take up this research project and complete my PhD.



## TABLE OF CONTENTS

DEDICATION .....	ii
ACKNOWLEDGEMENTS .....	iii
LIST OF TABLES .....	vi
LIST OF FIGURES .....	vii
NOMENCLATURE .....	ix
1. INTRODUCTION .....	1
ORC applications.....	2
ORC market.....	3
Literature review.....	4
Working fluid properties .....	5
Previous work on different heat sources .....	7
Previous studies on second law parameters of ORC .....	9
Objectives .....	11
2. WASTE HEAT SOURCES .....	14
Various Methods for Recovery of Waste Heat.....	17
Low-Temperature Waste Heat Recovery Methods .....	17
Geothermal waste heat sources .....	18
Biomass sources .....	19
Solar energy sources.....	20
Waste heat from engine exhaust.....	22
3. WORKING FLUIDS .....	24
Working Fluids for ORC Applications.....	24
Desirable characteristics.....	26
Organic Working Fluid Classification.....	29
Comparison of Organic Working Fluids and Water.....	34

4. FIRST AND SECOND LAW ANALYSIS OF BASIC ORC .....	38
Introduction.....	38
Analysis .....	39
Basic ORC .....	41
Conclusions.....	55
5. ANALYSIS OF REGENERATIVE ORC .....	56
Introduction.....	56
Analysis .....	57
Regenerative ORC.....	60
a. Feed-water Heater .....	60
b. Pump: (Processes 1-2 and 3-4).....	60
c. Evaporator: (Process 4-5) .....	61
d. Turbine: (Processes 5-6 and 5-7) .....	62
e. Condenser: (Process 7-1).....	62
f. Cycle Efficiency.....	63
g. Total Cycle Irreversibly .....	63
h. Second Law Efficiency .....	64
i. Electric Generator .....	64
Conclusions.....	75
6. EXERGY ANALYSIS OF ORC .....	77
Introduction.....	77
Analysis .....	79
Degree of thermodynamic perfection.....	81
Exergy efficiency .....	82
Influence coefficient.....	83
The different steps .....	83
Exergy Wheel Diagram .....	85
Results.....	86
Application of the Exergy Graph Methodology .....	88
Application of the Exergy Wheel Diagram .....	96
Effect of different parameters on the ORC performance .....	98
Conclusions.....	101
7. CONCLUSIONS.....	104
LIST OF REFERENCES.....	107

## LIST OF TABLES

2.1	Potential sources and sinks .....	16
3.1	Environmental parameters for some working fluids [Maizza et al., (1996)].....	27
3.2	Classification of working fluids ( Some of the data were taken from REFPROP).....	31
6.1	Exergy rates associated with the different components of an ORC [Bejan et al., 1996) .....	82
6.2	Matrix of incidence corresponding to the exergy flow graph for basic cycle [Step 3].....	90
6.3	Matrix of incidence corresponding to the exergy flow graph for regenerative cycle [Step 3].....	90
6.4	Flow parameters of the evaluated basic ORC [Step 4].....	91
6.5	Flow parameters of the evaluated regenerative ORC [Step 4] .....	91
6.6	Performance parameters of the evaluated basic ORC [Step 4].....	92
6.7	Performance parameters of the evaluated regenerative ORC [Step 4] .....	92
6.8	Thermodynamic characteristics of the evaluated basic ORC [Step 5].....	93
6.9	Thermodynamic characteristics of the evaluated regenerative ORC [Step 5] .....	93

## LIST OF FIGURES

1.1	A simple schematic of a Rankine cycle.....	1
3.1	Identification of the type using the shape of T-s diagram: a) Dry, b) Isentropic, c) Wet .....	33
4.1	Simple configuration of basic ORC to produce electrical power.....	40
4.2	Variation of the system thermal efficiency with the turbine inlet temperature ( $P_e = 1.5$ MPa and $T_c = 298$ K).....	46
4.3	Variation of the system irreversibility with the turbine inlet temperature ( $P_e = 1.5$ MPa and $T_c = 298$ K).....	48
4.4	Variation of the system second-law efficiency with the turbine inlet temperature ( $P_e = 1.5$ MPa and $T_c = 298$ K).....	49
4.5	Variation of the system thermal efficiency with the turbine inlet pressure ( $T_c = 298$ K).....	50
4.6	Variation of the system irreversibility with the turbine inlet pressure ( $T_c = 298$ K) for R113, R123, Propane, and Isobutane. ....	51
4.7	Mass flow rate needed to produce 122 kW of electric power versus turbine inlet pressure ( $T_c = 298$ K) for R113, R123, Propane and Isobutane. ....	52
4.8	Variation of the system thermal efficiency with the condenser outlet temperature ( $P_e = 3$ MPa). ....	53
4.9	Variation of the system second law efficiency with the condenser outlet Temperature ( $P_e = 3$ MPa) for R113, Isobutane, and Propane and R134a. ....	54
5.1	Outline of the procedure involved in the analysis of an Organic Rankine Cycle. ....	58
5.2.	Schematic and temperature-entropy diagram corresponding to the basic (a and c) and regenerative (b and d) ORC configurations.....	59
5.3	Variation of the system thermal efficiency with the turbine inlet pressure for Different ORC configurations ( $T_c = 298$ K): (a) basic and (b) regenerative.....	66

5.4	Comparison of the two ORC configurations for R113 and Isobutane ( $T_c = 298$ ).....	67
5.5	Variation of the specific system irreversibility with the turbine inlet pressure for R113 ( $T_c = 298$ K).....	68
5.6	Variation of the system second law efficiency with the turbine inlet temperature For R113 ( $T_c = 298$ K) .....	69
5.7	Variation of the heat transfer rate required in the evaporator to produce 100 kW Of electric power with the turbine inlet pressure for R113 ( $T_c = 298$ K).....	71
5.8	Variation of the mass flow rates required to produce 100 kW of electric power With the turbine inlet pressure for R113 ( $T_c = 298$ K).....	72
5.9	Variation of the system thermal efficiency with the turbine inlet temperature ( $P_e = 2$ MPa). .....	74
5.10	Variation of the system second law efficiency with the turbine inlet Temperature for R113 ( $P_e = 2$ MPa) .....	75
6.1	Flow chart of the network topological method adapted from Nikulshin et al. [2002, 2006] .....	80
6.2	Simple flow sheet diagram: (a) basic ORC and (b) regenerative ORC [Step 1].....	87
6.3	Exergy Flow Graph for the ORC presented in Figure 6.2: (a) basic and (b) Regenerative [Step 2] .....	89
6.4	Percentage of the exergy loss in each component: (a) basic and (b) regenerative .....	95
6.5	Exergy wheel diagram for a basic ORC.....	97
6.6	Exergy wheel diagram for a regenerative ORC. ....	97
6.7	Effect of the variation of the evaporator pressure on the system performance: a) Thermal efficiency, b) exergy efficiency and system total exergy loss .....	99
6.8	Variation of the system thermal and exergy efficiencies and the mass total System exergy loss with the hot gas inlet temperature: a) Basic ORC and b) Regenerative ORC.....	100

## NOMENCLATURE

$h$	Specific enthalpy, kJ/kg
$i$	Irreversibility rate, kW
$M$	Molecular weight, kg/mol
$\dot{m}$	Mass flow rate, kg/s
$\eta$	Efficiency, %
$P_{critical}$	Critical pressure, MPa
$P_{maximum}$	Maximum pressure of applicability, MPa
$q$	Specific heat, kJ/kg
$\dot{Q}$	Heat rate, kW
$S$	Entropy, kJ/K
$s$	Specific entropy, kJ/kg K
$T$	Temperature, K
$T_{BP}$	Boiling Point Temperature, °C
$T_{critical}$	Critical temperature, °C
$T_{maximum}$	Maximum temperature of applicability, °C
$T_H$	Temperature of the high-temperature reservoir, K
$T_L$	Temperature of the low-temperature reservoir, K
$\Delta T$	Temperature differential, K
$\rho_{critical}$	Critical density, kg/m <sup>3</sup>
$\dot{W}$	Power, kW

$\nu_i$	Degree of thermodynamic perfection, %
$\Pi_i$	Exergy loss, %
$\eta_{ex}^i$	Exergy efficiency of $i^{\text{th}}$ element, %
$E_i^u$	Exergy utilized by the $i^{\text{th}}$ element, kW
$E_i^a$	Exergy available at the $i^{\text{th}}$ element, kW
$\beta_i$	Coefficient of influence, %
$E_{\Sigma}^a$	Exergy available for the entire system, kW
$N$	Power
$K$	Number of primary flows
$L$	Number of secondary flows
$P_{out}$	Pressure at the exit of the boiler, MPa
$T_{out}$	Temperature at the exit of the boiler, K
$P_{out2}$	Pressure of the fluid leaving the condenser, MPa
$\dot{m}$	Mass flow rate of the working fluid, kg/sec
$T_0$	Reference temperature, K
$s_0$	Reference entropy, kJ/kg.K
$h_0$	Reference enthalpy, kJ/kg
$E_{x,i}$	Exergy loss

Subscripts:

*c* Condenser

*cycle* Cycle

*e* Evaporator

*exit* Conditions at the exit

*ideal* Isentropic case

*inlet* Conditions at the inlet

*p* Pump

*o* Ambient

*t* Turbine



## CHAPTER 1

### INTRODUCTION

The basic principles of the Organic Rankine Cycle (ORC) are similar to those of the conventional Rankine cycle. However the major difference is that the working fluid in the ORC is an organic fluid which has a lower boiling point and a higher vapor pressure than that of water. This improves the total performance or cycle efficiency of the ORCs significantly compared to the conventional Rankine cycle. The ORCs show characteristics similar to the ideal Carnot cycle. A Rankine cycle is used as a device to produce driving force by transforming the working fluid at a low temperature into steam at high temperature and high pressure. ORCs use organic fluids having a higher saturation vapor pressure and a lower boiling point than that of water to recover waste heat at low-temperature grade as power.

ORCs are similar to the large steam Rankine cycle engines typical to the coal-burning electric power plants. Heat is supplied to a heater where the compressed liquid is converted to a superheated vapor at constant pressure. The vapor is expanded through a turbine stage to produce a work output. Vapor leaving the turbine enters the condenser where heat is removed until the vapor is condensed into the liquid state. Saturated liquid is delivered to a pump, which raises the pressure of the liquid and is then delivered back to the heater where the cycle then repeats. The main difference between

the large steam Rankine engines and the ORCs is that ORCs utilize heavy working fluids, i.e., organic compounds, which result in superior efficiency over steam Rankine cycle engines for heat source temperatures below 370°C. Also, ORCs typically require only a single-stage expander in the turbine stage, making them much simpler than multi-stage expanders typical of the steam Rankine engines.

A simple ORC schematic for converting waste heat into useful electrical power is depicted in Figure 1.1.

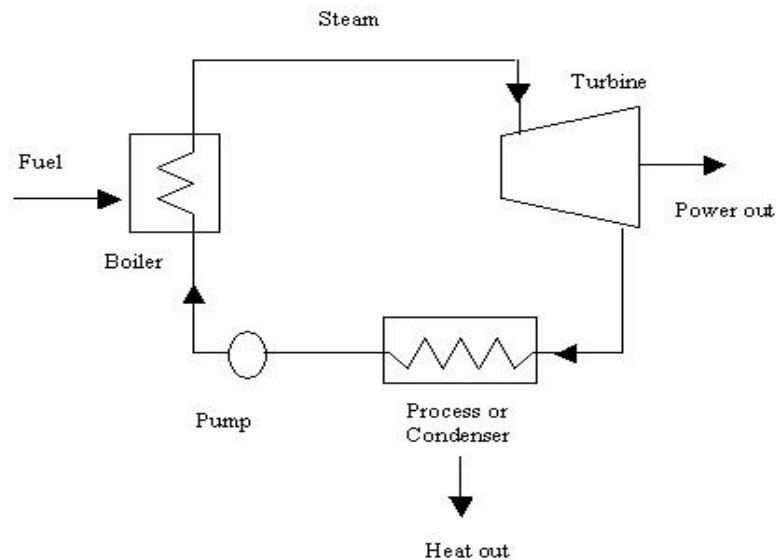


Figure 1.1 A simple schematic of a Rankine cycle

With the rapidly increasing cost of exhaustible energy resources, it is becoming increasingly important to find cost effective ways to reduce thermal discharges and to use those which remain. Since most of the thermal sources are available at a low temperature, the heat engine cycle selected must have a high efficiency at these temperatures. This

characteristic of the Organic Rankine cycle provides a unique match for low level waste heat streams.

Interest in alternative energy technologies is driven by two things:

1. The availability of fossil fuels
2. Environmental regulations

The low cost of fossil fuels cannot be sustained indefinitely due to both the inevitable depletion of resources and the political uncertainty associated with foreign markets. In addition, present day concern for global warming and pollution has already begun to create pressure, both internationally and domestically, to increase already existing environmental emissions regulations.

### **ORC applications**

ORCs are an appealing option for remote, low-power applications. One of the main advantages of ORCs lies in mechanical simplicity. As mentioned before, ORCs typically consist of a single-stage expander which consists of a single rotating component for the entire system. For the past several decades, thousands of ORCs have been developed and used for remote terrestrial applications with power outputs ranging from 1 to 1000 kW. A few examples of remote applications that have used efficient, reliable, unattended ORC power sources include communication stations, data gathering buoys, satellite communication power supplies, as well as irrigation pumps, air conditioners, and turbo-generators.

Several Organic Rankine Cycle Engines including solar dish-engines powered by solar energy have been successfully built and demonstrated. ORCs used to produce power from geothermal resources have also been developed and used. In addition, three U.S. companies have developed ORCs for use with waste heat streams resulting from industrial processes. All of the ORC research and development mentioned above find ORCs to be a more appropriate power system alternative over some of the other types listed above (e.g., fuel cells) for applications that seek to directly utilize a renewable energy source and require direct shaft power e.g. heat pumps, chillers, irrigation pumps, flywheel technologies, etc.

### **ORC market**

Currently the market for ORC power systems lies in the range of hundreds of millions of U.S. dollars annually. In the short term, an increase in environmental regulations will likely be the first catalyst to drive the market to a higher level before an increase occurs in the price of fossil fuels. Thus, the first area in which ORCs will find a potentially large market will be waste heat utilization. Utilizing waste heat will continue to increase due to the ongoing international effort to reduce the emission of greenhouse gases. The recent international environmental meetings in Kyoto, Japan, during December of 1997 and in Buenos Aires, Argentina during November of 1998 resulted in the "Kyoto Protocol" where several nations agreed to limit their generation of greenhouse gases. The United States has agreed to reduce its predicted greenhouse gas emissions by 40 percent over the next 15 years.

The developed nations require huge amounts of electrical power in order to produce the goods and lifestyle presently enjoyed. The developing nations are beginning to require similar electrical power requirements. Based on the "Kyoto Protocol" this increasing demand cannot be met by additional energy from fossil fuel. The only alternatives are nuclear, renewable sources, and better utilization of the fossil fuel that will be consumed. Considering these sources, the choice of better utilization of fossil fuel will clearly be the most significant, at least in the short term. This will require that all sources of so called waste heat be utilized to their maximum. ORC technology is a viable alternative for converting the waste heat streams to electricity and can be the power system of choice for such processes.

As the energy has become more precious, new energy technologies have emerged to exploit the resources which until now had been considered to be unsuitable for electrical power generation. Low grade heat as in the industrial waste streams, solar heat trapped in the collectors, cooling water streams of stationary diesel engines and the exhaust of diesel engines and biomass are the some of the examples of such resources. While the efficiency of conversion into electricity is an important factor, other aspects like reduction of emissions and low cost of the installed setup also play vital roles.

### **Literature review**

The working fluid is an important part of an organic cycle plant. The thermodynamic properties of the working fluids are key parameters for modeling of the plants [Kohler et al., (2003)]. The National Institute of Standards and Technology (NIST) database is extensively used for the evaluation of the properties of the refrigerants. These

data are used to find the cycle conditions with the help of Softwares like Cycle Tempo and REFPROP.

### **Working fluid properties**

In order to get the maximum out of a refrigerant, the refrigerant should satisfy some very important requirements. For ORC applications, flammable compounds could be employed if appropriate safety measures are employed. Fluids which are phased out are neglected owing to their high ozone depletion potential [Angelino et al., (1998)]. Also there are some general criteria [Vijayaraghavan et al., (2005)] like stability of the fluid, non-fouling nature, non-corrosiveness etc. To improve the heat transfer characteristics, the thermal conductivity of the selected refrigerants has to be high. The latent heat of vaporization should be high which means a smaller flow rate is required for a similar output from the plant. The liquid specific heat should be high meaning that less preheating is required [Vijayaraghavan et al., (2005)]. In addition to the above mentioned characteristics, there are many more features which will improve the heat transfer capability and thermo-physical performance of the plant that are worth mentioning. They are:

- high molecular weight
- low specific volume
- moderate vapor pressure in the heat exchanger units
- low viscosity and surface tension
- suitable thermal stability limits
- compatibility with engine materials

- low cost

Instead of using readily available property-evaluation tools like REFPROP, simple software which is custom-made based on the requirements can also be used. A similar attempt was made by Vlamincx et al., (1990) in which, the best available equations of state, equations of vapor pressure and the correlations for the prediction of the various properties were used, and software was developed. This software predicts all customary thermodynamic quantities with only a relatively small number of physical parameters of the fluid. As in the choice of the properties of the working fluids, the type of working fluids is also important.

The Rankine cycle can be modeled effectively using softwares like Cycle Tempo, REFPROP, and HYSYS. Yamamoto et al., (2001), in order to determine the optimum operating conditions, carried out a thermodynamic analysis of an ORC using a process simulator called HYSYS. This simulator is useful for thermodynamic analysis, especially at steady-state conditions. The simulator requires conditions like evaporator input, heat input, turbine inlet pressure, and turbine outlet pressure.

Maizza et al., (2001) reported that the fluid thermodynamic characteristics give rise to thermodynamic limitations to the amount of energy that can be extracted from the heat source. Some refrigerants satisfy the above mentioned criteria more than the others. One such refrigerant is R-245fa. An application development guide released by Honeywell gives some of the properties of HFC-245fa and also some of the applications of this refrigerant as the working fluid [Genetron®245fa, (2000)]. A benefit of the ORC is that they recover useful energy often as electrical output from low energy sources such

as low-pressure steam associated with steam driven turbines for electricity generation. Somayaji et al., (2006) and Mago et al., (2006) presented an analysis of the performance of ORC using R113 and R134a in which the use of organic fluids to generate power using low-temperature waste heat was studied. They have also shown that organic fluids must be operated at saturated conditions to reduce the total irreversibility of the system.

### **Previous work on different heat sources**

The limitation on the properties applies to both working fluids and the heat sources. Low grade (80°C to 200°C) as in the industrial waste heat stream, solar heat trapped by the collectors with low to medium ratios of concentration, low temperature geothermal sources , and cooling water streams of stationary engines are some of the sources which can be effectively used in ORC [Gurgenci et al., (1985)].

The amount of heat energy that can be extracted depends on the waste stream temperature and on the temperature of the cooling medium. The main advantage of the ORC is its superior ability in recovering waste heat with low to medium temperature. On the negative side, the temperature range limits the available heat sources dramatically. In general solar and geothermal sources which are usually available at low temperatures make up to 80% of the ORC heat source [Hung et al., (2001)]. The effect of the temperature of the heat source was also provided by Lee et al., (1996) in their investigation. They performed a systematic parametric analysis on an ORC using R-113 as working fluid and proved that the recovery of low temperature, low pressure waste steam by an ORC provided a high potential for moderate capacity plants. They also



indicated that the effects of the condensing and evaporating temperatures on the system's economic feasibility were significant.

Low grade heat sources account for more than 50% of the total heat generated in the industry. The recovery of the waste heat energy of different sources has been examined by many researchers. An ORC system combined with a space nuclear reactor in order to achieve higher efficiency was studied by Niggeman et al (1978). Some studies have also taken place to recover waste heat at temperatures around 700-1000°F in the chimney of a glass/ceramic furnace [Shai et al., (1996)]. Utilization of heat rejected from a condenser was examined by Angelino et al.,(2000) who concluded that a combined cycle with an ORC system as a bottoming cycle that utilizes the waste heat at a temperature greater than 200°C from the condenser has a return of investment less than conventional cycles. Some typical industrial waste heat sources are:

- hot gases from blast furnaces in steel industry
- exhaust gases of gas turbine and diesel engines
- hot gases from kilns in ceramic industry
- hot liquids in paper and pulp industry [Larjola et al., (1995)]

Thus, the most important characteristic of waste heat sources is their availability, the temperature at which they are available, and the cost of converting the waste heat into useful power. For example, the temperatures available from the Molten Carbonate Fuel Cell (MCFC) are suitable for the generation of additional power by means of a Rankine recovery cycle.

The thermodynamic modeling of a binary cycle with geothermal energy being used as the heat source was also investigated [Kohler et al., (2003)]. The possibility of using low-temperature, liquid-dominated geothermal sources was explored [Desidiri et al., (1997)]. The scope for optimization of the performance, by modifying the main parameters such as turbine inlet pressure and type of fluid being used was also studied. Much research work has been done on the parameters analysis on an ORC energy recovery system. Thermodynamic analysis, economic evaluation, sensitivity analysis, and economic design parameters study is widely covered [Yamamoto et al., (2000)].

### **Previous studies on second law parameters of ORC**

In contrast to the traditional methods of thermodynamic investigation, the exegetic analysis takes into account both quantity and quality of energy flow [Nikulshin et al., (2006)]. Analysis of system thermal performance also involves thermodynamic optimization of the system. Thermodynamic optimization is the determination and minimization of the thermodynamic factors causing the decrease in efficiency. Irreversibility in a real life thermodynamic system usually leads to inefficient conversion of all the available thermal energy into useful work [Hung et al., (2001)]. From the first and second laws of thermodynamics, we find the efficiency of an ORC can be obtained under various working conditions for a specific working fluid. Hung et al., (2001) conclude in their paper that when the associated state is a saturated vapor, the system thermal efficiency is commonly increased with respect to greater turbine inlet pressure which leads to less irreversibility when the temperature of the source is fixed. When the temperature difference in the evaporator is fixed, higher turbine inlet pressure leads to

larger irreversibility. In general they say that the waste heat boiler is a key component to cause irreversibility. The second law efficiency is the indicator for the amount of irreversibility present in a system.

Hung et al., (1997) in their work have done parametric analysis and compared the efficiencies and irreversibility of the ORC using various working fluids such as Benzene, Toluene, P-Xylene, R123, and R113. A 10-MW waste heat source was employed for this purpose. A computer program was developed to simulate the performance of the working fluids under various working conditions. The thermodynamic properties of the fluids were calculated using Peng-Robinson equations. They found that when the associated state is a saturated vapor, the system thermal efficiency would increase with turbine inlet pressure. When the temperature difference in the evaporator is fixed, higher turbine inlet pressure leads to larger irreversibility. Somayaji et al., (2006) and Mago et al., (2007) showed that ORCs using dry fluids have better performance than ORCs using wet fluids.

Diffuse introduction for biomass based power generation in an industrial district has been studied which can improve system efficiency and also at the same time reduce the emissions [Chinese et al., (2004)]. They investigated the impact of the introduction of ORC units in an industrial context from a system perspective. With particular reference to industrial districts, which are characterized by the concentration in small areas of a large number of medium and small sized firms. To this end, a mixed-integer, linear programming model oriented to economical optimization of the system is developed and a sensitivity analysis is carried out in order to determine the condition for the expansion of biomass based power generation and to evaluate potential CO<sub>2</sub> emissions.

In yet another method the potential role of organic bottoming Rankine Cycle in steam power stations [Angelino et al., (2000)] was studied to reduce emissions and improve system efficiency. A method proposed by which a fraction of the low pressure steam is extracted. This is fed to an auxiliary ORC module of small capacity. This auxiliary ORC module besides being perfectly suited to explore even the coldest cooling agent, improves the working condition of the main turbine by reducing the exhaust volume. With the help of a computer program, the performance of a typical power station supplemented with an ORC system was analyzed for different cooling situations. In this investigation, attention was focused on turbine optimization.

### **Objectives**

*1. To evaluate and optimize the use of ORC to convert low-grade waste energy to power using thermodynamically effective organic working fluids.* The selection of the organic working fluid forms an important part of the proposed research. One of the most important parameters of the operation of ORCs is to choose the organic working fluid, which passes the stringent environmental regulations. The organic working fluid must be carefully selected based on safety and technical feasibility. There is a wide selection of organic fluids that could be used in ORC.

*2. Study the effect of different ORC configurations to determine the configuration that gives best first and second law efficiencies, with minimum irreversibility.* All configurations will be modeled based on a combined first and second law analysis. This is one of the most important aspects of the proposed research since all the results will be based on the developed models. The optimization of ORCs include the effect of the

different configurations on the overall thermal efficiency of the cycle, the cycle total irreversibility, the cycle second law efficiency, the mass flow rate needed to generate a certain power output, and the amount of waste heat needed to operate the cycle. The analysis of an ORC can be carried out using different configurations. For each of the configurations, the turbine inlet pressure and turbine inlet temperature will be varied. Then system variables such as thermal efficiency, second-law efficiency, irreversibility rate, and mass flow rate needed to generate specified amount of power output will be determined. Different organic working fluids will be evaluated and their results will be compared with those of water operating under the same operating conditions.

*3. Study the influence of the boiling point temperature and molecular weight on the system performance for all ORC configurations.* The system performance is related to the molecular weight and the boiling point of the working fluid used. Therefore, analyzing this subject will also help in the selection of the organic working fluid.

*4. Propose a simple and effective method to classify the organic working fluids.* Working fluids will be classified as wet, dry, or isentropic fluids depending on the slope of the temperature - entropy curve. A simple method to classify organic working fluids will be developed in this investigation. The idea is to reduce the complex calculations involved in some of the current methods. The classification of the organic working fluids is very important because the type of fluid used will affect the cycle performance.

*5. Propose two different methods to perform a complete exergy analysis of ORCs.* The two proposed methods are: (1) The exergy wheel method and (2) The topological method. The topological method is useful to determine the influence of different

components on the performance of the system. Parameters like degree of thermodynamic perfection, exergy efficiency, and coefficient of influence will be found, and the effect of each component on the overall system will be studied. Also, the effect of varying the pressure at the evaporator on different parameters will be analyzed. The main purpose of this exergy analysis is to determine the component in a cycle, which has the highest influence on the system performance. These techniques also help better understand the energy and exergy interactions associated with any component of a system or the whole system. The approach will help in evaluating losses at different components and the whole cycle.

## CHAPTER 2

### WASTE HEAT SOURCES

In industrial processes, there are many low temperature heat sources which are available at less than 230 °C that cannot be effectively recovered by simple heat exchanger devices. However ORC heat engines have high potential to convert low grade waste heat into power.

In a typical developed country as much as 40% of the total fuel consumption is used for industrial and domestic space heating and process heating. Of this, around one third is wasted. This wasted heat can be lost to the atmosphere at all stages of the process, through inefficient generation, transmission, or during final use of the energy. Waste heat recovery aims to minimize the amount of wasted heat by reusing it in either the same or a different process. Waste heat can be recovered either directly (without using a heat exchanger-e.g., recirculation) or, more commonly, indirectly. Direct heat recovery is often the cheaper option, but its use is restricted by location and contamination considerations. In indirect heat recovery, the two fluid streams are separated by a heat transfer surface, which can be categorized as either a passive or active heat exchanger. Passive heat exchangers require no external energy input whilst active heat exchangers do

(e.g., thermal wheel and heat pump). When describing waste heat recovery, the nature of the waste heat is specified in terms of temperature and material phase. Waste heat can be considered as either low-grade ( $<100^{\circ}\text{C}$ ), medium grade ( $100^{\circ}\text{C}$ – $400^{\circ}\text{C}$ ) or high grade ( $>400^{\circ}\text{C}$ ). Low grade waste heat can only be recovered effectively when there is a high quantity of waste heat and a ready use for it. There are many examples of successful heat recovery projects for temperatures between  $100^{\circ}\text{C}$  and  $200^{\circ}\text{C}$ . At  $200^{\circ}\text{C}$  and above most users should be able to make significant cost savings from heat recovery. Different techniques and heat exchanger materials are used to recover heat above  $400^{\circ}\text{C}$ .

Since the recovery of heat from solid material is difficult, most heat is recovered from and passed to material in a gas or liquid phase. Many relatively simple processes have a surprisingly large number of potential waste heat sources and sinks. The identification of the sources and sinks and their relative suitability and proximity determines the cost-effectiveness of any heat recovery project. Some common sources and sinks for processes, utilities and buildings are listed in Table 2.1.

In general, high-grade waste heat is mainly limited to the iron and steel, glass, nonferrous metals, bricks and ceramics industries. Medium-grade waste heat is most widely found in the chemicals, food and drink, and other process industries, as well as building utilities. Low-grade waste heat can be found in virtually all areas of industry and buildings and is often the hardest to recover cost-effectively—typical examples of recovering low grade waste heat would be ventilation or hot water systems.



Waste heat recovery does not always require high capital investment and in some cases little or no cost is involved. The first and often easiest step is to ensure that the heat is not wasted in the first place.

Table 2.1. Potential sources and sinks

	<i>PROCESS</i>	<i>UTILITY</i>	<i>BUILDING</i>
<i>POTENTIAL SOURCES</i>	EXOTHERMIC REACTION	BOILER FLUE	VENTILATION SYSTEMS
	DRYER EXHAUST	STEAM CONDENSATE	EXHAUST AIR
	OVEN AND KILN EXHAUST	FURNACE EXHAUST	AIR CONDITIONING PLANTS
	CONDENSER	COMPRESSORS	
	EFFLUENT STREAMS	REFRIGERATION SYSTEMS	
<i>POTENTIAL SINKS</i>	PROCESS STEAM	BOILER FEED WATER	SPACE HEATING
	HEAT FOR A REACTION	AIR PRE HEATER	HOT WATER
	HEAT FOR SEPARATION	DISTRICT HEATING	
	REBOILER	POWER GENERATION	
	PREHEAT PROCESS FLUID		

This includes:

- Ensuring plant is operating at maximum efficiency;
- Reducing evaporation and heat loss from open tanks;
- Optimizing the scheduling and control of operations;
- Making sure there are no leaks in ducts and pipes;
- Fitting insulation and ensuring that it is replaced after maintenance.

Good housekeeping is essential before even considering any major capital investment in waste heat recovery. If wasted heat can be limited at source, then recovering it is made that much easier.

### **Various Methods for Recovery of Waste Heat**

A large amount of energy in the form of medium- to low-temperature gases or low-temperature liquids (less than about 250°C) is released from process heating equipment, and much of this energy is wasted.

#### **Low-Temperature Waste Heat Recovery Methods**

*Conversion of Low-Temperature Exhaust Waste Heat* – making efficient use of the low temperature waste heat generated by prime movers such as micro-turbines, IC engines, fuel cells and other electricity producing technologies. The energy content of the waste heat must be high enough to be able to operate equipment found in cogeneration and tri-generation power and energy systems such as absorption chillers, refrigeration applications, heat amplifiers, dehumidifiers, heat pumps for hot water, turbine inlet air cooling, and other similar devices.

*Conversion of Low Temperature Waste Heat into Power* –The steam-Rankine cycle is the principle method used for producing electric power from high temperature fluid streams. For the conversion of low temperature heat into power, the steam-Rankine cycle may be a possibility, along with other power cycles, such as the organic-Rankine cycle. Most 'alternative' thermal energy is found at a temperature below that of steam or boiling water (below 100 °C). Solar energy is most economically collected at 40 °C -65

°C; a geothermal temperature of 70 °C exists only 200 feet underground and industrial waste heat is most prevalent at temperatures between 60-120 °C.

Compared to 'alternative' thermal sources, commercial 'organic Rankine cycle' power plants generally require heat sources hotter than those that are economically obtained from renewable sources. Modern geothermal power plants require a minimum heat source of 320° F, largely in consequence to the mechanical inefficiency of the mechanical feed pump required by all Rankine cycles.

There are a number of waste heat sources which can be used very effectively in Organic Rankine cycle system. They are:

- geothermal sources
- biomass sources
- solar waste heat sources
- waste heat from engine exhaust, engine coolants

### ***Geothermal waste heat sources***

Geothermal energy has been exploited since the beginning of this century in order to produce electric power and domestic hot water. When compared to other renewable energy sources, its main advantages consist of direct technology transfer from conventional steam power plants and continuous availability of fluid output in the geothermal fields.

A deterrent for the geothermal industry growth is the economical risk in identifying the source. Locating geothermal sources can prove costly. Indications of potential sources may include geysers, seismic or volcanic activity, and hot springs. The

high cost has hindered extensive exploration. Once a geothermal site is found, it can also be difficult to determine the total available energy of the site, which is necessary to gauge the worth of the investment. Exploitation of geo-fluids will undoubtedly prompt a geological response, which could result in a finite lifetime for a geothermal site before it cools off (Dickson and Fanelli, 1995). So although the global geothermal potential is virtually limitless, local concentrations with high geothermal gradients are bounded and not renewable (Armstead, 1978). Estimates must be made for the geothermal gradient, heat flow to the surface, and heat capacity of the fluid holding rocks, which are often only accurate to within an order of magnitude. The potential site must be selected prudently.

Geothermal sources are generally divided into two classes. One is vapor dominated and the second is water dominated. From the first, steam at saturated condition exits from the ground and can be directly expanded in a turbine to generate power. Since the steam is at saturated state high pressure sources are also at high temperature. The power plants with vapor dominated sources are quite simple and are based on conventional steam power plant technology. In water dominated geothermal fields hot water is available at a nearly saturated state and at various temperatures of up to over 200° C. Those sources with the highest temperature can be exploited to generate power.

### ***Biomass sources***

Biomass is the term used to describe all the organic matter produced by photosynthesis that exists on the Earth. The source of all energy in biomass is the sun, the biomass acting as a kind of chemical energy store. Biomass is constantly undergoing a complex series of physical and chemical transformations and being regenerated while

giving off energy in the form of heat to the atmosphere. For many, this is in the simplest form of an open fire used to provide heat for cooking, heating water or heating the air in a home. More sophisticated technologies also exist for extracting biomass energy and converting it into useful heat or power in an efficient way.

The biomass fuelled ORCs have many advantages: 1) low temperature and pressure levels. 2) higher plant performance in comparison to pure heat production 3) higher electrical efficiency 4) small space required 5) higher cost effectiveness 6) good partial load behavior. Small scale turbines for organic working fluids are well developed and optimized with respect to their efficiency. This increase in efficiency increases the electricity production in comparison to conventional steam turbines.

Waste heat is another energy source that can be converted to useful energy by using expanders in an Organic Rankine Cycle (ORC) system. Potential heat sources include: tail gas from industrial furnaces or combustion engines, waste vapor from chemical and petrochemical processes, and solar heat from flat or parabolic reflectors and collectors.

### *Solar energy sources*

The energy from the sun varies from place to place and is very dependent on weather conditions. Without an atmosphere  $1453 \text{ W/m}^2$  per hour is available, but with an atmosphere we can only count on  $1000 \text{ W/m}^2$  per hour in the absence of clouds. Though sunshine is free, the cost of a large, curved, shiny mirrored assembly that must swivel to track the sun, and concentrate sunshine into a  $400^\circ\text{-}700^\circ\text{F}$  fluid has to be considered. The

cost of curved collectors can also be compared with that to the cost of a simple immobile flat plate collector, producing equal Btu's per square meter, but at a temperature of 150°F.

The higher temperatures produced by the parabolic collector would produce a Rankine cycle of a higher efficiency. Parabolic trough power plants are the only type of solar thermal power plant technology with existing commercial operating systems. In capacity terms, 354 MWe of electrical power are installed in California, and some new plants are currently in the planning process in other locations. The parabolic trough collector consists of large curved mirrors that concentrate the sunlight by a factor of 80 or more to a focal line. Parallel collectors usually make a 300–600 meter long collector row. This multitude of parallel rows form the solar collector field.

Solar thermal use for power generation has been limited to mid and high temperature collection, as efficient power cycles for low temperature resources have not been thoroughly explored. The power production cost has been found to go down dramatically with system size, so most systems are on the large commercial scales. Systems using parabolic trough concentrators obtain fluid temperatures around 700 °C. Parabolic dish concentrators can achieve temperatures up to 3250 °C (Twidell and Weir, 1986). For large solar systems, two methods are used for mid temperature cycles. In the first method, with distributed collection, many collectors are networked, which heat a fluid to high temperatures. This fluid can be steam, which is expanded through a turbine, or an intermediary fluid such as ammonia, which is dissociated to store chemical energy. The heat from the collector can power a steam turbine. In the second method, power

towers are used, with an array of reflectors focused on a single collection point (Twidell and Weir, 1986). Both of these methods for solar thermal electricity are infeasible on residential scales, as the cost would be prohibitive to the homeowner. The typical efficiency for mid and high temperature solar thermal power generation is about 20%. The cost of solar collection is minimized in using flat plate collectors, although the temperatures produced in the transfer fluid are not sufficiently high to efficiently fuel conventional power cycles. The proposed cycle addresses this issue by being able to utilize low temperature resources, providing a cost savings potential by being able to use inexpensive flat plate collectors.

#### ***Waste heat from engine exhaust***

The waste heat recovery research and development (R&D) focuses on technologies that can recover and convert engine waste heat to electrical energy to improve the overall engine thermal efficiency and reduce emissions. Recovery of energy from the engine exhaust represents a potential for at least a 10% improvement in the overall engine thermal efficiency. The efficiency of turbochargers used to recover part of this energy could be increased from the current 50% to 58% to about 72% to 76% with enhancements such as variable geometry. An electrically driven turbocharger with increased transient response would be another approach. Turbo-compounding and direct thermal-to-electric conversion could also improve the overall thermal efficiency. Bulk semiconductor thermoelectric devices are currently 6-8% efficient. However, recent developments in quantum well thermo-electrics suggest a potential improvement to over 20% is possible.

There are four sources of usable waste heat from a reciprocating engine: 1) exhaust gas, 2) engine jacket cooling water, 3) lube oil cooling water, and 4) turbocharger cooling. Recovered heat is generally in the form of hot water or low pressure steam (<30 psig). The high temperature exhaust can generate medium pressure steam (up to about 150 psig), but the hot exhaust gas contains only about one half of the available thermal energy from a reciprocating engine. Some industrial CHP applications use the engine exhaust gas directly for process drying. Generally, the hot water and low pressure steam produced by reciprocating engine CHP systems is appropriate for low temperature process needs, space heating, and portable water heating. There were an estimated 1,055 engine-based CHP systems operating in the United States in 2000, representing over 800 MW of electric capacity. SI engines fueled by natural gas or other gaseous fuels represent 84% of the installed reciprocating engine CHP capacity.



## CHAPTER 3

### WORKING FLUIDS

#### **Working Fluids for ORC Applications**

One of the most important parameters of the operation of ORCs is the selection of the organic working fluid. The organic working fluid must be carefully selected based on safety and technical feasibility. There is a wide selection of organic fluids that could be used in ORC. Information regarding different working fluids that could be used in ORC applications can be found in Maizza and Maizza (1996), Vijayaraghavan and Goswami (2005), and Maizza and Maizza (2001).

The fully-halogenated compounds should be replaced by ozone-safe substances in the near future to protect global environment. CFCs were widely used as refrigerants, cleaning agents, and propellants. Some CFCs such as CFC-11, CFC-113, and CFC-114 were also employed as working fluids for organic Rankine Cycle (ORC) engines to recover low-temperature waste heat [Lee et al. (1993)]. Utilization of waste heat is not economically attractive when the waste heat goes below a certain temperature level because the amount of power that can be recovered from the low-grade waste heat source is dependent on the temperature. The temperature of the low-grade waste heat source will directly affect the thermal efficiency of the whole system. The

selection of the working fluid and other operating conditions has to be taken very seriously in order to have good system performance. The proper choice of the working fluid is as important a parameter as the waste heat source temperature for an effective Organic Rankine Cycle power plant. [Liu et al.(2004)]

In processes involving Rankine cycles, water is generally used as the working fluid. A difficulty that arises with the use of water is the need to superheat the water to prevent turbine blade erosion. Organic working fluids, on the other hand, can be used at lower temperatures and do not require superheating [Somayaji et al., (2006) and Mago et al., (2006)]. The use at low temperatures with organic fluids result in a practical increase in efficiency over the use of the cycle with water as the working fluid. Also when the available heat source which is used to heat the working fluid in the boiler is at very low temperatures we tend to opt for organic working fluids.

Drescher (2007) mentioned that in contrast to water, the expansion of an organic working fluid in a turbine ends in the dry state rather than in the wet state. He also points out that organic working fluids are more useful when the maximum available temperature is low and the size of the power plant is relatively small. Although less thermodynamically efficient than the Carnot cycle, the Rankine cycle is practical and adaptable. The Rankine cycles utilizing the organic fluids tend to give higher thermal efficiency compared with water.

Besides water, no other inorganic working fluid is found to be suitable to effectively use the processes involved in the Rankine cycle. This necessitates the need to use organic fluids. Further, even in the large pool of organic fluids available, no single

working fluid satisfies all the desirable characteristics needed for a working fluid. This calls for a compromise between different properties and, thereby, selecting one which best fits all requirements. The range of organic fluids is such that there are hundreds of working fluids in the market. However, the available pool of refrigerants narrows down significantly, once cost and environmental standards are considered. Because of the zero ozone depletion potential (ODP) hydro-fluorocarbons have been predominantly chosen as alternative refrigerants replacing CFCs and HCFCs. Since HFCs have a high global warming potential (GWP) there is still a search for the next generation refrigerants that might have better cycle performance.

An efficient operation of the organic Rankine cycle depends heavily on the type of cycle and the thermodynamic properties of the working fluids. In Organic Rankine cycle (ORC) applications, the choice of working fluid is critical since the fluid must have not only thermo-physical properties that match the application but also adequate chemical stability at the desired working temperature.

### **Desirable characteristics**

A good working fluid for an ORC should have the following desirable characteristics:

- High cycle efficiency
- Low critical temperature and pressure
- Low specific volume
- Low vapor superheat requirement
- Moderate vapor pressure in the heat exchange units

- Low viscosity
- Low surface tension
- High thermal conductivity
- A high decomposition temperature so that a high bottom cycle temperature can be employed.
- High molecular weight
- Mollier diagram close to isentropic
- Suitable thermal stability limits
- Compatible with engine materials and lubricating oil
- Non-corrosive
- Non-inflammable
- Non-toxic
- Low cost

As mentioned before, no fluid will satisfy all of these characteristics. Prediction of the thermodynamic capability of substances with the aid of proper thermodynamic models could help to select potential working media from numerous compounds. Lee et al. (1993) used the Iwai-Margerum-Lu equation of state to predict the thermodynamic properties of the working fluids and evaluated the heat transfer capability of these fluids. A detailed list of some environmentally acceptable working fluid with their different characteristics is given in Table 3.1 [Maizza and Maizza (1996)].

Table 3.1 Environmental parameters for some working fluids [Maizza et al., (1996)]

Table 1. Possible environmentally acceptable fluids

Fluid (name)	Chemical formula	Molecular weight <i>M</i>	Boiling point (°C)	ODP <sup>a</sup>	GWP <sup>a</sup>	LFL <sup>c</sup> (%)	TOX <sup>d</sup> (ppm)
HCFC-21	CHCl <sub>2</sub> F	102.92	8.9	—	—	none	1000
HCFC-22	CHClF <sub>2</sub>	86.47	-40.5	0.055	510	none	1000
HCFC-23	CHF <sub>3</sub>	70.01	-82.03	0	12000	none	1000
R-25 Toluene	(e)	92.14	110.6	—	—	—	100
HFC-32	CH <sub>2</sub> F <sub>2</sub>	52.02	-51.2	0	220	14.6	—
HC-40 Methyl chloride	CH <sub>3</sub> Cl	50.48	-24	—	—	—	100
FC-116	CF <sub>3</sub> CF <sub>3</sub>	138.01	-78.2	—	—	—	1000
HCFC-123	C <sub>2</sub> HCl <sub>2</sub> F <sub>3</sub>	152.91	-27.75	0.02	29	none	10
HCFC-124a	C <sub>2</sub> HClF <sub>4</sub>	136.5	-12.03	0.02	150	none	500
HFC-125	C <sub>2</sub> H <sub>2</sub> F <sub>5</sub>	120.02	-48.3	0	860	none	1000
HFC-134a	C <sub>2</sub> H <sub>2</sub> F <sub>4</sub>	102.03	-26.1	0	420	none	1000
HCFC-142b	C <sub>2</sub> H <sub>3</sub> ClF <sub>2</sub>	100.5	36	0.06	540	6.9	1000
HFC-143a	C <sub>2</sub> H <sub>3</sub> F <sub>3</sub>	84.041	-47.4	0	1000	7.1	—
HFC-152a	C <sub>2</sub> H <sub>4</sub> F <sub>2</sub>	66.05	-24.2	0	47	3.7	1000
HC-160 Chloroethane	C <sub>2</sub> H <sub>5</sub> Cl	64.5	12.3	—	—	—	1000
HC-170 Ethane	C <sub>2</sub> H <sub>6</sub>	30.07	-88.6	—	—	—	800
HC-270	C <sub>2</sub> H <sub>6</sub>	42.08	-32.9	0	—	—	400
HC-290 Propane	C <sub>3</sub> H <sub>8</sub>	44.1	-42.1	0	3	2.1	Asphyx.
HC-600a Isobutane	(CH <sub>3</sub> ) <sub>2</sub> CH	58.12	-11.7	0	3	1.8	1000
R-401A	(f)	94.44	-32.97	0.03	0.22	none	800/9/
R-401B	(f)	92.8	-34.67	0.035	0.24	none	840/9/
R-401C	(f)	101	-28.4	0.03	0.17	none	720/9/
R-402A	(g)	101.55	-49.19	0.02	0.63	none	1000/10/
R-402B	(g)	94.71	-47.4	0.03	0.52	none	1000/10/
HFC-404A	(g)	97.6	-46.45	0	0.94	none	1000/10/
HFC-407C	(h)	86.2	-43.56	0	1600(1)	none	1000
HFC-SUVA 9100	(i)	75.57	-51.8	0	2020(1)	—	—

<sup>a</sup>ODP: Ozone depletion potential (rel. to CFC-11).

<sup>a</sup>GWP: Global warming potential (rel. to CO<sub>2</sub>; integration time = 500 yr).

<sup>c</sup>LFL: Lower flammability limit (vol% in dry air).

<sup>d</sup>TOX: Toxicity (threshold limit value = the max time-weighted average concentration for a normal 8 hr workday).

<sup>e</sup>R-25 is a mixture of methylbenzene, toluene, toluall, C<sub>8</sub>H<sub>7</sub>.

<sup>f</sup>Azeotrope mixture of HCFC-22, HCFC-124a, HFC-152a /9/.

<sup>g</sup>Azeotrope mixture of HCFC-22, HFC-125, HC-290 /10/.

<sup>h</sup>Azeotrope mixture of HFC-32, HFC-125, HFC 134a (23/25/52% by weight).

<sup>i</sup>Azeotrope mixture of HFC-32, HFC-125 (45/55% by weight). A new product of Du Pont De Nemours (October 1994).

<sup>a</sup>GWP: Global warming potential (rel. to CO<sub>2</sub>; integration time = 100 yr).

The thermal stability of an organic working fluid can also be tested experimentally [Anderson (2005)]. He uses a simple technique where the decomposition reaction rate constant of the working fluid is studied. In addition to this, literature is available for the analytical aspects involved in the selection of the proper working fluid, for example Liu et al. (2004). High heat source temperatures require correspondingly high critical temperatures. But in general, organic working fluids should have a lower critical temperatures than steam. This property has one adverse effect for organic working fluids, which is, low operating temperature range. Higher molecular weight means higher molecular complexity. Water, for instance, has a simple molecular structure. Thus organic fluids with complex molecular structure are preferred. The

organic working fluids are generally made up of carbon and fluorine molecules which tend to be heavy. When the fluids are heavy, the turbines tend to have lower peripheral speed and lower number of stages. Thus, heavier working fluids will reduce the work required thus increasing the system performance [Angelino (1998, 2000)]. The cycle efficiency is also affected by the shape of the mollier diagram for a particular working fluid. Maizza et al (2001) have done an excellent study on the properties of the working fluids. From their research they found that a vertical or near vertical saturated liquid line is needed so that most of the heat is added during the change of phase without the need for the complexity of regenerative feed heating to carnotize the cycle to realize high cycle efficiency. This will also help in reducing the moisture content resulting during the expansion. On the other hand, there is no need to condense a superheated vapor.

### **Organic Working Fluid Classification**

Another characteristic that must be considered during the selection of organic fluid is its saturation vapor curve. This characteristic affects the fluid applicability, cycle efficiency, and arrangement of associated equipment in a power generation system. Basically, the working fluid can be classified into three categories. Those are dry, isentropic, and wet depending on the slope of the  $T-s$  curve. A dry fluid has a positive slope; a wet fluid has a negative slope; while an isentropic fluid has an infinitely large slopes. These characteristic curves are shown in Figure 3.1 for a basic ORC configuration. The working fluids of dry or isentropic type are more appropriate for ORC systems, since both are superheated after isentropic expansion thereby eliminating the concerns of impingement of liquid droplets on the turbine blades [Liu et al. (2004)].

Using the fluid properties available in REFPROP software, the approximate shape of the T-s diagram and the working pressure range of all the working fluids considered was noted. The ratio of the temperature difference to the entropy difference was then calculated as given in equation 3.1 is,

$$\frac{dT}{dS} = \frac{T_1 - T_2}{S_1 - S_2} \dots\dots\dots (3.1)$$

Table 3.2 Classification of working fluids (Data used in the calculation are taken from REFPROP)

short name	full name	$T_{cr}$ (°C)	$P_{cr}$ (Mpa)	$T_{min}$ (°C)	$T_{max}$ (°C)	$P_{max}$ (Mpa)	M (kg/kmol)	$P_1$ (Mpa)	$P_2$ (Mpa)	$T_1$ (°C)	$T_2$ (°C)	$s_1$ (kJ/kg.K)	$s_2$ (kJ/kg.K)	X	type
ammonia	ammonia	132.25	11.333	-77.65	326.85	100	17.03	5	10	88.882	125.17	5.106	4.515	-61.401	wet
argon	argon	-122.46	4.863	-189.34	426.85	1000	39.94	0.5	1.5	-167.35	-149.19	2.9602	2.7605	-90.9364	wet
butane	butane	151.98	3.796	-138.28	315.85	69	58.12	0.5	1.5	50.288	99.108	2.4397	2.4964	861.0229	dry
CO2	carbon dioxide	30.97	7.37	-56.55	826.85	800	44.01	5	7	14.284	28.683	1.7544	1.5844	-84.7	wet
ethane	ethane	32.18	4.87	-182.8	351.85	70	30.07	0.5	1.5	-52.732	-18.071	2.4143	2.2516	-213.036	wet
isobutane	2-methylpropane	134.67	3.64	-159.59	299.85	35	58.12	0.5	1.5	37.729	85.463	2.3211	2.3695	986.2397	dry
methane	methane	-85.58	4.59	-182.46	351.85	1000	16.04	0.5	1.5	-137.8	-114.62	4.0716	3.6887	-60.538	wet
nitrogen	nitrogen	-146.96	3.39	-210	1726.9	2200	28.01	0.5	1.5	-179.15	-162.75	5.084	4.8157	-61.1256	wet
oxygen	oxygen	-118.57	5.043	-218.79	726.85	82	31.99	1	2	-153.53	-140.41	4.8958	4.7461	-87.642	wet
propane	propane	96.67	4.24	-187.67	349.85	103	44.09	0.5	1.5	1.7185	43.989	2.3699	2.3376	-1308.68	wet
propylene	propene	92.42	4.66	-173.15	326.85	200	42.08	0.5	1.5	1.7185	43.989	2.3699	2.3376	-1308.68	wet
R11	trichlorofluoromethane	197.96	4.4	-110.47	351.85	30	137.37	0.5	1.5	78.124	130.31	1.6763	1.677	74551.43	isen
R12	dichlorodifluoromethane	111.97	4.13	-157.05	251.85	200	120.91	0.5	1.5	15.648	59.333	1.5535	1.5407	-3412.89	wet, isen
R13	chlorotrifluoromethane	28.85	3.879	-181.15	129.85	35	104.46	0.5	1.5	-45.3	-10.322	1.3757	1.3428	-1063.16	wet
R14	tetrafluoromethane	-45.64	3.75	-174.21	349.85	51	88	0.5	1.5	-100.56	-74.105	1.2788	1.214	-408.256	wet
R22	chlorodifluoromethane	96.14	4.99	-157.42	276.85	60	86.46	0.5	1.5	0.12398	39.095	1.7505	1.6996	-765.639	wet
R23	trifluoromethane	26.14	4.832	-155.13	201.85	120	70.01	0.5	1.5	-48.938	-17.665	1.645	1.5577	-358.225	wet
R32	difluoromethane	78.1	5.78	-136.81	161.85	70	52.02	0.5	1.5	-14.331	20.619	2.2083	2.0809	-274.333	wet
R41	fluoromethane	44.13	5.89	-98.15	226.85	60	34.03	0.5	1.5	-43.613	-10.991	2.4795	2.2702	-155.862	wet
R113	1,1,2-trichloro-1,2,2-trifluoroethane	214.06	3.39	-36.22	251.85	200	187.38	0.5	1.5	105.87	161.75	1.6336	1.6682	1615.029	dry



Table 3.2 Continued

short name	full name	$T_{cr}$ (°C)	$P_{cr}$ (Mpa)	$T_{min}$ (°C)	$T_{max}$ (°C)	$P_{max}$ (Mpa)	M (kg/kmol)	$P_1$ (Mpa)	$P_2$ (Mpa)	$T_1$ (°C)	$T_2$ (°C)	$s_1$ (kJ/kg.K)	$s_2$ (kJ/kg.K)	X	Type
R115	chloropentafluoroethane	79.95	3.12	-99.39	226.85	60	154.47	0.5	1.5	4.2441	45.467	1.3989	1.4133	3076.336	dry,isen
R116	hexafluoroethane	19.87	3.05	-87.15	149.85	50	138.01	0.5	1.5	-42.261	-7.808	1.2317	1.2306	-31320.9	isen
R123	1,1-dichloro-2,2,2-trifluoroethane	183.68	3.66	-107.15	326.85	40	152.93	0.5	1.5	80.88	131.5	1.6785	1.6973	2692.553	dry,isen
R124	1-chloro-1,2,2,2-tetrafluoroethane	122.28	3.62	-153.15	196.85	40	136.48	0.5	1.5	33.948	77.718	1.59	1.5989	4917.978	isen
R125	pentafluoroethane	66.02	3.61	-100.63	226.85	60	120.02	0.5	1.5	-8.9571	28.258	1.4886	1.4823	-5907.16	isen
R134a	1,1,1,2-tetrafluoroethane	101.06	4.05	-103.3	181.85	70	102.03	0.5	1.5	15.735	55.233	1.7197	1.7049	-2688.78	wet
R141b	1,1-dichloro-1-fluoroethane	208.81	4.46	-103.3	226.85	100	116.95	0.5	1.5	86.93	139.5	1.8633	1.8805	3056.395	dry,isen
R142b	1-chloro-1,1-difluoroethane	137.11	4.07	-130.43	226.85	60	100.5	0.5	1.5	38.361	83.72	1.7834	1.783	-113397	isen
R143a	1,1,1-trifluoroethane	72.7	3.76	-111.81	376.85	100	84.04	0.5	1.5	-6.714	31.794	1.6927	1.6636	-1323.3	wet
R152a	1,1-difluoroethane	113.26	4.51	-118.59	226.85	60	66.05	0.5	1.5	19.173	59.979	2.0963	2.0481	-846.598	wet
R218	octafluoropropane	71.95	2.67	-160.15	226.85	30	188.02	0.5	1.5	5.9444	46.606	1.3361	1.3685	1254.988	dry
RC318	octafluorocyclobutane	115.23	2.77	-39.8	349.85	60	200.03	0.5	1.5	40.582	85.026	1.4605	1.5021	1068.365	dry
R227ea	1,1,1,2,3,3,3-heptafluoropropane	101.65	2.928	-128.8	226.85	60	170.03	0.5	1.5	28.119	70.408	1.4752	1.5038	1478.566	dry
R230ea	1,1,1,2,3,3-hexafluoropropane	139.29	3.502	-31.15	226.85	60	152.04	0.5	1.5	53.219	97.811	1.6502	1.683	1359.512	dry
R236fa	1,1,1,3,3,3-hexafluoropropane	124.92	3.2	-83.63	226.85	40	152.04	0.5	1.5	44.52	88.081	1.6102	1.6355	1721.779	dry
R245ca	1,1,2,2,3-pentafluoropropane	174.42	3.925	-73.15	226.85	60	134.05	0.5	1.5	75.05	122.15	1.8194	1.8539	1365.217	dry
R245fa	1,1,1,3,3-pentafluoropropane	154.05	3.64	-73.15	226.85	60	134.05	0.5	1.5	62.692	108	1.7747	1.803	1600.989	dry
water	water	373.95	22.06	0.01	1001.9	1000	18.01	5	15	263.94	342.16	5.9737	5.3106	-117.961	wet

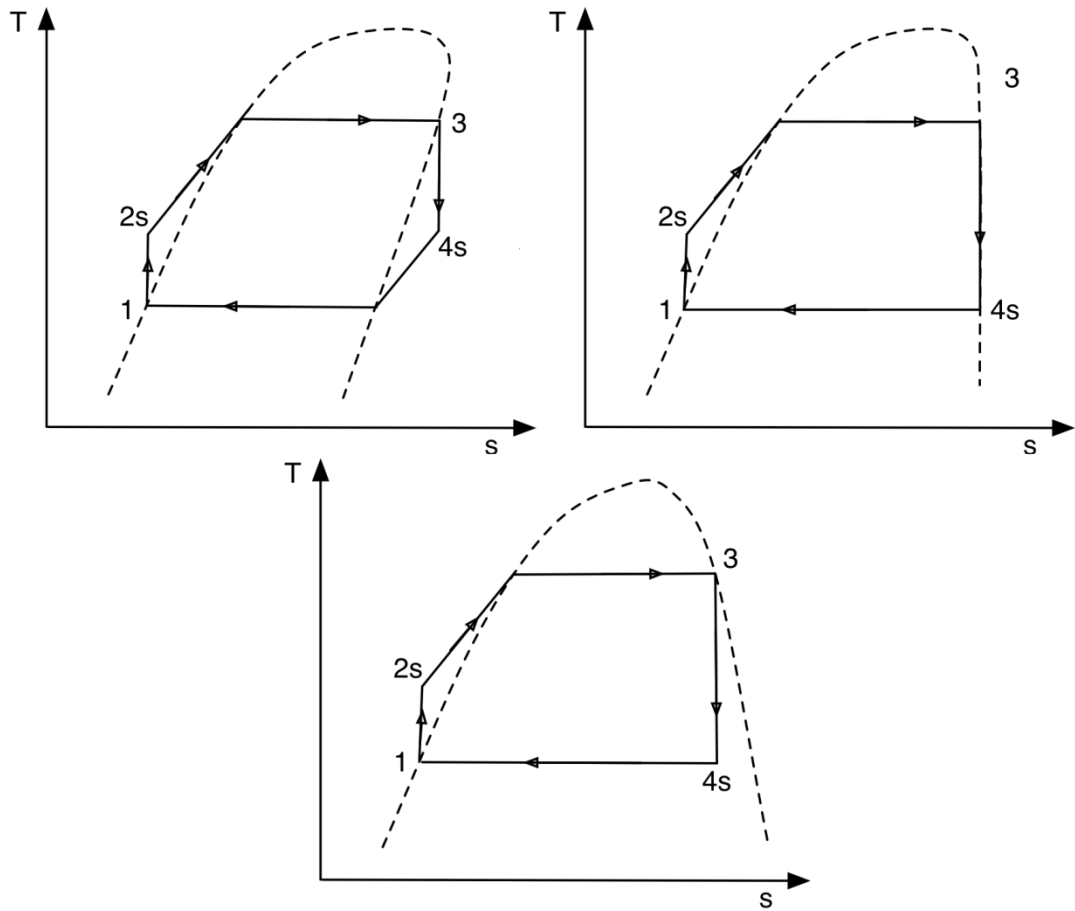


Figure 3.1. Identification of the type using the shape of T-s diagram: a) Dry, b) Isentropic, c) Wet

The shape of the temperature-entropy diagram gives a clear indication of the type of working fluid. If the slope of the curve on the vapor side is positive, then the working fluid is a dry fluid. If the slope is negative, then the working fluid is a wet fluid. If the slope is infinite, then the working fluid is isentropic.

## Comparison of Organic Working Fluids and Water

Comparison of performance of water and organic fluids for low temperature applications is useful in determining the organic fluids to be used. Water is the working fluid of choice for the majority of large scale fossil-fired Rankine cycle power plants. Water is well-suited for those high-temperature applications, but water has its limitations for low temperature operation. However, organic fluids excel during low temperature operations. The main difference between organic fluids and water is their behavior when expanding from a saturated or superheated state through a turbine at low to moderate temperature (200°C-400°C). This behavior is best observed by examining a turbine expansion in this temperature regime. Since water is a wet fluid, in the absence of superheat the isentropic expansion of water results in a relatively low-quality two-phase mixture (<80%). A low quality flow through a turbine is unacceptable as it can result in significant equipment damage. Organic fluids show a much different behavior than that observed for water. Since most of the organic fluids are dry or isentropic, an isentropic expansion from a saturated vapor state results in a superheated vapor, rather than the two-phase mixture as with water. Dry or isentropic fluids eliminate the possibility of low-quality turbine flows and the associated complications to cycle design.

A system with lower irreversibility results in a better performance. In practice the temperature of the waste heat medium varies along the evaporator rather than remaining constant. With constant evaporator temperature, the irreversibility as well as the exergy efficiency depends on the type of the working fluid and the type of heat source implemented. Higher power output can be obtained when the working fluid closely

follows the heat source fluid to be cooled. In other words, a system has better performance if the temperature difference between the heat source and the temperature of the working fluid in an evaporator is reduced due to its lower irreversibility.

According to a study presented by Lee et al. (1993), since dry type fluids (fluids with a positive slope of the saturation vapor curve in the T-S diagram) have no condensation problems in the expansion process. This is possible only when the turbine inlet vapor is saturated. This characteristic is generally observed in dry, or isentropic fluids. Therefore, these types of fluids are preferred to the wet type of fluids. They also mentioned that fluid molecular weight, normal boiling points and critical pressures could be key properties for preliminarily selecting working fluids. Fluids with molecular weight smaller than 90 g/mole, a normal boiling point between 570 °C and 600 °C and a critical pressure higher than 35 bar are potentially able to provide a good thermo-physical capability for the ORC energy recovery system. This study presents an analysis of the performance of Organic Rankine Cycle (ORC) subjected to the influence of working fluids. The effects of various working fluids on the thermal efficiency and on the total heat recovery efficiency have been investigated. The presence of hydrogen bonds in certain molecules such as water, ammonia and ethanol may result in wet fluid conditions due to larger vaporizing enthalpy and is regarded as inappropriate for ORC systems. The calculated values show that the thermal efficiency is a weak function of critical temperature.

The effect of various working fluids on the thermal efficiency and on the total heat recovery efficiency has been studied [Liu et al. (2004)]. The results were as follows:

1) The presence of a hydrogen bond in certain molecules such as water, ammonia and ethanol results in wet fluids due to larger vaporizing enthalpy and is regarded as inappropriate for the ORC systems.

2) The thermal efficiency for various working fluids is a weak function of the critical temperature regardless of the fact that the thermal efficiency for the working fluids with the low critical temperature is lower.

3) In general, the maximum value of total heat recovery efficiency occurs at an appropriate evaporating temperature that is between the inlet temperature of the waste heat and the condensing temperature. The maximum value of the total heat recovery efficiency increases with an increase of the inlet temperature of the waste heat and decreases with working fluids of the lower critical temperature.

Since the purpose of an ORC is the recovery of low-grade heat to power, a superheated approach is not appropriate. Therefore, the wet fluids are not appropriate for ORC systems because they become saturated once they go through a large enthalpy drop after producing work in the turbine and the condensate of the fluids imposes a threat of damage to the turbine. However, the dry and isentropic fluids can prevent the above disadvantage. Due to the irreversibility of the thermodynamic system, the conversion of all the available thermal energy into useful work is not possible. Using the first and second laws of thermodynamics, the efficiency of an ORC can be obtained under various working conditions for a specific working fluid.

When the associated state is a saturated vapor the system thermal efficiency is usually increased with respect to a greater inlet turbine pressure. This factor leads to less

irreversibility when the temperature of the source is fixed. For systems with saturated vapor as working fluid, the thermal efficiency increases with higher turbine inlet pressure. When the temperature difference in the evaporator is fixed, a higher turbine inlet pressure leads to larger irreversibility.

The fluid thermodynamic properties give rise to thermodynamic limitations to the amount of energy that can be extracted from the heat source. The amount of energy extracted also depends on the waste stream temperature and on the temperature of the cooling medium. The amount of energy which can be recovered is greater if the waste source temperature is higher and if the cooling source temperature is lower.

To conclude, the properties of the working fluid affect the cycle efficiency and capital cost involved. Selection of a proper working fluid for an ORC is very important since the ORC is a special purpose cycle which is specifically used to recover the low-grade heat to power. The purpose of using the ORC will not be served if proper care is not taken in the selection of the working fluid.

CHAPTER 4  
FIRST AND SECOND LAW ANALYSIS OF BASIC ORC

**Introduction**

Energy supply trends as well as the environmental regulations have made it necessary to closely scrutinize the way energy is utilized. As a result the importance given to the analysis of the thermodynamic cycle has increased over the years. Effective energy utilization thus needs accurate and advanced thermodynamic analysis of the thermal systems. The first law of thermodynamics and second law of thermodynamics analysis are particularly useful for understanding the thermodynamic system. In the simplest terms, the laws of thermodynamics indicate the details for the movement of heat and work. Basically, the first law of thermodynamics is a statement of the conservation of energy, and the second law is a statement about the direction of that conservation, and the combined first and second law of thermodynamics is the most effective method for evaluating a thermal system performance.

In this chapter different organic working fluids were used to evaluate the effect of the fluid boiling point temperature as well as fluid classification on the

performance of basic ORCs. The results are compared with those of water under similar conditions.

Using the first and second laws of thermodynamics, parameters like thermal efficiency, second-law efficiency, and irreversibility are found. In addition, using the first and second laws of thermodynamics, the best working fluid, based on both analysis is chosen. The organic-fluid boiling point and the working fluid used also have a strong influence on the system thermal efficiency and the electric power production.

To evaluate the performance of electric power generation systems, ORCs in this specific case, thermodynamic models of the different components have to be developed. Although the analysis of simplified thermodynamic models generally leads only to qualitative conclusion about the cycle performance, these models allow evaluating how the changes in operating parameters affect the actual cycle performance. Also, different parameters can be evaluated to improve the cycle overall performance by utilizing these models. The purpose of this chapter is to evaluate the performance of organic Rankine cycle using the combined first and second law of thermodynamics for a basic Rankine cycle. Though the approach of first and second law analyses is not new, for an Organic Rankine cycle this technique is unique.

### **Analysis**

The equations used to determine the cycle efficiencies as well as the cycle irreversibility for basic ORC configurations are presented in this section. The thermodynamic model presented in this chapter assumes the following: 1) steady state conditions, 2) no pressure drop in the evaporator, condenser, and pipes, and 3) isentropic



efficiencies for the turbine and pump. The components of a basic ORC for converting waste heat into useful electrical power are shown in figure 4.1. As observed in Figure, basic ORC consists of four different processes: Process 1-2 (pumping process), Process 2-3 (constant-pressure heat addition), Process 3-4 (expansion process), and Process 4-1 (constant-pressure heat rejection).

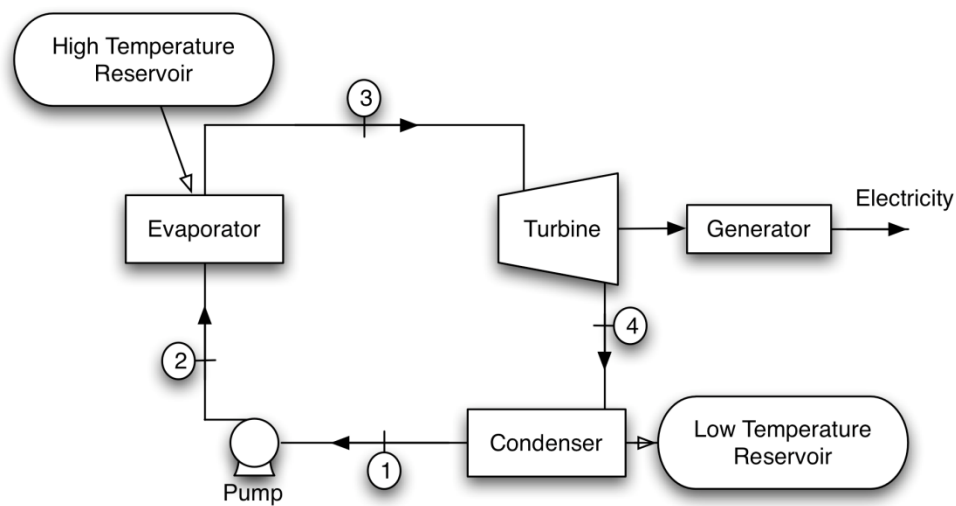


Figure 4.1. Simple configuration of basic ORC to produce electrical power.

For each individual component, the first and second laws of thermodynamic are applied to find the work output, the heat added or rejected, and the components and system irreversibility. The energy balance equation is,

$$\sum_i E_i + \dot{Q} = \sum_o E_o + \dot{W} \quad (4.1)$$

where  $E_i$  and  $E_o$  are the energy rate in and out,  $\dot{Q}$  is the heat transfer rate, and  $\dot{W}$  is the power.

The irreversibility rate for uniform flow conditions is given by,

$$\dot{I} = T_o \frac{dS}{dt} = T_o \dot{m} \left[ \sum S_{exit} - \sum S_{inlet} + \left( \frac{ds_{system}}{dt} \right) + \sum_j \frac{q_j}{T_j} \right] \quad (4.2)$$

where the subscript “j” stands for the heat transfer for different reservoirs and the term

$$\frac{ds_{system}}{dt} = 0 \text{ for steady state conditions.}$$

### Basic ORC

**a. Process 1-2 (Pump):** The liquid leaving the condenser at Point 1 is pumped into the evaporator. Taking a control volume around the pump, using Equation (4.1) and assuming a pump isentropic efficiency, the pump power can be expressed as,

$$\dot{W}_p = \frac{\dot{W}_{p,ideal}}{\eta_p} = \frac{\dot{m}(h_1 - h_{2s})}{\eta_p} \quad (4.3)$$

where  $\dot{W}_{p,ideal}$  is the ideal power of the pump,  $\dot{m}$  is the working fluid mass flow rate,  $\eta_p$  is the pump isentropic efficiency, and  $h_1$  and  $h_{2s}$  are the enthalpies of the working fluid at the inlet and outlet of the pump for the ideal case.

The pump irreversibility rate can be determined as,

$$\dot{I}_p = T_o \dot{m}(s_2 - s_1) \quad (4.4)$$

where  $s_1$  and  $s_2$  are the specific entropies of the working fluid at the inlet and exit of the pump for the actual conditions, respectively.

**b. Process 2-3 (Evaporator):** The evaporator heats the working fluid from the pump outlet to the turbine inlet condition. Taking a control volume enclosing the evaporator, the heat transfer rate from the energy source into the working fluid is given by,

$$\dot{Q}_e = \dot{m}(h_3 - h_2) \quad (4.5)$$

where  $h_3$  and  $h_2$  are the enthalpies of the working fluid at the exit and inlet of the evaporator, respectively.

The evaporator irreversibility rate can be determined as,

$$\dot{I}_e = T_o \dot{m} \left[ (s_3 - s_2) - \frac{h_3 - h_2}{T_H} \right] \quad (4.6)$$

where  $s_3$  and  $s_2$  are the specific entropies of the working fluid at the inlet and exit of the evaporator, respectively, and  $T_H$  is the temperature of the high-temperature heat source.

This temperature is considered to be equal to  $T_H = T_3 + \Delta T_H$

**c. Process 3-4 (Turbine):** Vapor from the evaporator at Point 3, with a high temperature and pressure, expands through the turbine to produce mechanical work and then is passed to the condenser at Point 4. For a control volume around the turbine and assuming a turbine isentropic efficiency, the turbine power is given by,

$$\dot{W}_t = \dot{W}_{t,ideal} \eta_t = \dot{m}(h_3 - h_{4s}) \eta_t \quad (4.7)$$

where  $\dot{W}_{t,ideal}$  is the ideal power of the turbine,  $\eta_t$  is the turbine isentropic efficiency, and  $h_3$  and  $h_{4s}$  are the enthalpies of the working fluid at the inlet and outlet of the turbine for the ideal case.

The turbine irreversibility rate is,

$$\dot{I}_t = T_o \dot{m}(s_4 - s_3) \quad (4.8)$$

where  $s_3$  and  $s_4$  are the specific entropies of the working fluid at the inlet and exit of the turbine for the actual conditions, respectively.

**d. Process 4-1 (Condenser):** The condenser heat rejection rate can be expressed as,

$$\dot{Q}_c = \dot{m}(h_1 - h_4) \quad (4.9)$$

The condenser irreversibility rate can be determined as follows,

$$\dot{I}_c = T_o \dot{m} \left[ (s_1 - s_4) - \frac{h_1 - h_4}{T_L} \right] \quad (4.10)$$

where  $s_1$  and  $s_4$  are the specific entropies of the working fluid at the inlet and exit of the condenser, respectively, and  $T_L$  is the temperature of the low temperature reservoir. This temperature is considered to be equal to  $T_L = T_1 - \Delta T_L$

***e. Cycle efficiency:***

The thermal efficiency is defined as the ratio between the net power of the cycle to the evaporator heat rate. It gives a measure about how much of the waste heat input to the working fluid passing through the evaporator is converted to the net work output and can be expressed as,

$$\eta_{cycle} = \frac{\dot{W}_t + \dot{W}_p}{\dot{Q}_e} \quad (4.11)$$

Substituting Equations (4.3), (4.5), and (4.7) into Equation (4.11) the thermal efficiency for a basic ORC can be written as,

$$\eta_{cycle} = \frac{(h_3 - h_{4s}) \cdot \eta_t + (h_1 - h_{2s}) \cdot \eta_p^{-1}}{(h_3 - h_2)} \quad (4.12)$$

***f. Total-Cycle Irreversibly:***

The total irreversibility can be obtained adding Equations (4.4), (4.6), (4.8), and (4.10) as follows,

$$\dot{I}_{cycle} = \sum_j \dot{I}_j = \dot{I}_p + \dot{I}_e + \dot{I}_t + \dot{I}_c = T_o \dot{m} \left[ -\frac{h_3 - h_2}{T_H} - \frac{h_1 - h_4}{T_L} \right] \quad (4.13)$$

**g. Second-Law Efficiency:**

The second law cycle efficiency can be calculated using the following equation,

$$\eta_{II} = \frac{\dot{W}_{net}}{\dot{Q}_e \left(1 - \frac{T_L}{T_H}\right)} = \left( \frac{(h_3 - h_{4s})\eta_t + (h_1 - h_{2s})\eta_p^{-1}}{(h_3 - h_2)} \right) \left(1 - \frac{T_L}{T_H}\right)^{-1} \quad (4.14)$$

**h. Electric Generator:** The mechanical power produced in the turbine is converted to electric power in the generator. The total electric power is,

$$\dot{W}_{electric} = \dot{W}_{net} \eta_{generator} = (\dot{W}_t + \dot{W}_p) \eta_{generator} \quad (4.15)$$

where  $\eta_{generator}$  is the generator efficiency.

For the purpose of this study, seven organic fluids with different boiling points ranging from -43°C to 48°C were employed. These organic fluids are R134a, R113, R245ca, R245fa, R123, isobutane, and propane and were selected to investigate the effect of the boiling point and the effect of the fluid classification on the performance of basic ORC. The selected fluids are dry and wet. Isentropic fluids such as R12 and R22 were not included since they are being phased-out and replaced with alternative refrigerants.

To investigate the effect of the turbine inlet temperature on the cycle efficiency, system specific irreversibility and second-law efficiency the following operating conditions were used. The evaporator pressure and condenser temperature were kept constant at 1.5 MPa and 298 K, respectively. The isentropic efficiencies of the turbine and pump were 80% and 85%, respectively, while the temperature differential was kept constant at 15 K for all cases. The variation of the system thermal efficiency with the turbine inlet temperature is given in Figure 4.2. Basically, this figure shows the effect of

superheating of the working fluid over the thermal efficiency of the cycle. The range of temperature used to analyze each fluid varies from the saturation temperature to the critical temperature. This figure illustrates that the cycle thermal efficiency for the evaluated organic fluids is a weak function of the turbine inlet temperature since thermal efficiency remains approximately constant or slightly decreases with the increment of the turbine inlet temperature. This reflects the fact that organic fluids do not need to be superheated to increase the cycle thermal efficiency as opposed to water, for which increasing the inlet turbine temperature increases the thermal efficiency. Even though only one evaporator pressure is illustrated in figure 4.2, the performance for other pressures is similar to the one presented here. Figure 4.2 can also be used to analyze the influence of the fluid boiling-point temperature on the system thermal efficiency. The boiling point temperatures are presented next to each fluid in Figure 4.2. It can be observed that the organic fluid that has the best thermal efficiency is R113, which has the highest boiling-point among the selected fluids (47.59°C), while the fluid with the lowest thermal efficiency is propane, which has the lowest boiling point temperature (-42.09°C). Similar trends are observed for the remaining working fluids in this investigation. Thus the results presented above show higher the boiling point temperature of the fluid leads to better cycle thermal efficiency.

From Figure 4.2, it can also be observed that R113 shows the maximum efficiency among the organic fluids for temperatures above 430 K, while R123, R245ca, and R245fa have the best efficiencies for temperatures between 380 K and 430 K. For temperatures below 380 K, isobutane shows the best efficiency, while water is the best

fluid when temperatures go above 470 K. This figure also illustrates that the selected organic dry fluids (R113, R123, R245ca, R245fa, and Isobutane) have better performance than the selected organic wet fluids (R134a and propane). As mentioned before, one of the reasons dry fluids seem to better thermal efficiencies is because they do not condense after the fluid goes through the turbine as opposed to wet fluids that condense in the turbine. However, important point to be noted is that independent of the fluid classification, organic fluids can be used to produce power from low temperature waste heat.

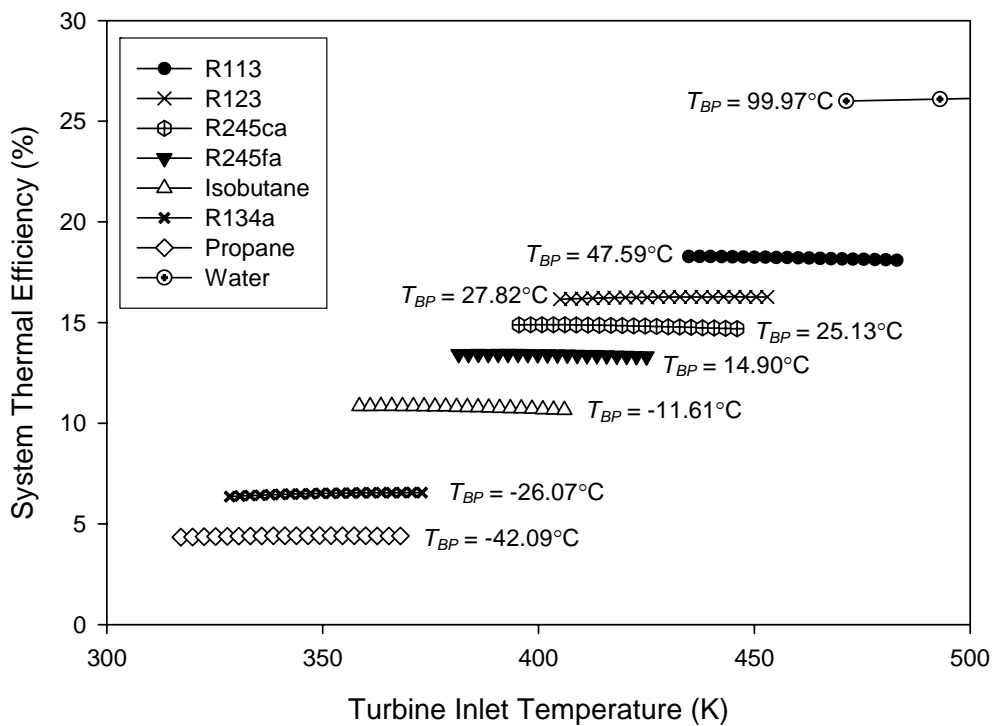


Figure 4.2. Variation of the system thermal efficiency with the turbine inlet temperature ( $P_c = 1.5$  MPa and  $T_c = 298$  K).

However, organic fluids are restricted to a small range of applicability depending on their thermodynamic conditions. This means that one organic fluid best suited for application for a temperature range, may not be so good for other temperature ranges. It is possible to have many organic fluids which satisfy the desirable characteristics at different temperature ranges.

The variation of the system specific irreversibility with the turbine inlet temperature is given in figure 4.3. It can be observed that the total system irreversibility increases with turbine inlet temperature for all the fluids. The results presented in this figure underline the importance of performing a second law analysis. According to the results presented in Figure 4.2, the thermal efficiency is approximately constant with the increment of the turbine inlet temperature. However, from a combined first and second-law analysis, the best case scenario is obtained when the fluid is operated at saturated conditions before the turbine. This yields the same thermal efficiency with lower irreversibility than operating under superheated conditions. Figure 4.3 illustrates how the system with higher (R113) and lower (propane) thermal efficiencies present the lower and higher irreversibility, respectively. Water has higher specific irreversibility compared with the evaluated organic fluids. The effect of the boiling point temperature in this figure does not present a consistent trend as in figure 4.2.



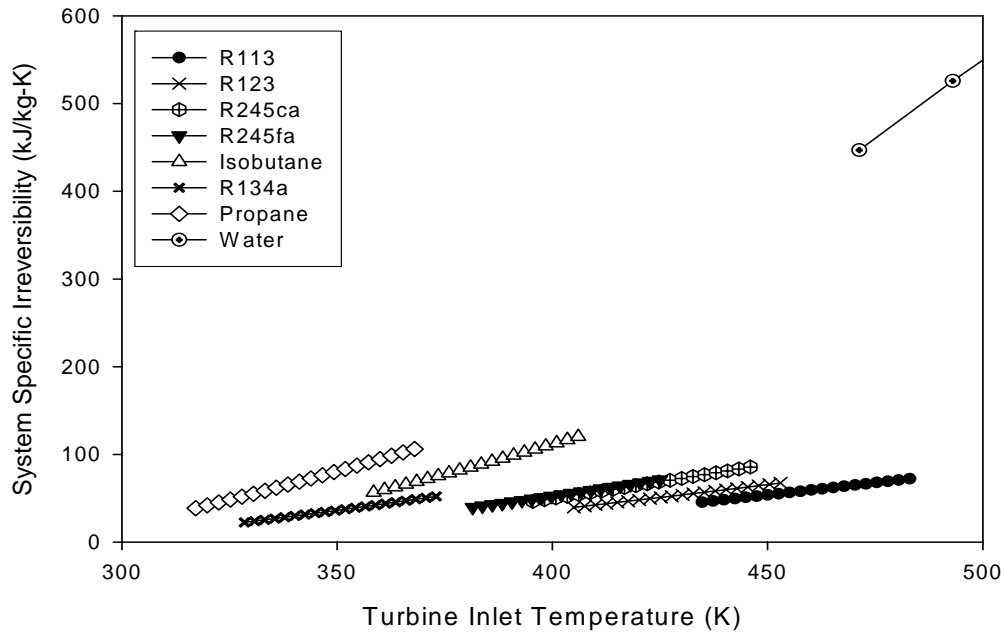


Figure 4.3. Variation of the system irreversibility with the turbine inlet temperature ( $P_e = 1.5 \text{ MPa}$  and  $T_c = 298 \text{ K}$ )

Figure 4.4 illustrates the effect of the turbine inlet temperature on the system second-law efficiency. The second law efficiency decreases with the turbine inlet temperature for all the fluids. These results agree well with the results presented in figure 4.3, since an increase in the system irreversibility yields a decrease in the system second-law efficiency. For temperatures between 430K and 525K, R113 shows the best second-law efficiency, for a range of 400K to 430K, R123 shows the best efficiency, R245ca and R245fa present the best second-law efficiency for temperatures between 380K and 400K. Isobutane shows the best efficiencies for a temperature range of 360K to 380K, R134a for a temperature range of 330K to 360K, while propane shows the low second-law efficiency among all the evaluated fluids. The effect of the turbine isentropic efficiency on the system second law efficiency was also evaluated. It was found that increase of the

turbine isentropic efficiency represent an increase of the second law efficiency for all the evaluated fluids.

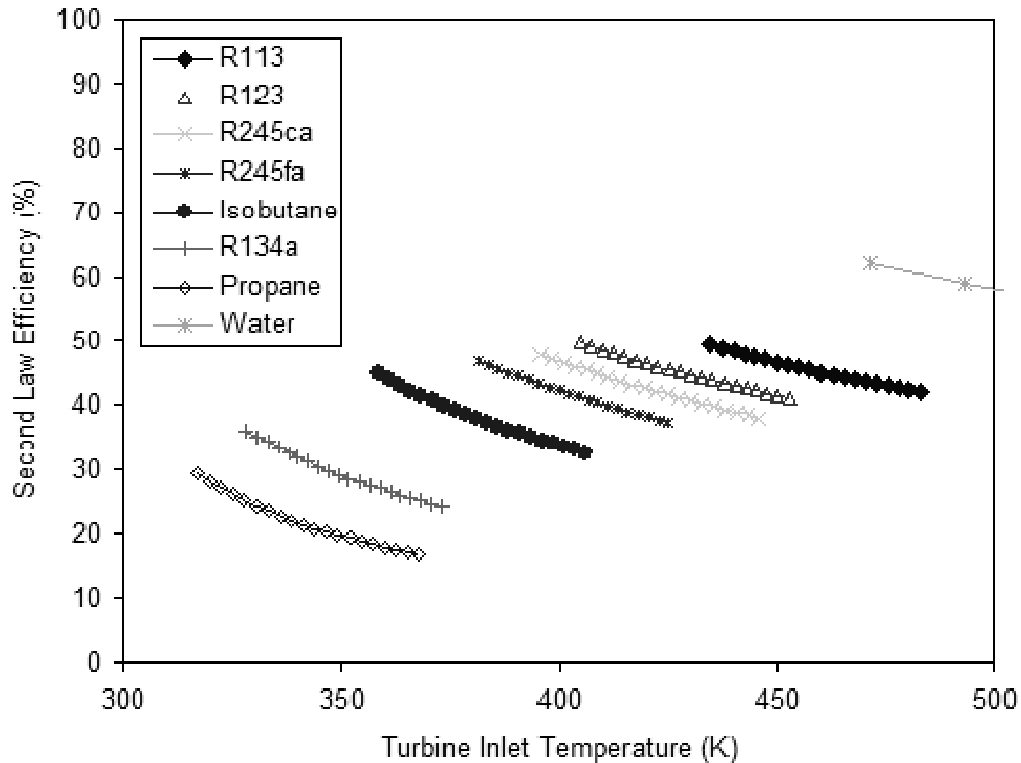


Figure 4.4. Variation of the system second-law efficiency with the turbine inlet temperature ( $P_c = 1.5$  MPa and  $T_c = 298$  K).

The next parameter to be evaluated is the effect of the turbine inlet pressure on the system performance. For this case, the condenser temperature was kept constant at 298 K, while the maximum pressure used for each fluid was the critical pressure. The isentropic efficiencies of the turbine and pump were 80% and 85%, respectively, while the temperature differential was kept constant at 15 K. Figure 4.5 illustrates the variation of the system thermal efficiency with the turbine inlet pressure while keeping the turbine

inlet temperature at saturated conditions. The results are consistent for all the fluids, since the system thermal efficiency increases with the turbine inlet pressure for all of them. This can be explained since the inlet turbine pressure increases both the net work and the evaporator heat. However, the percentage of increase of the net work is higher than the percentage of increase of the evaporator heat. Therefore the ratio of the net work and the evaporator heat increases with the turbine inlet pressure.

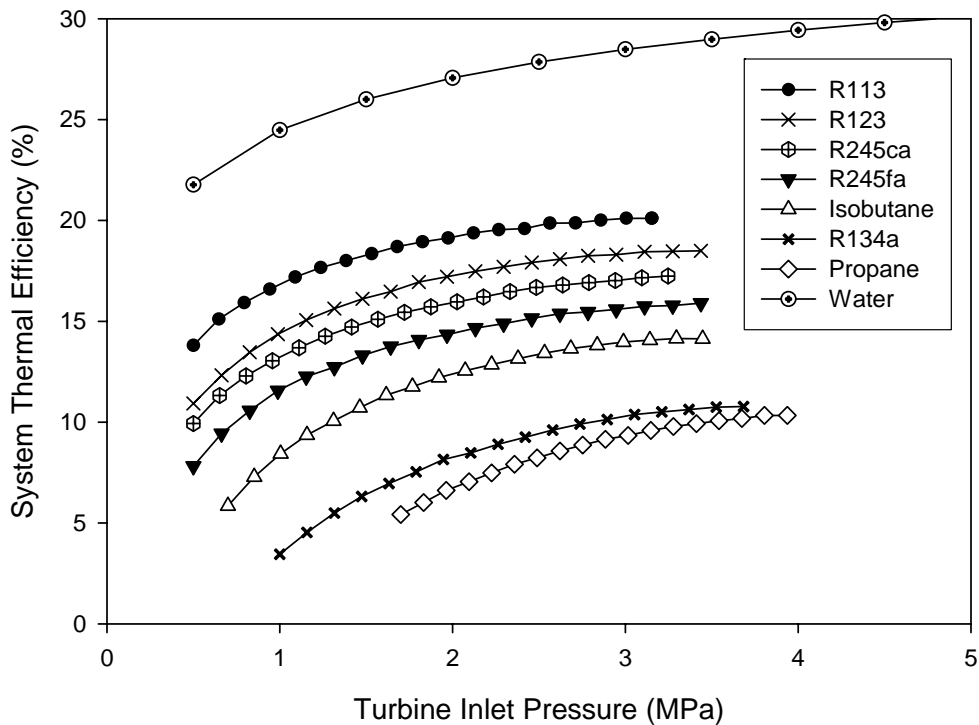


Figure 4.5. Variation of the system thermal efficiency with the turbine inlet pressure ( $T_c = 298 \text{ K}$ )

Similar to the results presented in figure 4.2, this figure shows that R113 has the best performance among the organic fluids for pressures below 3.4 MPa; R123 and R245ca present the best efficiencies for a range of pressures between 3.4 and 3.6 MPa,

while R134a presents the best efficiency for a range of pressure between 3.6 and 4.2 MPa. Water has the best thermal efficiency under the conditions analyzed in this case. The trend observed with the boiling point described in Figure 4.2 is also consistent with the results presented in figure 4.5.

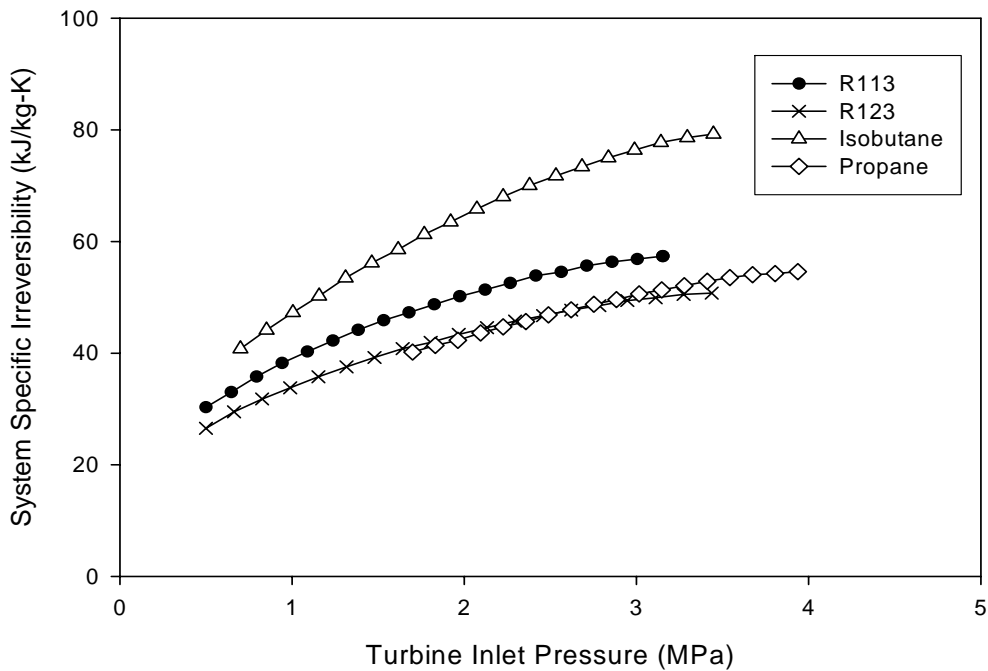


Figure 4.6. Variation of the system irreversibility with the turbine inlet pressure ( $T_c = 298$  K) for R113, R123, Propane, and Isobutane.

Figure 4.6 demonstrates the total specific irreversibility versus the turbine inlet pressure for the same conditions used to generate figure 4.5 for R113, R123, propane, and isobutane. Some of the fluids were omitted from this figure to improve its readability. From this figure, it can be observed how the irreversibility increases with the increase of the turbine pressure for all the fluids. Water has the highest irreversibility values, and they are not shown in the figure in order to be able to observe the values for the

remaining fluids. Among the organic fluids, isobutane and R134a has the highest and lowest irreversibility values, respectively. Similar to Figure 4.3, the effect of the boiling point temperature in this figure does not present a consistent trend as the ones in previous figures.

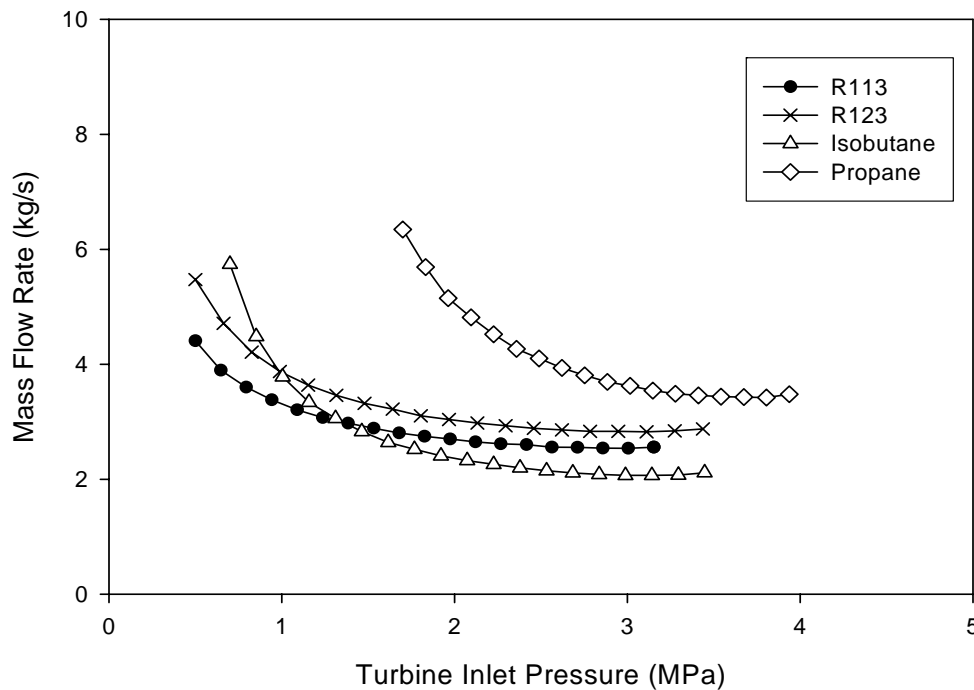


Figure 4.7. Mass flow rate needed to produce 122 kW of electric power versus turbine inlet pressure ( $T_c = 298$  K) for R113, R123, Propane and Isobutane.

The variation of the mass flow rate needed to generate the same electric power output with the turbine inlet pressure is evaluated in figure 4.7. This figure was generated using the same conditions described in figure 4.5 for a fixed electric power output of 60 kW and a generator efficiency of 82%. For all the fluids, the mass flow rate needed to produce the same electric power decreases with the increase of the turbine inlet pressure. This is due to the increase in the net work of the cycle with the increase in turbine inlet

pressure. Propane requires the highest mass flow rates among the organic working fluids, while for pressures below and above 1.5 MPa, R113 and isobutane require the lowest mass flow rates, respectively.

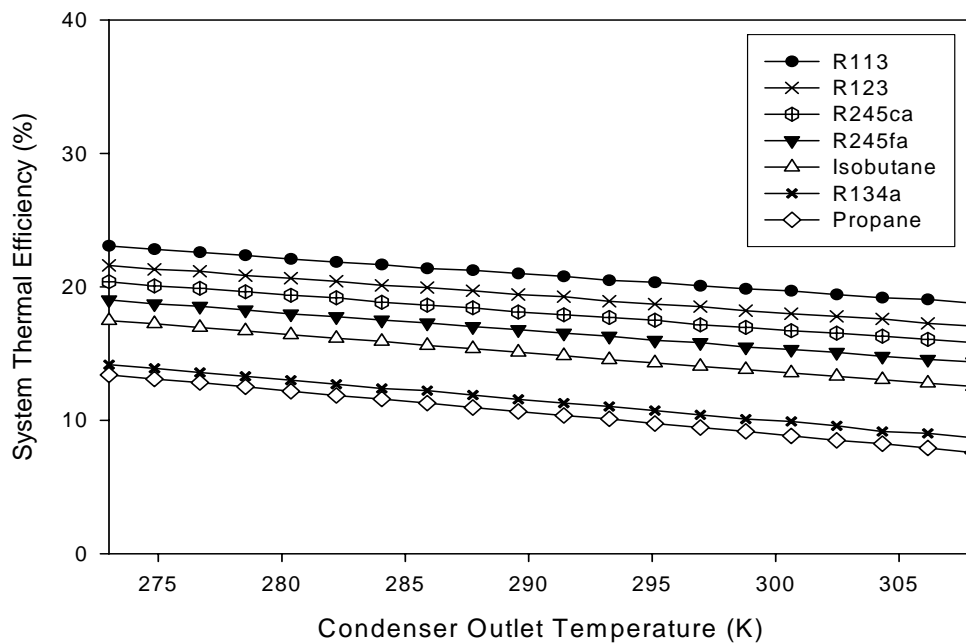


Figure 4.8. Variation of the system thermal efficiency with the condenser outlet temperature ( $P_e = 3$  MPa).

Figure 4.8 illustrates the variation of thermal efficiency with the condenser outlet temperature. This figure was generated keeping the evaporator pressure constant at 3 MPa. The isentropic efficiencies of the turbine and pump were 80% and 85%, respectively. For all the working fluids, the system thermal efficiency decreases linearly with the increase in condenser outlet temperature. The trend observed in this figure is consistent with the results shown in figures 4.2 and 4.5, where R113 and R123 have the best thermal efficiencies while propane the lowest among the organic fluids. From this

figure, the influence of the boiling point on the system thermal efficiency can be observed once again, since fluids with higher boiling point temperatures have the best thermal efficiency.

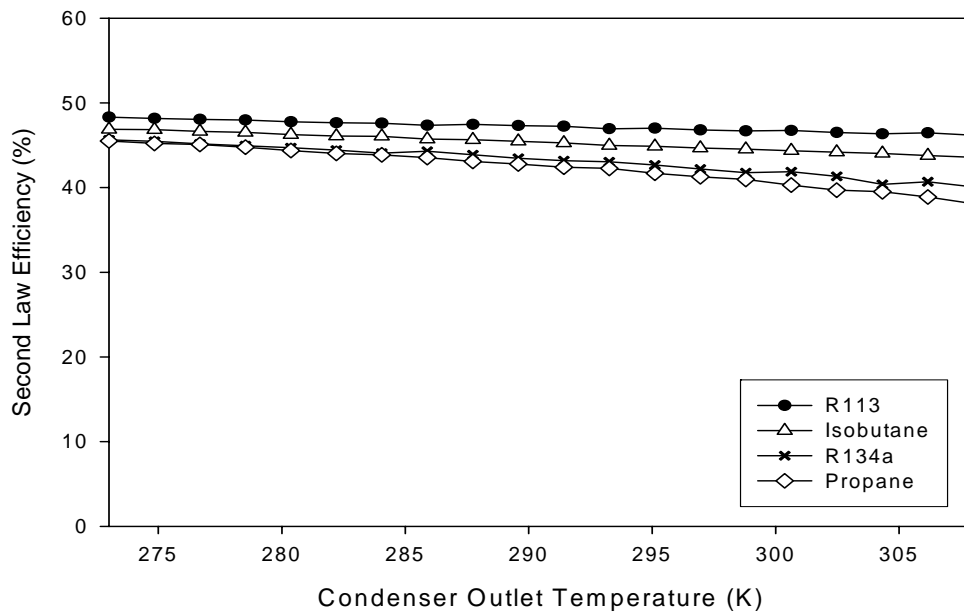


Figure 4.9. Variation of the system second law efficiency with the condenser outlet temperature ( $P_c = 3$  MPa) for R113, Isobutane, and Propane and R134a.

Figure 4.9 illustrates the variation of the system second-law efficiency with the condenser outlet temperature for R113, isobutane, and propane and R134a. Some fluids were left out of this figure in order to make it clear to read. The second-law efficiency decreases for all the fluids with the increase of the condenser outlet temperature. The results presented in Figures 4.8 and 4.9 indicate that ORC will be more beneficial in places with annual low ambient temperatures, since ORC will have higher first and second law efficiencies.

## Conclusions

This chapter presents an analysis of the performance of basic ORC to produce electric power. This analysis was based on the first and second-laws of thermodynamics, and parameters such as thermal efficiency, irreversibility, and second-law efficiency were evaluated and compared with the results for water under the same conditions. It was demonstrated that the organic fluids examined could be used to generate power using low-temperature waste heat.

Organic fluids do not need to be superheated since the cycle thermal efficiency remains approximately constant when the inlet temperature of the turbine is increased. However, using the second law analysis it can be seen that superheating the organic fluids, increases the irreversibility. Therefore, organic fluids must be operated at saturated conditions to reduce the total irreversibility of the system. The thermal efficiency of ORC increases when the condenser temperature is decreased. Therefore, using ORC in locations with low ambient temperatures will be more effective. Organic dry fluids (R113, R123, R245ca, R245fa, and isobutane) have better performance than wet fluids (R134a and Propane). This is because they do not condense after the fluid goes through the turbine as wet fluids do.



## CHAPTER 5

### ANALYSIS OF REGENERATIVE ORC

#### **Introduction**

In the previous chapter, the performance of a basic ORC was studied. Also different organic working fluids were evaluated. In order to understand the performance of ORC, the studies on just the basic cycle are not sufficient. Advancements in thermodynamics have made it possible to further explore the possibilities of improving the system performance. One of these modifications is the regenerative ORC which is a variation to basic Rankine cycle. This cycle utilizes the partially expanded steam extracted from turbine at various points to heat the condensate and feedwater on its way back to the boiler. Regenerative ORC configurations are analyzed and compared with the basic ORCs in order to determine the configuration that presents the best performance.

The finite temperature difference during the heat transfer process is the main reason for irreversibility. The regenerative cycle reduces the irreversibility by using heat input from other parts of the system.

This chapter includes the effect of the different configurations on the overall thermal efficiency of the cycle, the cycle total irreversibility, cycle second law efficiency, the mass flow rate needed to generate a certain power output, and the amount of waste heat needed to operate the cycle.

The purpose of this section is to analyze the ORC for regenerative cycle. The analysis was also carried out for reheat cycle. However the reheat cycle does not add much to the system performance as compared to the basic cycle. In fact, in some cases it was found that, basic cycle gives better performance than reheat ORCs. The need for clarity of graphs as well as the simplicity in the presentation of the results were the other reasons for the omission of reheat cycle from the analysis in this chapter. The regenerative cycle is better than the basic cycle for a conventional Rankine cycle, this chapter validates the results for organic Rankine cycle. Also effort has been made to measure exactly by what percentage the regenerative cycle outperforms the basic cycle with respect to various system parameters. This chapter as well as the preceding chapter serves as reference when both basic and regenerative cycles are analyzed and compared in the next chapter using another approach.

### **Analysis**

The outline of the procedure involved in this chapter for the analysis of ORC is given in Figure 5.1. For each of the cycle turbine inlet pressure and turbine inlet temperature is varied. Then the system variables such as thermal efficiency, irreversibility rate, second law efficiency and mass flow rate needed to generate a fixed power output are determined. For the analysis, seven working fluids are considered and are compared with water.

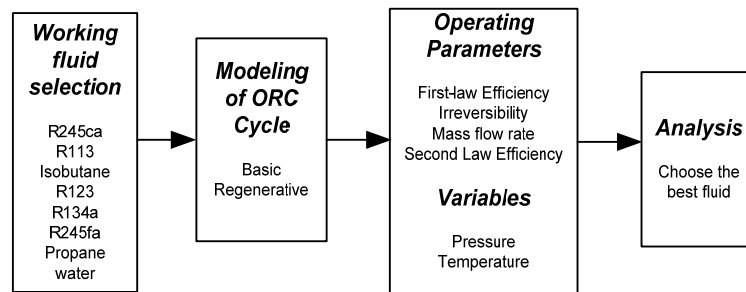
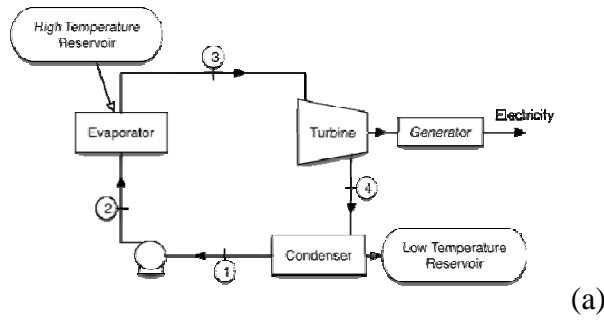


Figure 5.1. Outline of the procedure involved in the analysis of an Organic Rankine Cycle.

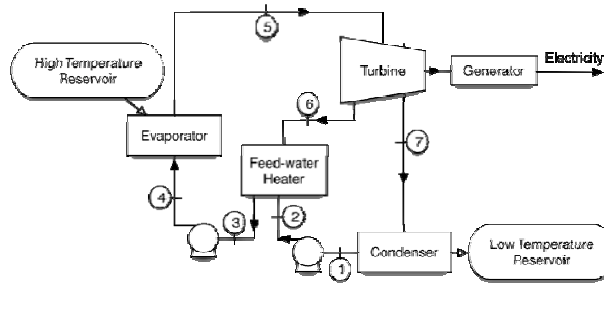
The equations used to determine the performance of the regenerative ORC configuration are presented in this chapter and are slightly different from those of the basic cycle. The equations of basic cycle have been already discussed in the previous chapter. Using the First and Second Law of Thermodynamics, the performance of an ORC can be evaluated under diverse working conditions for different organic working fluids. For all the configurations, this analysis assumes the following: 1) steady state conditions, 2) no pressure drop in the evaporator, condenser, feed-water heater, and pipes, and 3) isentropic efficiencies for the turbine and pumps.

The different configurations of an ORC for converting waste heat into useful electrical power as well as the temperature entropy diagram are illustrated in Figure 5.2.

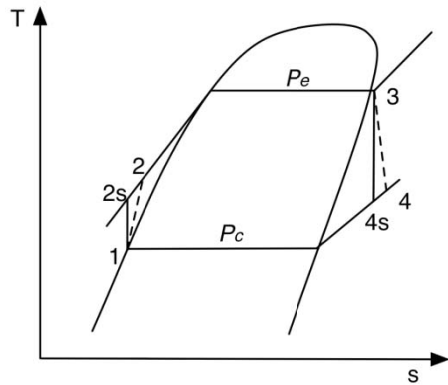
In Figure 5.2 (b), a feed-water heater is incorporated into the ORC. The vapor extracted from the turbine mixes with the feed-water exiting the pump. Ideally, the mixture leaves the heater as a saturated liquid at the heater pressure.



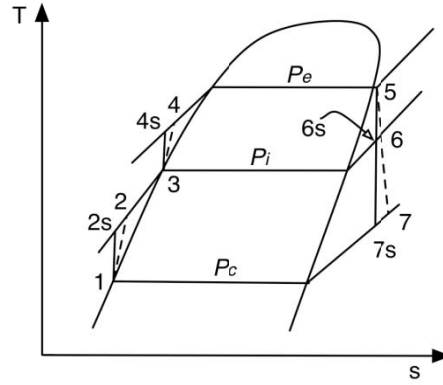
(a)



(b)



(c)



(d)

Figure 5.2. Schematic and temperature-entropy diagram corresponding to the basic (a and c) and regenerative (b and d) ORC configurations.

For the different configurations the irreversibility rate for uniform flow conditions can be expressed as,

$$\dot{I} = T_o \frac{dS}{dt} = T_o \dot{m} \left[ \sum s_{exit} - \sum s_{inlet} + \left( \frac{ds_{system}}{dt} \right) + \sum_j \frac{q_j}{T_j} \right] \quad (5.1)$$

A detailed study and equations for a basic ORC configuration can be found in Somayaji et al. [2006].

Figure 5.2(a) and (b) shows the temperature-entropy diagram corresponding to the basic and regenerative configurations.

## Regenerative ORC

### *a. Feed-water Heater*

In order to determine the fraction of the flow rate that goes into the feed-water heater and the fraction that goes into the condenser, a mass and energy balance is applied in the feed-water heater. The fraction of the flow rate that goes into the feed-water heater is given by,

$$X_1 = \frac{h_3 - h_2}{h_6 - h_2} \quad (5.2)$$

### *b. Pump: (Processes 1-2 and 3-4)*

The pump power for pump I (Process 1-2) can be expressed as

$$\dot{W}_{p,1} = \frac{\dot{W}_{p,ideal}}{\eta_p} = \frac{(1 - X_1)\dot{m}(h_1 - h_{2s})}{\eta_p} \quad (5.3)$$

and the pump power for pump II (Process 3-4) can be expressed as

$$\dot{W}_{p,2} = \frac{\dot{W}_{p,ideal}}{\eta_p} = \frac{\dot{m}(h_3 - h_{4s})}{\eta_p} \quad (5.4)$$

where  $\dot{W}_{p,ideal}$  is the ideal power of the pump,  $\dot{m}$  is the working fluid mass flow rate,  $\eta_p$  is the pump isentropic efficiency,  $h_1$  and  $h_{2s}$  are the enthalpies of the working fluid at the inlet and outlet of pump I for the ideal case, and  $h_3$  and  $h_{4s}$  are the enthalpies of the working fluid at the inlet and outlet of pump II for the ideal case.

Adding Equations (5.3) and (5.4) the total pump power can be determined as

$$\dot{W}_p = \dot{m} \left[ \frac{(1 - X_1)(h_1 - h_{2s}) + (h_3 - h_{4s})}{\eta_p} \right] \quad (5.5)$$

Using Equation (5.1), the total pump irreversibility rate is

$$\dot{i}_p = T_o \dot{m} [(1 - X_1)(s_1 - s_2) + (s_3 - s_4)] \quad (5.6)$$

where  $s_1$  and  $s_2$  are the specific entropies of the working fluid at the inlet and exit of Pump I for the actual conditions, respectively, and  $s_3$  and  $s_4$  are the specific entropies of the working fluid at the inlet and exit of Pump II for the actual conditions, respectively.

### ***c. Evaporator: (Process 4-5)***

The evaporator heat transfer rate is,

$$\dot{Q}_e = \dot{m}(h_5 - h_4) \quad (5.7)$$

where  $h_4$  and  $h_5$  are the enthalpies of the working fluid at the inlet and exit of the evaporator, respectively.

The evaporator irreversibility rate can be expressed as:

$$\dot{I}_e = T_o \dot{m} \left[ (s_5 - s_4) - \frac{(h_5 - h_4)}{T_H} \right] \quad (5.8)$$

where  $s_4$  and  $s_5$  are the specific entropies of the working fluid at the inlet and exit of the evaporator, respectively, and  $T_H$  is the temperature of the high temperature heat source.

Similarly to the other configurations, this temperature is considered to be equal to

$$T_H = T_3 + \Delta T_H$$

#### ***d. Turbine: (Processes 5-6 and 5-7)***

The turbine power for this configuration is given by:

$$\dot{W}_t = \dot{W}_{t,ideal} \eta_t = \dot{m} \eta_t [(h_5 - h_{7s}) + X_1 (h_{7s} - h_{6s})] \quad (5.9)$$

where  $W_{t,ideal}$  is the ideal power of the turbine,  $\eta_t$  is the turbine isentropic efficiency,  $h_5$  is the enthalpy of the working fluid at the inlet of the turbine, and  $h_{6s}$  and  $h_{7s}$  are the enthalpies of the working fluid at the exit of the turbine for the ideal case.

The turbine irreversibility rate can be expressed as,

$$\dot{I}_t = T_o \dot{m} [(s_7 - s_5) + X_1 (s_6 - s_7)] \quad (5.10)$$

where  $s_5$  is the specific entropy of the working fluid at the inlet of the turbine, and  $s_6$  and  $s_7$  are the specific entropies of the working fluid at the exit of the turbine for the actual conditions.

#### ***e. Condenser: (Process 7-1)***

The condenser heat rate is given by,

$$\dot{Q}_c = \dot{m} (1 - X_1) (h_1 - h_7) \quad (5.11)$$

where  $h_1$  and  $h_7$  are the enthalpies of the working fluid at the exit and inlet of the condenser, respectively. The condenser irreversibility rate is,

$$\dot{i}_c = T_o \dot{m} (1 - X_1) \left[ (s_1 - s_7) - \frac{h_1 - h_7}{T_L} \right] \quad (5.12)$$

where  $s_1$  and  $s_7$  are the specific entropies of the working fluid at the inlet and exit of the condenser, respectively, and  $T_L$  is the temperature of the low temperature reservoir. This temperature is considered to be equal to  $T_L = T_1 - \Delta T_L$

#### ***f. Cycle Efficiency***

The thermal efficiency can be determined as,

$$\eta_{cycle} = \frac{\dot{W}_t + \dot{W}_p}{\dot{Q}_e} \quad (5.13)$$

Substituting Equations (5.5), (5.7), and (5.9) into Equation (5.13), the thermal efficiency of a regenerative ORC can be expressed as

$$\eta_{cycle} = \frac{\eta_t [(h_5 - h_{7s}) + X_1 (h_{7s} - h_{6s})] + (1 - X_1) (h_1 - h_{2s}) + (h_3 - h_{4s}) \eta_p^{-1}}{(h_5 - h_4)} \quad (5.14)$$

#### ***g. Total Cycle Irreversibly***

The total irreversibility can be obtained adding Equations (5.6), (5.8), (5.10), and (5.12) as follows,

$$\dot{i}_{cycle} = \dot{m} T_o \left[ \left( -\frac{(h_5 - h_4)}{T_H} \right) - (1 - X_1) \left( \frac{h_1 - h_7}{T_L} \right) \right] \quad (5.15)$$



### *h. Second Law Efficiency*

The second law cycle efficiency for the regenerative cycle can be expressed as,

$$\eta_{II} = \frac{\dot{W}_{net}}{\dot{Q}_e \left(1 - \frac{T_L}{T_H}\right)} = \left( \frac{\eta_t [(h_5 - h_{7s}) + X_1 (h_{7s} - h_{6s})] + (1 - X_1) (h_1 - h_{2s}) + (h_3 - h_{4s}) \eta_p^{-1}}{(h_5 - h_4) \left(1 - \frac{T_L}{T_H}\right)} \right) \quad (5.16)$$

### *i. Electric Generator*

Similar to the basic ORC the total electric power generation can be determined as,

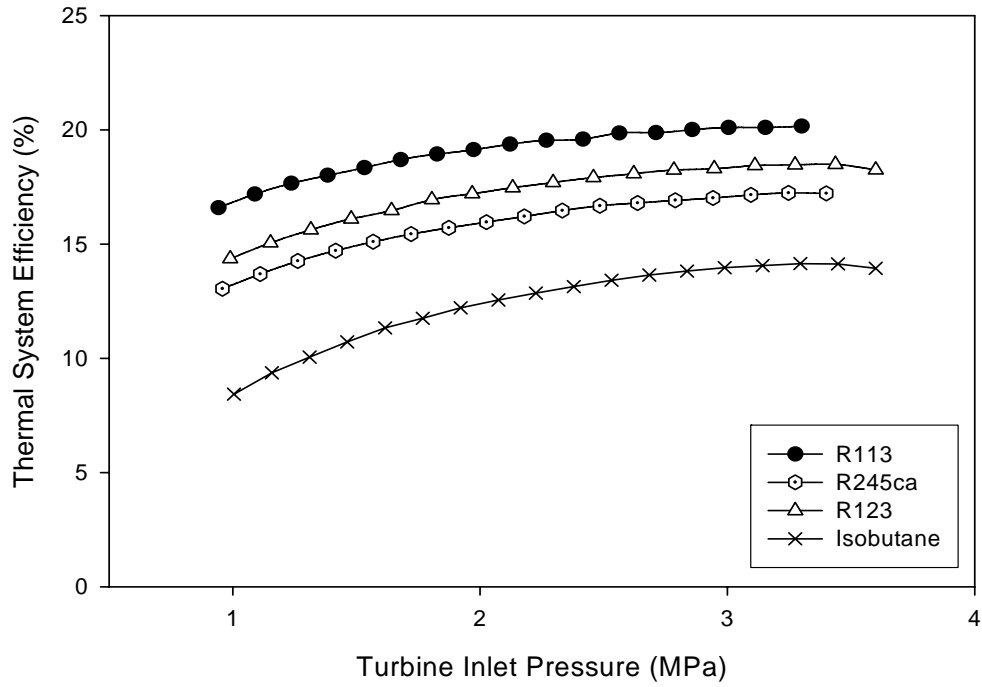
$$\dot{W}_{electric} = \dot{W}_{net} \eta_{generator} = (\dot{W}_t + \dot{W}_p) \eta_{generator} \quad (5.17)$$

Previous results showed that dry fluids have a better performance than wet fluid for basic ORC applications. Therefore, this section focuses on the use of regenerative ORC to produce electric power using only dry fluids. Four organic dry fluids, with boiling points ranging from -12°C to 48°C, were selected: R113, R245ca, R123, and isobutane.

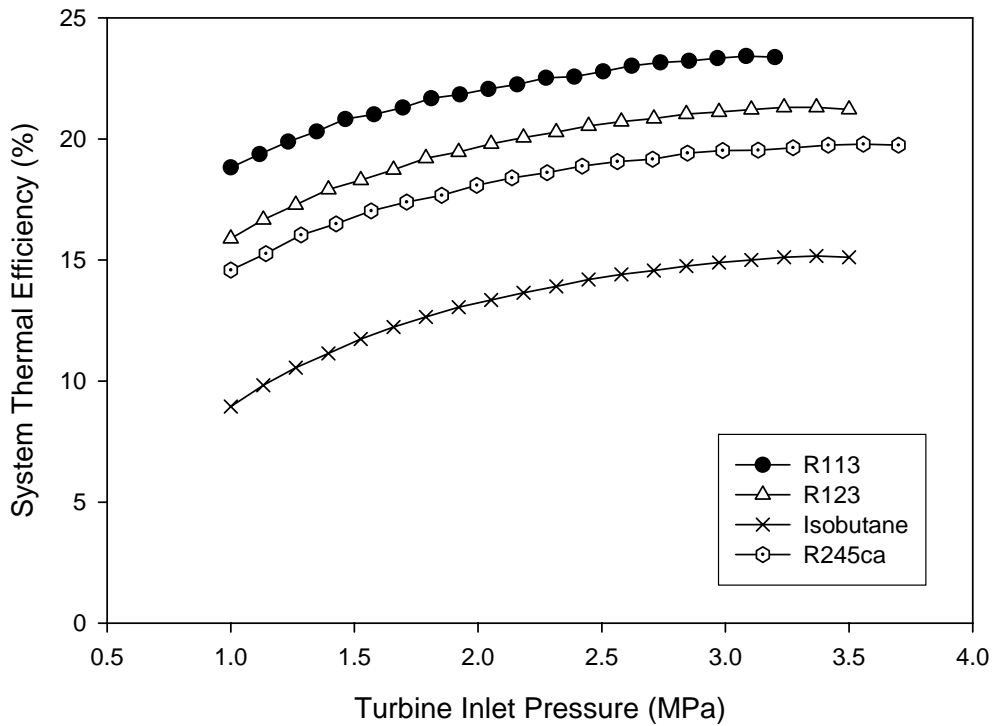
Figure 5.3 demonstrates the variation of the system thermal efficiency with the turbine inlet pressure while keeping the turbine inlet temperature at saturated conditions for the different ORC configurations (basic and regenerative). For both configurations the condenser temperature was kept constant at 298 K, while the maximum pressure used for each fluid was the critical pressure. The isentropic efficiencies of the turbine and pump were 80% and 85%, respectively, while the temperature difference was kept constant at 15 K. Figure 5.3 demonstrates that the system thermal efficiency increases

with the turbine inlet pressure, the results are consistent for all the fluids used in both configurations. This figure illustrates that for both configurations R113 has the best performance between the organic fluids, while isobutane has the worst performance. For both configurations, the fluid that shows the best thermal efficiency is R113, which has the highest boiling point among the selected fluids (47.59°C), while the fluid with the worst thermal efficiency is isobutane, which has the lowest boiling point temperature (-11.61°C). Similar trend is observed for the remaining working fluids selected in this investigation. Therefore, the above results show that the higher the boiling point temperature of the fluid the better the cycle thermal efficiency for both basic and regenerative cycle.

Comparison of the system thermal efficiency for the two cases presented in figure 5.3 is given in figure 5.4. This comparison was performed for R113 and Isobutane since they represent the best and worst cases, respectively. The regenerative ORC has better thermal efficiencies than the basic ORC for both fluids. The Regenerative ORC using R113 shows an increase of 13.4% to 16% in thermal efficiency from the lowest and highest turbine inlet pressure, respectively. On the other hand, isobutane has an increase of 6% to 8.5% for the lowest and highest pressure, respectively. These results clearly demonstrate that using regenerative ORC the system thermal efficiency of the basic ORC can be increased. It is also important to point out that the use of the regenerative ORC is not justified for all fluids from the thermal efficiency point of view, since the differences



(a)



(b)

Figure 5.3. Variation of the system thermal efficiency with the turbine inlet pressure for different ORC configurations ( $T_c = 298$  K): (a) basic and (b) regenerative

between this configuration and the basic ORC is negligible for some organic fluids. However, there are other parameters to be considered in this analysis, such as: the total irreversibility of the system, second law efficiency, and the amount of heat required to produce the same electric power.

Figure 5.5 demonstrates the variation of the system specific irreversibility with the turbine inlet pressure using R113 under the same conditions used to generate the results given in Figure 5.3. To improve the readability of the figure, R113 was the only organic fluid included. It can be observed that the total system irreversibility increases with increasing turbine inlet pressures for both configurations. A comparison between the two configurations indicates that regenerative ORC has approximately 42% less specific irreversibility than the basic ORC for the pressure range evaluated.

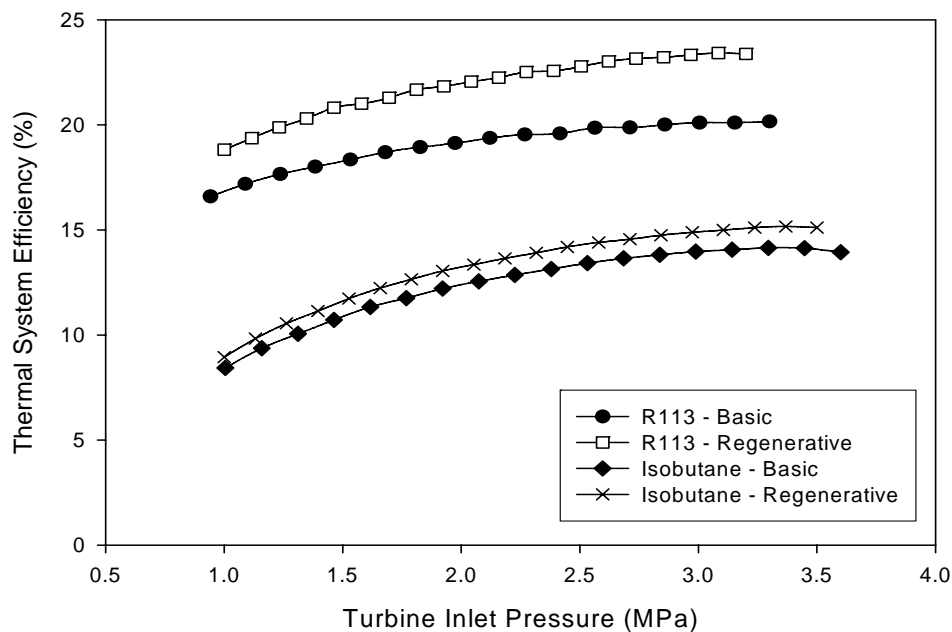


Figure 5.4. Comparison of the two ORC configurations for R113 and Isobutane ( $T_c = 298$  K)

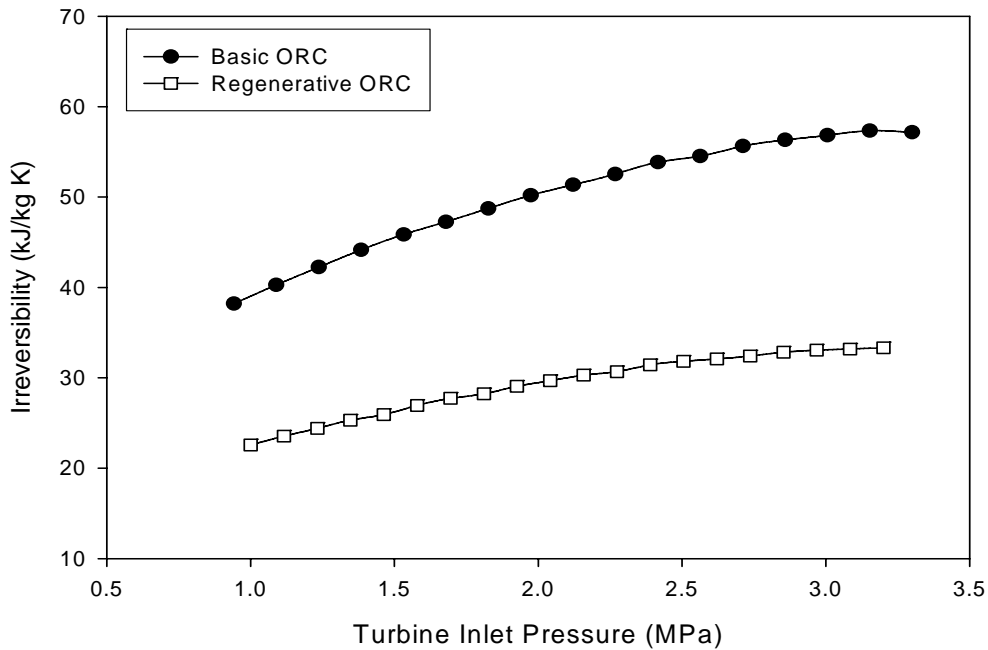


Figure 5.5. Variation of the specific system irreversibility with the turbine inlet pressure for R113 ( $T_c = 298$  K)

Figure 5.6 illustrates the variation of the system second-law efficiency with the turbine inlet temperature for R113 for both ORC configurations. For both configurations the second-law efficiency decreases with the turbine inlet temperature. The results presented in this figure agree well with the results presented in Figure 5.4, since an increment in the system irreversibility represent a decrease in the system second law efficiency. The second-law efficiencies obtained for regenerative ORC are higher than those obtained for basic ORC. For low inlet turbine temperatures, the second-law efficiencies for the regenerative ORC using R113 are approximately 12% higher than those obtained for basic ORC, while for high turbine inlet temperatures, the second-law efficiencies for regenerative ORC are approximately 17% higher than those obtained for

basic ORC. Figures 5.5 and 5.6 demonstrate the importance of performing a second law analysis.

According to the results presented in Figure 5.4 using regenerative ORC, employing R113, the thermal efficiency can be increased by approximately 15% compared with basic ORC. However, a combined first and second law analysis demonstrates that using regenerative ORC not only increases the system thermal efficiency but also reduces the system irreversibility by 42%, or increases the second law efficiency by an average of 14.5% compared with the basic ORC.

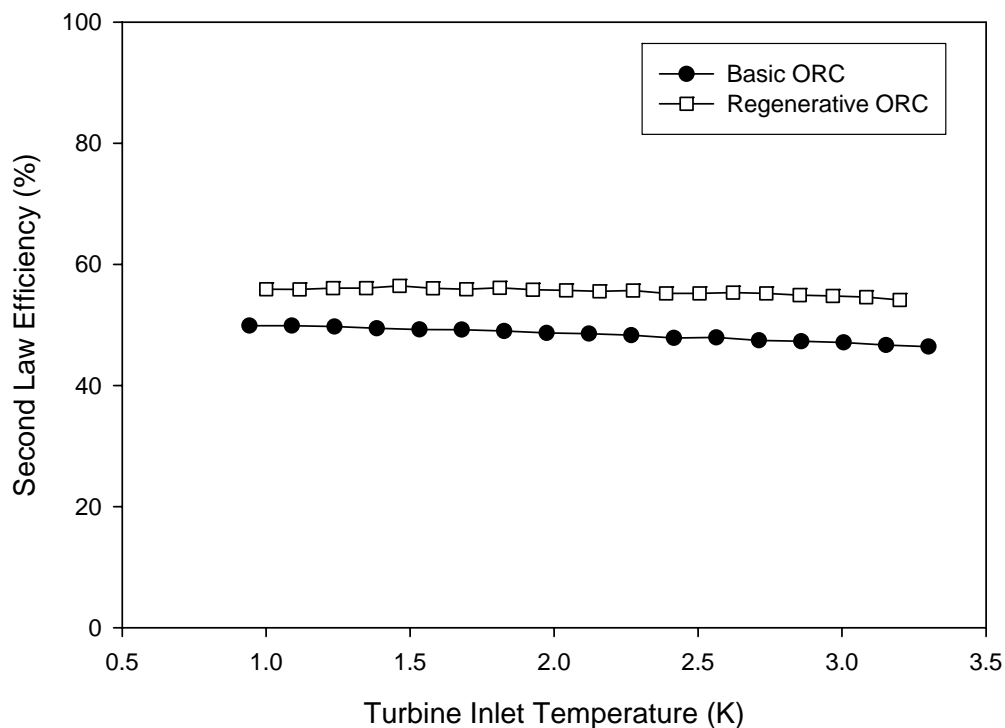


Figure 5.6. Variation of the system second law efficiency with the turbine inlet temperature for R113 ( $T_c = 298$  K)

The heat transfer rate required in the evaporator to generate the same power output with the turbine inlet pressure is evaluated in Figure 5.7. This figure was generated

using R113 for the different configurations using the same conditions described in Figure 4.2 of chapter 4 and for an electric power output of 100 kW with a typical generator efficiency of 82%. The generator efficiency is defined as the ratio of the electric power and the net power produced by the ORC. It can be seen that for R113 the heat rate needed decreases with increasing turbine inlet pressures. This is due to the decrease in the mass flow rate needed and the increase in the net work of the cycle with an increase in turbine inlet pressure. Figure 5.7 demonstrates that the regenerative ORC requires lower heat rates than the basic ORC to produce the same power. The amount of heat required for the regenerative ORC is 7.5% to 9.7% less than the heat required for a basic ORC, for the lowest and highest turbine inlet pressures, respectively. From Figures 5.4, 5.5, 5.6, and 5.7, the regenerative ORC is found to, not only increase the first and second law efficiencies, but also decrease the amount of heat required and system irreversibility to produce the same power output as compared to a basic ORC.

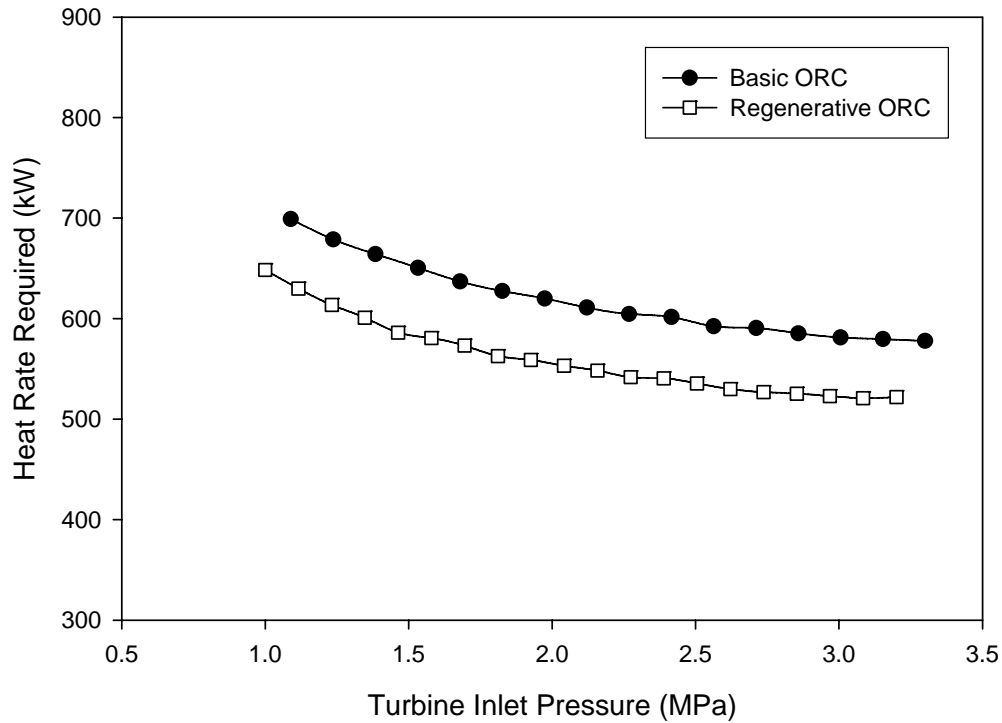


Figure 5.7. Variation of the heat transfer rate required in the evaporator to produce 100 kW of electric power with the turbine inlet pressure for R113 ( $T_c = 298$  K).

The mass flow rate needed for R113, to produce the same electric power, for the cases analyzed in Figure 5.7 is given in Figure 5.8. The required mass flow rate decreases with the increment of the turbine inlet pressure. This is due to the increase in the net work of the cycle with the increment in turbine inlet pressure. Another interesting point is that the basic configuration requires lower mass flow rates compared to the regenerative ORC. This can be explained since the basic ORC generates higher specific net works than the regenerative ORC. However, the ratio between the net work and the total heat input (thermal efficiency) is lower for this configuration than for the regenerative ORC.



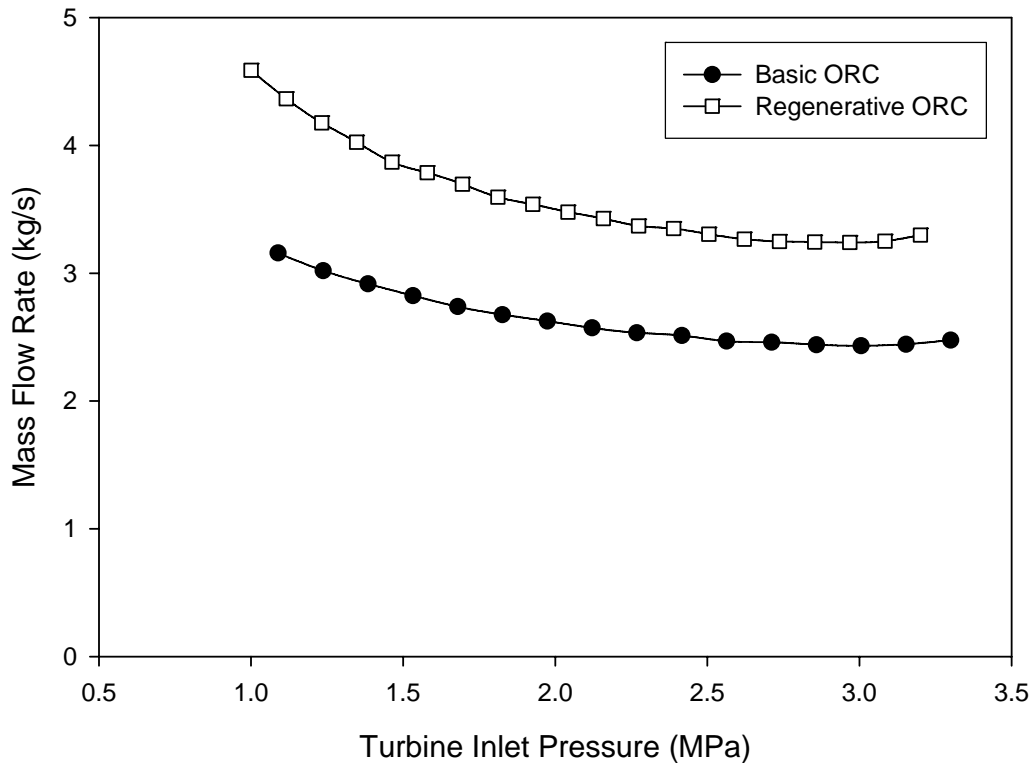


Figure 5.8. Variation of the mass flow rates required to produce 100 kW of electric power with the turbine inlet pressure for R113 ( $T_c = 298$  K).

Figure 5.9 illustrates the variation of the system thermal efficiency with the turbine inlet temperature. To generate this figure, the evaporator pressure and condenser temperature were kept constant at 2 MPa and 298 K, respectively. Similar to the previous case, the isentropic efficiencies of the turbine and pump were maintained at 80% and 85%, respectively, and the temperature differential was kept constant at 15 K for all cases. The effect of superheating the working fluid on the thermal efficiency of the cycle is seen from the figure 5.9. The temperature range for each fluid used to analyze the different configurations is from the saturation temperature to the critical temperature. Figure 5.9 illustrates that the efficiency of the cycle slightly decreases for some fluids or

remains approximately constant for others with the turbine inlet temperature for all the configurations. This reflects the fact that organic fluids do not need to be superheated to increase the cycle thermal efficiency as opposed to water where increasing the inlet turbine temperature increases the thermal efficiency. The trend observed with the boiling point described in Figure 5.4 is also consistent with the results presented in this figure. Figure 5.9 demonstrates that the regenerative ORC has the best thermal efficiency for the analyzed organic fluids. Among the three organic fluids included in this figure, R113 has the maximum efficiency for a temperature above 450 K. R123 has the best efficiencies for temperatures between 420 K and 450 K, while isobutane is the best fluid for temperatures between 375 K and 410 K. It is important to point out, how organic fluids can be used to produce power from low temperature waste heat; however, organic fluids are restricted to a small range of applicability depending on their thermodynamic characteristics.

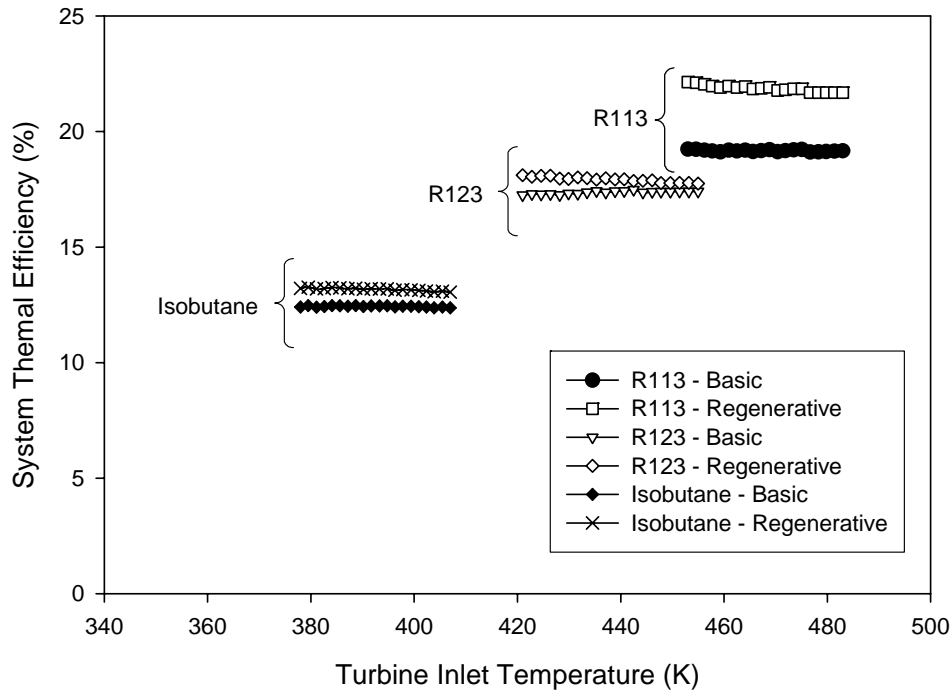


Figure 5.9. Variation of the system thermal efficiency with the turbine inlet temperature ( $P_e = 2$  MPa).

The variation of the system second law efficiency with the turbine inlet temperature using R113 for both configurations is observed in Figure 5.10. For both configurations the second law efficiency decreases with the turbine inlet temperature. The Regenerative ORC shows an increase on the second law efficiency of about 14% compared with the basic ORC. According to the results presented in Figure 5.9, the thermal efficiency is approximately constant with the turbine inlet temperature. However, a combined first and second-law analysis proves that the best case scenario is obtained when the fluid is operated at saturated conditions before the turbine since this produces the same thermal efficiency with lower irreversibility and higher second law efficiencies than operating under superheated conditions.

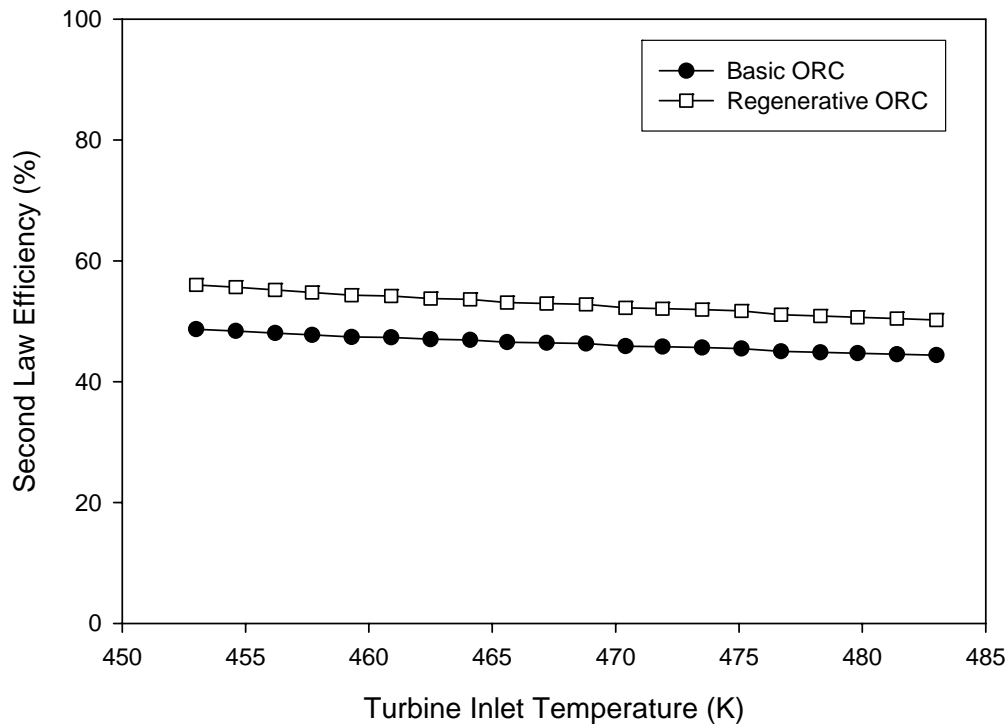


Figure 5.10. Variation of the system second law efficiency with the turbine inlet temperature for R113 ( $P_e = 2$  MPa)

### Conclusions

The regenerative ORC not only has higher first and second law efficiencies than basic ORC but also has lower irreversibility and lower heat required to produce the same power. Dry organic fluids do not need to be superheated since the cycle thermal efficiency remains approximately constant when the inlet temperature of the turbine is increased. Moreover, the second law analysis illustrated that superheating organic fluids increases the irreversibility and decreases the second law efficiency. Therefore, organic fluids should be operated at saturated conditions to reduce the total irreversibility of the system.

The influence of the boiling point temperature on the system thermal efficiency for both configurations was determined. The fluid that has the best thermal efficiency is the one that has the highest boiling point among the selected fluids (R113,  $T_{bp} = 47.59^{\circ}\text{C}$ ), while the fluid with the worst thermal efficiency has the lowest boiling point temperature (propane,  $T_{bp} = -42.09^{\circ}\text{C}$ ). Therefore, the higher the boiling point temperature of the organic fluid, the better the thermal efficiency that will be achieved by the ORC.

For the different scenarios analyzed in this investigation, ORCs using R113 give the best thermal efficiency while those using propane show the worst efficiencies. However, some organic fluids show better performance within a range of temperature. Therefore, designers have to closely monitor the operating conditions to select the right organic fluid.

## CHAPTER 6

### EXERGY ANALYSIS OF ORC

#### **Introduction**

Traditional first-law analysis, based upon performance characteristics coupled with energy balances, usually leads to the correct conclusions. However, many times it is not possible to predict the reason for a particular system behavior just with the first law analysis. This is because the first law embodies no distinction between work and heat, no provision for quantifying the quality of energy. These limitations are not a serious drawback when dealing with familiar systems. For these, one can develop an intuitive understanding of the different parametric influences on system performance. However, when analyzing novel and complex thermal systems, such an understanding should be complemented by a more rigorous quantitative method. Second-law analysis, or exergy analysis, provides such a tool. Second-law analysis is no substitute for first-law analysis, but rather a supplement.

ORCs are usually defined by the type of processes involved in the system and how the different components of the system are connected. Also, many times, valid conclusions cannot be drawn based only on the results of first law of thermodynamics. The thermodynamic analysis of such systems requires combined application of both laws of thermodynamics and demands the exergy approach. The Exergy-topological method is the combination of the exergy flow graph and the different steps.

involved in arriving at that graph. Bejan [2006] reported that exergy is the maximum useful work delivered to an external user as the stream reaches the restricted dead state. Thermodynamics tells us that different kinds of energy are not equal. Mechanical and electrical energy are converted ultimately to one another, less the dissipative energy of friction and electrical resistance. The less valuable kinds of energy, such as heat, cannot be completely converted to other forms at all times. Thus, the concept of available energy, or exergy, is introduced and described as the part of thermal energy which can be completely converted to shaft work. In other words, the exergy of a system is the maximum available work to be obtained from a system at equilibrium via a reversible process (Spurrier 1990).

The evaluation of Organic Rankine Cycles (ORCs) cannot be limited to the application of the conservation of mass and conservation of energy. These two principles can be used to obtain the performance of ORCs, but an exergy analysis is needed to determine the irreversibility present in the various components and the losses associated with those components. This chapter presents an exergy analysis of the overall performance of ORCs using the exergy graph methodology and the exergy wheel calculations. The working fluids used in ORC are organic substances which have a low boiling point and a low latent heat for using low-grade waste heat sources. For this analysis R113, which is a dry fluid, was selected as the working fluid since it has been shown to be a good candidate for ORC applications. Using the exergy graph methodology, parameters like degree of thermodynamic perfection, exergy efficiency, and coefficient of influence are found and the effect of each component on the overall

system is studied. In addition, using the first and second laws of thermodynamics, an exergy flow wheel is produced from which the losses involved with the components are found.

The main purpose of exergy analysis is to determine the component in a cycle, that has the most influence on the system performance. The exergy analyses techniques also help in better understanding the energy and exergy transactions associated with any component of a system or the whole system. This in turn will help in evaluating losses in different components and the cycle. Even though the topological method is not a new concept, this technique has been applied only on very few systems, for example air refrigerator. This method has never been used on an Organic Rankine Cycle.

### **Analysis**

This section presents a methodology to perform an exergy analysis of Organic Rankine Cycles. The methodology is called the topological method (*or the exergy graph method*). A flowchart with the different steps involved to apply the topological methodology is presented in Figure 6.1. In addition, an exergy map of the entire process is represented using the exergy wheel diagram.

#### **Network Topological method (or the exergy graph method)**

Network topology is the study of the arrangement or mapping of elements (links and nodes) of a network, especially the physical and logical interconnections between the nodes. In this chapter, the topological method is employed only by graphical mapping of nodes, which in itself is nothing but graph theory.



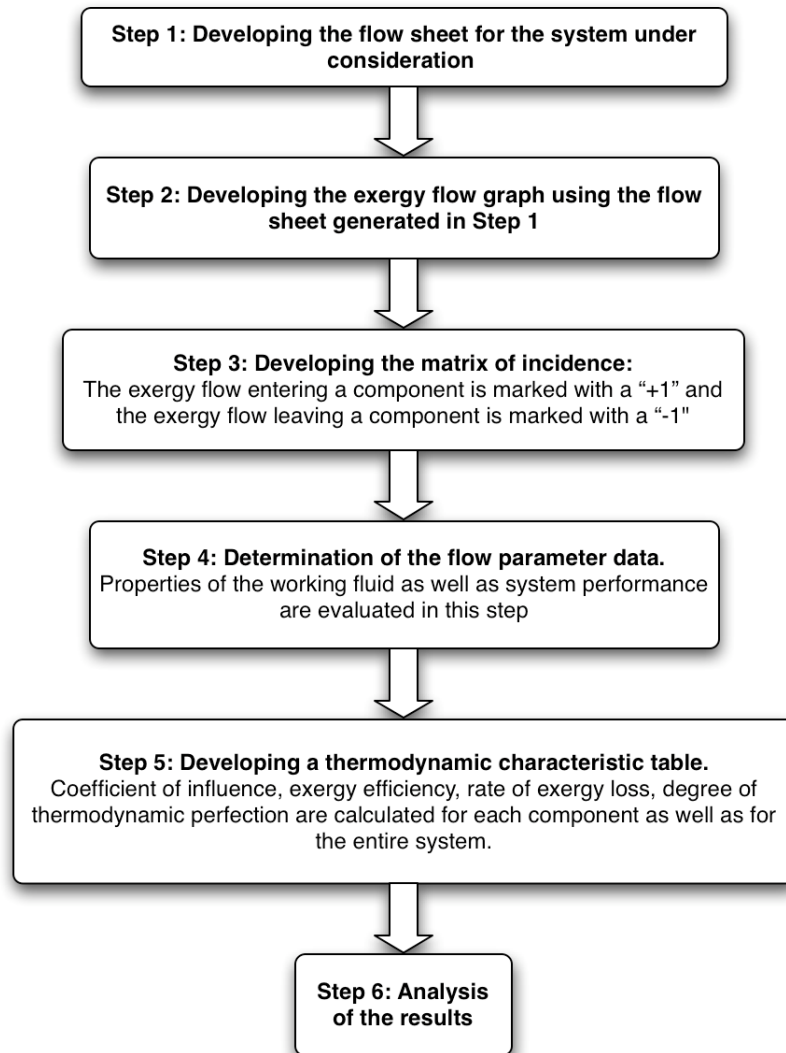


Figure 6.1. Flow chart of the network topological method adapted from Nikulshin et al. [2002, 2006]

The structure of the exergy flow graph and the structure of the modeling system are uniquely described by a matrix known as the matrix of incidence (Nikulshin and Nikulshina, 2002). The basis for the matrix is the flow sheet of the system under consideration. The elements of the exergy flow graph matrix of incidence are:

0: where the  $j^{th}$  flow and  $i^{th}$  element are not tied.

+1: where the  $j^{th}$  flow entering the  $i^{th}$  element.

-1: where the  $j^{th}$  flow leaves the  $i^{th}$  element.

The exergy loss graph is particularly useful for determining exergy losses in any element of the system or the system as a whole. From the thermodynamic point of view the value of exergy losses in any element indicates the importance of the element and provides possible ways to improve the overall system performance. In the analysis of an ORC, the calculation of exergy fluxes for different types of elements is very important to evaluate the overall performance of the cycle. The important parameters that can be determined using the exergy graph method are discussed as following,

### *Degree of thermodynamic perfection*

The degree of thermodynamic perfection of element  $i$  is the ratio of the exergy leaving the element,  $E_i^{out}$ , to the exergy flow into the element,  $E_i^{in}$ . It can be defined as (Nikulshin et al., 2006)

$$v_i = \frac{E_i^{out}}{E_i^{in}} = 1 - \frac{\xi_i}{E_i^{in}} \quad (6.1)$$

where  $\xi_i$  is the exergy loss associated with element  $i$ .

The exergy loss associated with element  $i$  can be determined as

$$\xi_i = E_i^{in} - E_i^{out} \quad (6.2)$$

The overall exergy loss of the system is the sum of the exergy loss associated with all the elements of the system:

$$\xi_{total} = \sum_{i=1}^n \xi_i \quad (6.3)$$

The degree of thermodynamic perfection of the system can be defined as:

$$v_{total} = \frac{E_{total}^{out}}{E_{total}^{in}} \quad (6.4)$$

### Exergy efficiency

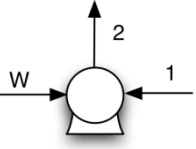
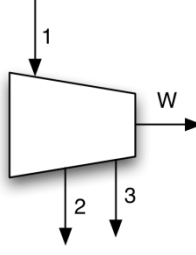
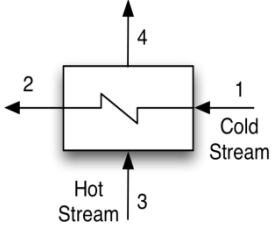
The exergy efficiency of element  $i$  is defined as the ratio of used exergy of element  $i$ ,  $E_i^u$ , to the available exergy for the same element,  $E_i^a$ . It can be determined as

[Bejan et al., 2006]

$$\eta_{exergy}^i = \frac{E_i^u}{E_i^a} \quad (6.5)$$

The available and used exergy for various components can be determined using the equations presented in Table 6.1.

Table 6.1. Exergy rates associated with the different components of an ORC [Bejan et al., 1996a)

Component	Pump	Turbine	Heat Exchanger
Schematic			
Used Exergy ( $E_i^u$ )	$E_2 - E_1$	$W$	$E_2 - E_1$
Available Exergy ( $E_i^a$ )	$W$	$E_1 - E_2 - E_3$	$E_3 - E_4$

The overall system exergy efficiency is the ratio of the total system exergy used to the total available exergy of the system. It can be determined as:

$$\eta_{\text{exergy,total}} = \frac{E_{\text{total}}^u}{E_{\text{total}}^a} \quad (6.6)$$

### ***Influence coefficient***

The influence coefficient of element  $i$  is defined as the ratio of the exergy available for element  $i$  to the total available exergy of the system,  $E_{\text{total}}^a$ . The influence coefficient is given by (Nikulshin et al., 2006)

$$\beta_i = \frac{E_i^a}{E_{\text{total}}^a} \quad (6.7)$$

This parameter gives the influence of any element on the total system performance.

One advantage of exergetic analysis is that the method makes the estimation of the flux and balance of energy and exergy for every element of the system. One of the most effective methods of thermodynamic analysis and optimization is to merge the method of exergetic analysis with the mathematical method of graph theory, commonly known as exergy-topological method.

### **The different steps**

The different steps involved in the exergy-graph method are:

*Step 1: Developing the flow sheet for the system*

Development of the flow sheet involves extensive work with regard to the different components that make up the system. This step also involves the analysis of

different components, which are inter-related to each other, as well as finding information about the operation of components when they are connected.

*Step 2: Developing the exergy-flow graph using the flow sheet generated in Step 1.*

The development of the exergy-flow graph involves a detailed study of the processes involved in the system. The elements present in the system differ from each other. Each element used in the system serves a particular purpose and has its own working principles. This step makes sure that the thermal form of exergy, which flows into and out of various elements, is properly accounted for. The exergy flow diagram is schematic in nature and shows the exergy entering and leaving various elements.

*Step 3: Developing the matrix of incidence*

The data from the exergy flow graph is used to develop the matrix of incidence. In this matrix, the number of rows corresponds to the number of elements in the system, while the number of columns corresponds to the number of flows involved in the entire system. The incidence matrix is very useful, especially for very complex systems with a large number of elements. Using the matrix, different parameters such as degree of thermodynamic perfection, influence coefficient, and exergy efficiency can be estimated. These parameters help in predicting a system's behavior as well as in analyzing the contribution of different components to the system.

*Step 4: Flow parameter data*

This step involves the calculation of the organic working fluid properties like specific enthalpy, specific entropy, mass flow rate, specific exergy, and exergy flow rate for different temperatures and pressures. The performance of the system is calculated

using the obtained flow parameter data. Parameters such as turbine and pump powers, evaporator and condenser heat rates, mass flow rate of the organic working fluid, mass flow rate of the condensing water, as well as the mass flow rate of the hot gases used in the evaporator are calculated using the flow parameter data.

#### *Step 5: Thermodynamic characteristic table*

Thermodynamic characteristic table is obtained using the data obtained in *Steps 3 and step 4*. The coefficient of influence, exergy efficiency, rate of exergy loss, degree of thermodynamic perfection, and the used and available exergy are calculated for each component as well as the entire system.

#### *Step 6: Analysis*

The final step involves the complete analysis of the results obtained in previous steps. The main criterion of the analysis is to correctly interpret the results and derive useful conclusions from the results. Also, the results of the analysis usually lead to further improvement in the system set up and may provide useful information that can be used beyond the thermodynamic aspect of the system, such as in economics.

### **Exergy Wheel Diagram**

Exergy wheel diagram is an effective method of studying the exergy losses in a system. It allows to easily observe the component-by-component contribution to the destruction of exergy. The exergy wheel diagram presented in this chapter is similar to the one proposed by Bejan et al., (2006) with the only difference being that, the approach used by Bejan uses the flow availability instead of heat supplied and rejected in the

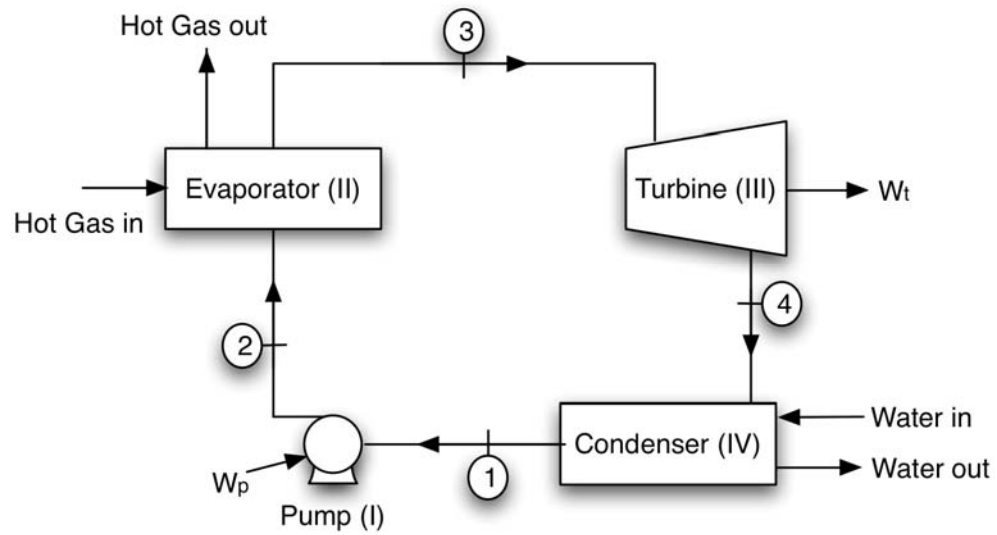
condenser. Using the results obtained from the topological methodology, the exergy wheel diagram is created.

## Results

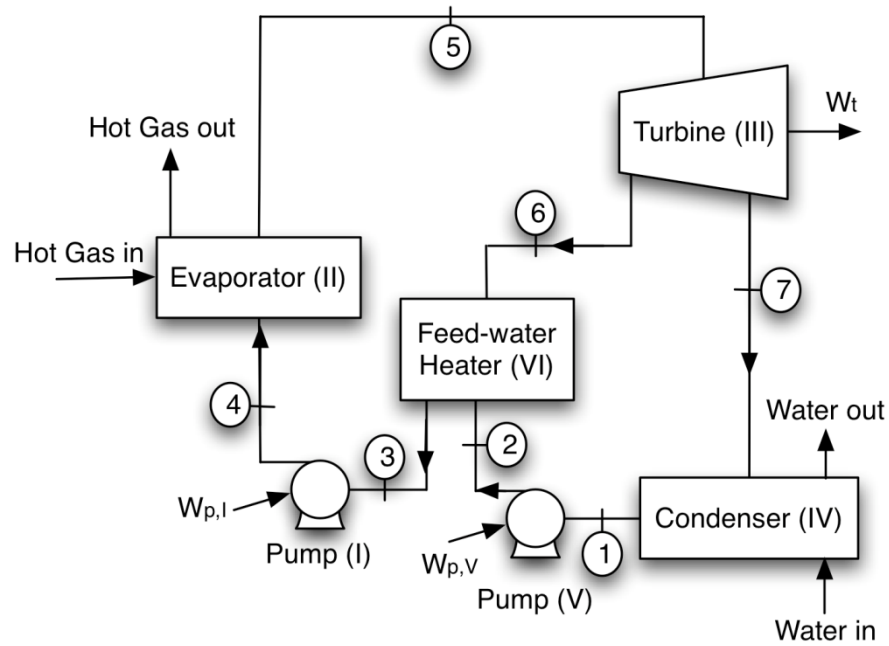
The exergy-graph method and the exergy wheel diagram are applied to two different ORC configurations namely, basic and regenerative. For the purpose of this study R113, which has been proved to be a good candidate for ORC applications [Mago et al., 2006 (a), (b)], was selected.

To apply the methodology, the following system conditions are used: 1) The evaporator pressure and condenser temperature were 2.5 MPa and 298 K, respectively. 2) The isentropic efficiencies of the turbine and pump were 80% and 85%, respectively. 3) The ORC receives heat from a heat source at a rate of 254 kW. 4) The heat required in the evaporator is provided by a steady stream of hot gases initially at 1000K and 0.1 MPa pressure. 5) The hot gases exhaust at a temperature of 450K to the ambient atmosphere, which is at 298K and 0.1MPa. 6) The mean specific heat at constant pressure for the hot gases was assumed as 1.1 kJ/kg K. 7) For the regenerative ORC calculations, an intermediate pressure of 1 MPa was assumed. 8) Steady state conditions 9) No pressure drops in the evaporator and condenser 10) Isentropic efficiencies for the turbine and pump.

A schematic of basic and regenerative ORCs for converting waste heat into useful power is shown in Figure 6.2. As observed in Figure 6.2(a) there are four different processes: Process 1-2 (pumping process), Process 2-3 (constant-pressure heat addition), Process 3-4 (expansion process), and Process 4-1 (constant-pressure heat rejection). For the regenerative cycle, Figure 6.2(b), a feed-water heater is incorporated into the ORC.



(a)



(b)

Figure 6.2. Simple flow sheet diagram: (a) basic ORC and (b) regenerative ORC [Step 1]



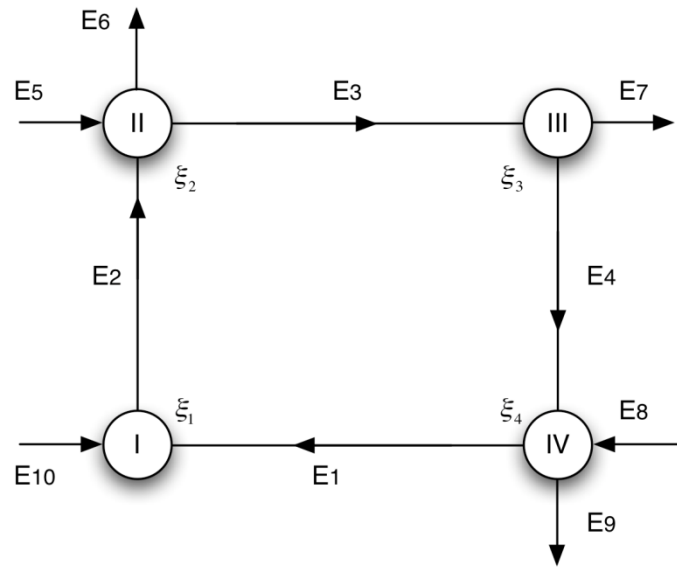
The vapor extracted from the turbine mixes with the feed-water exiting the pump. Ideally, the mixture leaves the heater as a saturated liquid at the heater pressure.

### **Application of the Exergy Graph Methodology**

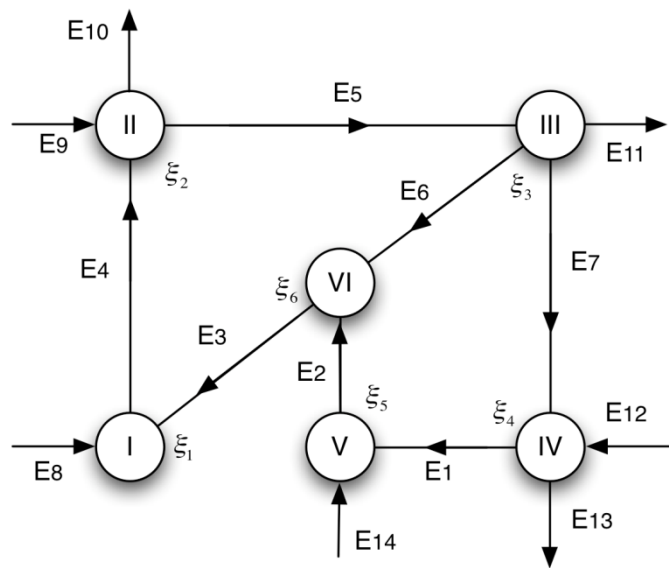
Step 1: The first step in the exergy graph methodology is to develop the flow sheet for different systems under consideration. The flow sheets are presented in figure 6.2 for both basic and regenerative configurations. Each element as well as each flow are identified with numbers. The numbering of different components and flows is useful in step 2 of this methodology.

Step 2: The exergy flow graph is created using the flow sheet generated in step 1. Figure 6.3 shows the exergy flow graph for the two ORCs configurations presented in figure 6.2. The different circles represent elements and the arrows entering and leaving the elements represent the exergy flow. Once the exergy flow graph has been created, the corresponding matrix of incidence can be constructed.

Step 3: This step involves creating the matrix of incidence for the evaluated system. Table 6.2 gives the matrix of incidence for the basic ORC corresponding to the exergy flow graph shown in Figure 6.3(a) while Table 6.3 gives the matrix of incidence for the regenerative ORC corresponding to the exergy flow graph shown in Figure 6.3(b). In the matrix of incidence, the different components which are connected are easily identified. The exergy flow entering a component from another is marked with a “+1” and the exergy flow leaving the component is marked with a “-1”.



(a)



(b)

Figure 6.3. Exergy Flow Graph for the ORC presented in Figure 6.2: (a) basic and (b) regenerative [Step 2]

Table 6.2. Matrix of incidence corresponding to the exergy flow graph for basic cycle [Step 3]

Flow	Element			
	I	II	III	IV
1	+1	0	0	-1
2	-1	0	0	0
3	0	-1	+1	0
4	0	0	-1	+1
5	0	+1	0	0
6	0	-1	0	0
7	0	0	-1	0
8	0	0	0	+1
9	0	0	0	-1
10	+1	0	0	0

Table 6.3. Matrix of incidence corresponding to the exergy flow graph for regenerative cycle [Step 3]

Flow	Element					
	I	II	III	IV	V	VI
1	0	0	0	-1	+1	0
2	0	0	0	0	-1	+1
3	+1	0	0	0	0	-1
4	-1	+1	0	0	0	0
5	0	-1	+1	0	0	0
6	0	0	-1	0	0	+1
7	0	0	-1	+1	0	0
8	+1	0	0	0	0	0
9	0	+1	0	0	0	0
10	0	-1	0	0	0	0
11	0	0	-1	0	0	0
12	0	0	0	+1	0	0
13	0	0	0	-1	0	0
14	0	0	0	0	+1	0

Step 4: In step 4, the flow parameter data for the cycle is determined. Table 6.4 shows the flow parameter data for the basic ORC while Table 6.5 for the regenerative ORC. Both tables include the following parameters, pressure, temperature, specific enthalpy, specific entropy, specific exergy, and exergy rate associated with each of the components. The data for the flow parameter table were obtained using software called

REFPROP (NIST). Using the information provided in Tables 6.4 and 6.5, the boiler heat rate, the condenser heat removal rate, the organic fluid mass flow rate, the pump power, and the turbine power can be determined. All the values are tabulated in Table 6.6 and 6.7 for basic ORC and regenerative ORC, respectively.

Table 6.4. Flow parameters of the evaluated basic ORC [Step 4]

<i>Point</i>	<i>T (°C)</i>	<i>P (MPa)</i>	<i>h (kJ/kg)</i>	<i>s (kJ/kg K)</i>	<i>E (kJ/kg)</i>	<i>E (kW)</i>
1	25	0.044831	222.67	1.0793	0	0.00
2	25.75	2.5	224.39	1.0799	1.533	1.62
3	193.52	2.5	464.23	1.6776	63.156	66.89
4	67.68	0.044831	415.21	1.7121	3.673	3.89
5	300	0.1	-	-	88.186	165.55
6	177	0.1	-	-	32.095	60.25
7	-	-	-	-	49.024	51.92
8	25	-	-	-	0	0.00
9	35	-	-	-	0.684	3.34
10	-	-	-	-	1.72	1.83

Table 6.5. Flow parameters of the evaluated regenerative ORC [Step 4]

<i>Point</i>	<i>T (°C)</i>	<i>P (MPa)</i>	<i>h (kJ/kg)</i>	<i>s (kJ/kg K)</i>	<i>E (kJ/kg)</i>	<i>E (kW)</i>
1	25	0.044831	222.67	1.0793	0	0.00
2	25.29	1	223.27	1.0793	0.575	0.59
3	139.26	1	335.5	1.3965	18.243	36.34
4	140.63	2.5	336.72	1.3965	19.450	38.74
5	193.52	2.5	464.23	1.6776	63.156	125.81
6	152.87	1	454.09	1.6836	51.237	49.63
7	85.09	0.044831	415.21	1.7127	3.6731	3.76
8	-	-	-	-	1.220	2.43
9	300	-	-	-	88.187	165.55
10	177	-	-	-	32.096	60.25
11	-	-	-	-	30.116	59.99
12	25	0.1	-	-	0	0
13	35	0.1	-	-	0.684	3.226
14	-	-	-	-	0.308	0.614

Table 6.6. Performance parameters of the evaluated basic ORC [*Step 4*]

<i>Boiler Heat Rate (kW)</i>	254.00
<i>Condenser Heat Rejection (kW)</i>	203.91
<i>Turbine Power (kW)</i>	51.92
<i>Pump Power (kW)</i>	1.83
<i>Net Power (kW)</i>	50.09
<i>Thermal Efficiency (%)</i>	19.72
<i>Mass Flow Rate (Organic Fluid) (kg/s)</i>	1.06
<i>Mass Flow Rate (Water) (kg/s)</i>	4.88
<i>Mass Flow Rate (Gas) (kg/s)</i>	1.88

Table 6.7. Performance parameters of the evaluated regenerative ORC [*Step 4*]

<i>Boiler Heat Rate (kW)</i>	254.00
<i>Condenser Heat Rejection (kW)</i>	197.05
<i>Turbine Power (kW)</i>	59.99
<i>Pump Power (kW)</i>	3.04
<i>Net Power (kW)</i>	56.95
<i>Thermal Efficiency (%)</i>	22.42
<i>Mass Flow Rate (Organic Fluid) (kg/s)</i>	1.99
<i>Mass Flow Rate (Water) (kg/s)</i>	4.71
<i>Mass Flow Rate (Gas) (kg/s)</i>	1.88

Step 5: In step 5, the calculations to determine the thermodynamic characteristics of the evaluated system are performed. Tables 6.8 and 6.9 show the thermodynamic characteristics of the analyzed basic and regenerative ORCs, respectively. Tables 6.8 and 6.9 include parameters such as exergy leaving and entering each component, the exergy loss associated with each component, used and available exergy of each component, exergy efficiency, degree of thermodynamic perfection, and coefficient of influence for each component. Also, the exergy loss, degree of thermodynamic perfection, and exergy efficiency for the entire system is presented.

Table 6.8. Thermodynamic characteristics of the evaluated basic ORC [Step 5]

<i>Element</i>	$E_i^{in}$ (kW)	$E_i^{out}$ (kW)	$\xi_i$ (kW)	$E_i^u$ (kW)	$E_i^a$ (kW)	$v_i$ (%)	$\beta_i$ (%)	$\eta_{exergy}^i$ (%)
<i>Pump (I)</i>	1.8	1.6	0.2	1.6	1.8	88.6	1.1	88.6
<i>Evaporator (II)</i>	167.2	127.1	40.0	65.3	105.3	76.1	63.6	62.0
<i>Turbine (III)</i>	66.9	55.8	11.1	51.9	63.0	83.4	38.1	82.4
<i>Condenser (IV)</i>	3.9	3.3	0.6	3.3	3.9	85.8	2.3	85.8
<i>Total System</i>	167.4	115.5	51.9	51.9	165.6	69.0	-	31.4

Table 6.9. Thermodynamic characteristics of the evaluated regenerative ORC [Step 5]

<i>Element</i>	$E_i^{in}$ (kW)	$E_i^{out}$ (kW)	$\xi_i$ (kW)	$E_i^u$ (kW)	$E_i^a$ (kW)	$v_i$ (%)	$\beta_i$ (%)	$\eta_{exergy}^i$ (%)
<i>Pump (I)</i>	38.77	38.74	0.03	2.40	2.43	99.9	1.5	98.9
<i>Evaporator (II)</i>	204.3	186.1	18.2	87.1	105.3	91.1	63.	82.7
<i>Turbine (III)</i>	125.8	113.4	12.4	60.0	72.4	90.1	43.	82.8
<i>Condenser (IV)</i>	3.8	3.2	0.5	3.2	3.8	85.8	2.3	85.8
<i>Pump (V)</i>	0.61	0.59	0.03	0.59	0.61	95.8	0.4	95.8
<i>Feed water Heater (VI)</i>	50.2	36.3	13.9	36.3	50.2	72.4	30.	72.4
<i>Total System</i>	168.6	123.5	45.1	60.0	165.6	73.2	-	36.2

Step 6: The results from table 6.8 indicate that the evaporator is the component that has the highest exergy losses (40kW). Also, it is the component with the lowest second law efficiency (62%). The exergy loss in the evaporator is mainly due to the irreversibility associated with heat transfer and the exergy loss associated with the hot gas stream. For this particular case, the exergy loss rate is about 36% of the initial exergy of the source fluid. The high exergy loss also causes a decrease in the degree of thermodynamic perfection, which shows its lowest value in the evaporator. On the other hand, the evaporator is the component with the highest influence coefficient, which reflects the fact

that the evaporator is the critical component of the evaluated basic ORC. The second component that has more influence on the ORC performance is the turbine. The turbine shows the second highest coefficient of influence (38%). However, the degree of thermodynamic perfection and exergy efficiency are higher for the turbine compared to the evaporator.

The total system exergy loss is 51.9 kW; the degree of thermodynamic perfection is 69%; while the thermal and exergy efficiencies are 19.72% and 31.4%, respectively. The overall system degree of thermodynamic perfection as well as the system exergy efficiency are lower than the same parameters for each individual component.

From Table 6.9, it can be observed that the highest exergy loss still occurs in the evaporator (18kW). However exergy loss is reduced by 55% as compared with the basic ORC (40kW). This reduction in the exergy loss corresponds to an improvement in the exergy efficiency from 62% (*for a basic ORC*) to 82.7% (*for a regenerative ORC*). The increase is due to the fact that the exergy used in the evaporator is more for a regenerative cycle compared to the basic cycle. The reduction in the exergy loss also causes an increase in the degree of thermodynamic perfection from 76.1% (basic) to 91.1% (regenerative). Similar to the basic ORC, the evaporator is the component with the highest coefficient of influence (63.6%) followed by the turbine (43.7%). The total system exergy loss is reduced by 13% (45.1 kW) compared with basic ORC. For the analyzed case, the degree of thermodynamic perfection is 73.2%; while the thermal and exergy efficiencies are 22.4% and 36.2%, respectively. Both efficiencies are higher compared with the efficiencies obtained for basic ORC.

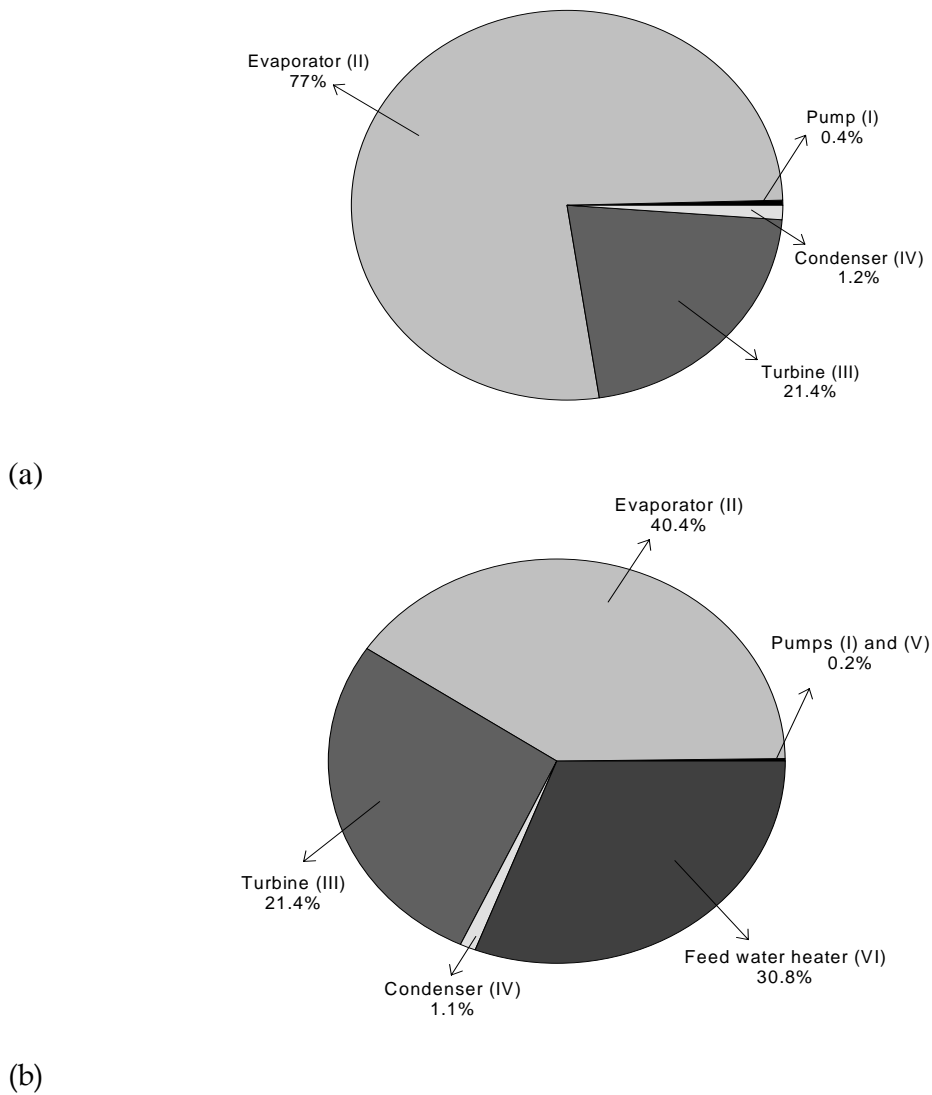


Figure 6.4. Percentage of the exergy loss in each component: (a) basic and (b) regenerative

From the results presented in Tables 6.8 and 6.9, it can be concluded that for the same heat rate available for the evaporator, from a hot gas stream, the regenerative ORC shows higher thermal and exergy efficiencies than basic ORC, reducing the total system exergy losses and increasing the degree of thermodynamic performance. Figure 6.4 illustrates the percentage of the exergy destroyed in each component with respect to the



total system exergy loss for both configurations. Figure 6.4 demonstrates that for the basic ORC the evaporator is the component with the highest exergy loss contribution (77%) followed by the turbine with (21.4%). For the regenerative ORC, the evaporator is still the highest contributor to the total exergy loss of the system. However, the exergy loss is reduced from 77% to 40.4% for the regenerative ORC compared to the basic ORC. The exergy reduction is mainly due to the presence of the feed water heater which accounts for 30.8% of exergy losses.

### **Application of the Exergy Wheel Diagram**

The results obtained from the topological methodology can be easily represented using an exergy wheel diagram. Using the exergy rate values presented in table 6.5, together with the exergy flow graph presented in figure 6.3, the exergy wheel was assembled for both configurations. The exergy wheel diagram for the basic ORC is presented in figure 6.5 while the exergy wheel diagram for the regenerative ORC is presented in figure 6.6. The exergy in-flow and exergy out-flow at various components can be identified using the exergy wheel diagram presented in figure 6.5 and figure 6.6.

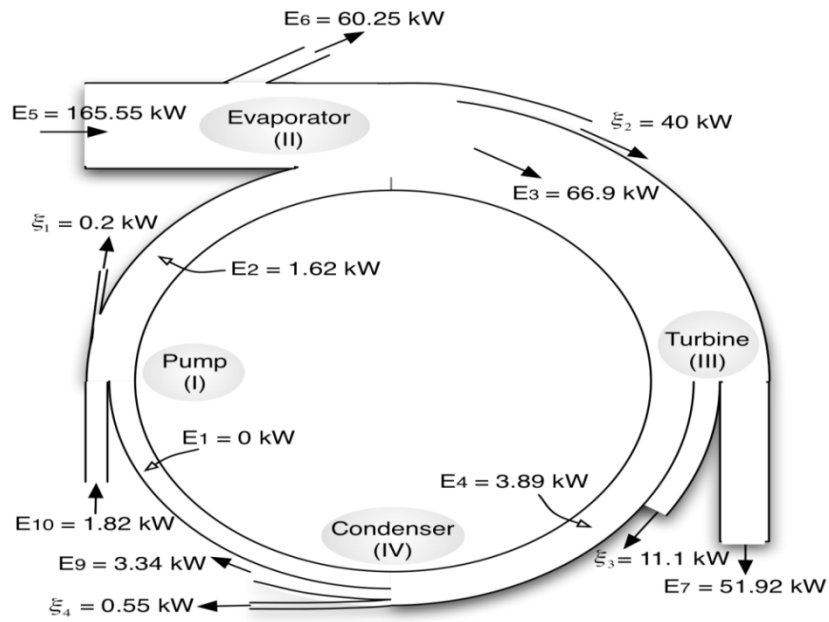


Figure 6.5. Exergy wheel diagram for a basic ORC.

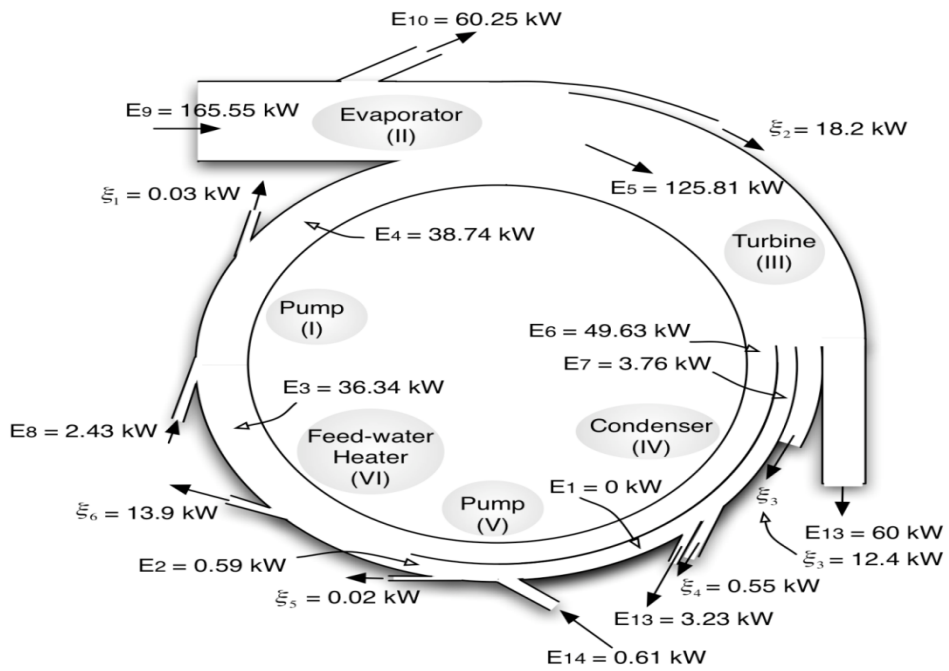
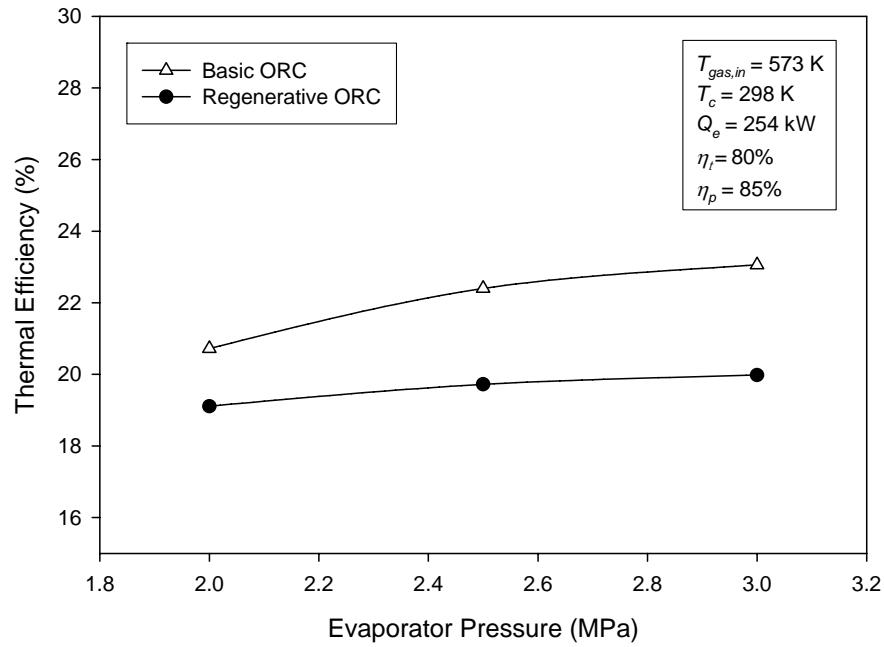


Figure 6.6. Exergy wheel diagram for a regenerative ORC.

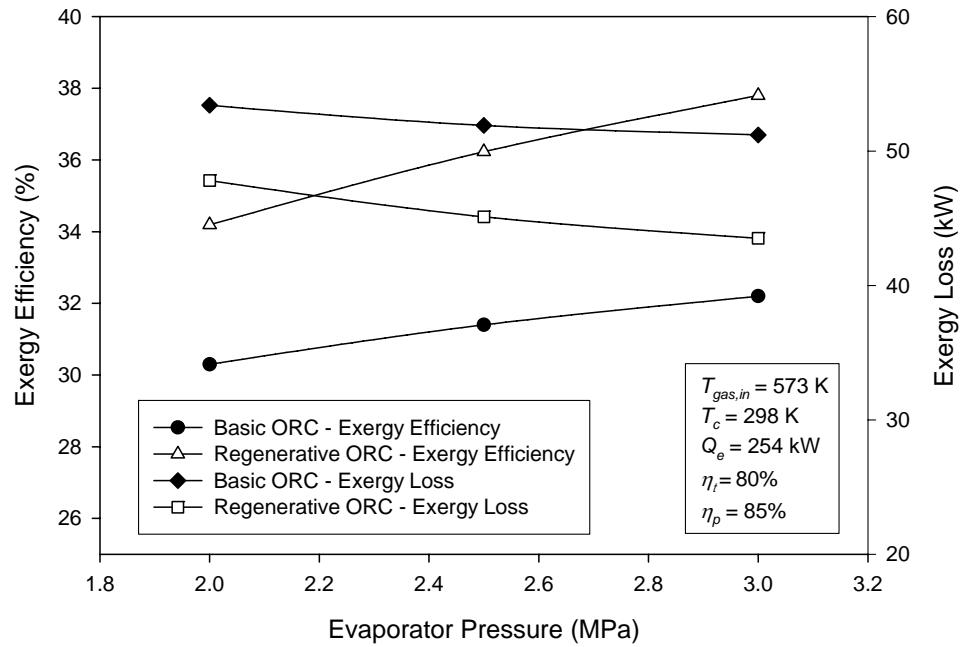
### **Effect of different parameters on the ORC performance**

Figure 6.7 illustrates the variation of the thermal and exergy efficiencies and the total system exergy loss with the evaporator pressure while keeping the turbine inlet temperature at saturated conditions for basic and regenerative configurations. The evaporator pressure was varied from 2 MPa to 3 MPa while keeping the same operating conditions. The thermal efficiency increases with the increase of the evaporator pressure for both configurations and the regenerative ORC present higher efficiency than basic ORC. The regenerative ORC shows an increase of the thermal efficiency of 8.4% to 15.4% from the lowest to the highest turbine inlet pressure. Higher evaporator pressure increases the specific net work and the specific evaporator heat. However, the percentage increase in the net work is higher than the increase in the evaporator heat rate, which leads to improvement in the first law efficiency.

Figure 6.7 also illustrates that the exergy efficiency increases and the system total exergy loss decreases with the increase in the evaporator pressure for both configurations. Both results are consistent, since a decrease of the total system exergy loss corresponds to an increase in the system exergy efficiency. This is due to the fact that when the evaporator pressure is increased, the difference between the evaporator temperature and the temperature of the hot gas stream entering the evaporator is reduced. The reduction in the temperature difference leads to an improvement of the exergy efficiency or a reduction of the system exergy loss. For low inlet turbine pressures, the second law efficiencies for regenerative ORC are approximately 12.8% higher than those obtained for basic ORC; while for high inlet turbine pressures the second law efficiencies for regenerative ORC are approximately 17.4% higher than those obtained for basic ORC.

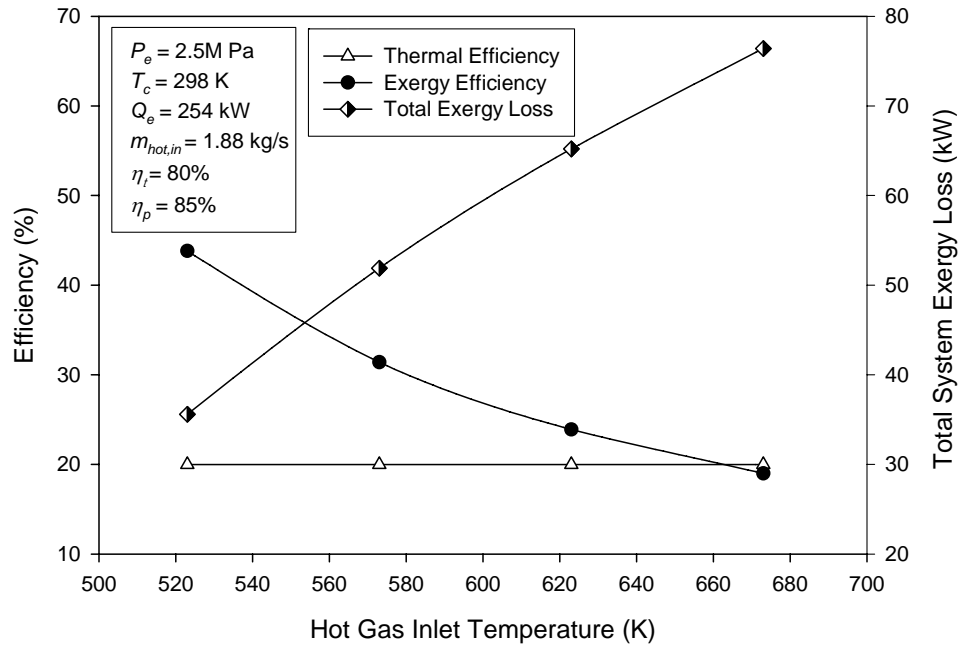


(a)

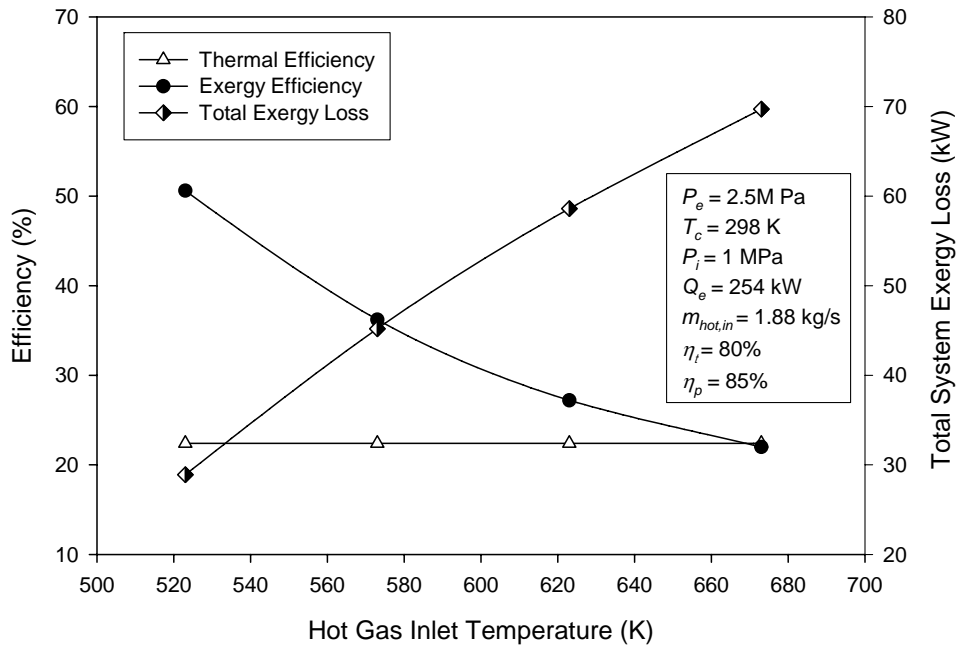


(b)

Figure 6.7. Effect of the variation of the evaporator pressure on the system performance: a) thermal efficiency, b) exergy efficiency and system total exergy loss



(a)



(b)

Figure 6.8. Variation of the system thermal and exergy efficiencies and the mass total system exergy loss with the hot gas inlet temperature: a) Basic ORC and b) Regenerative ORC

Figure 6.8 shows the effect of the hot gas inlet temperature on the thermal efficiency, exergy efficiency, and the total system exergy loss for both configurations. To generate this figure, the evaporator pressure was kept constant at 2.5 MPa while the condenser temperature was kept constant at 298 K. The ORC receives heat from a heat source at a rate of 254 kW at a constant mass flow rate of 1.88 kg/s. The hot gas inlet temperature was changed from 523 K to 673 K. As expected, the ORC thermal efficiency remains constant for basic as well as regenerative configurations with the increase of the hot gas stream temperature. However, it is demonstrated that regenerative ORC produces better thermal efficiencies than basic ORC. Additionally, the exergy efficiency decreases while the system exergy loss increases, with the increase of the hot gas temperature. Similar to the results presented in Figure 6.7, an increase of the inlet hot gas temperature leads to a decrease of the exergy efficiency. Figure 6.8 basically shows how the difference between the evaporator temperature and the hot gas temperature entering the evaporator affects the system performance. The smaller the temperature difference, better the exergy efficiency of the system. The lower temperature difference also leads to lower exergy losses in the system.

### Conclusions

The exergy-topological method developed by Nikulshin et al., (2002) was used to present a quantitative estimation of the exergy destroyed in an Organic Rankine Cycle (ORC) operating on R113. A detailed roadmap of exergy flow is presented using an exergy wheel diagram and parameters such as degree of thermodynamic perfection,

exergy efficiency, and influence coefficient were evaluated and compared for both ORC configurations. The analysis presented in the chapter leads to the following conclusions.

1. The regenerative ORC not only produces higher thermal and exergy efficiencies and higher degree of thermodynamic perfection than basic ORC, but also has lower total system exergy loss.
2. For both ORC configurations, the evaporator is the component with the highest influence coefficient and highest exergy loss with respect to the overall system exergy loss. For basic ORC, the evaporator exergy loss contribution is around 77%, while for regenerative ORC, the evaporator exergy loss contribution is around 40.4%. This reduction in exergy loss is mainly due to the presence of the feed water heater, which increases the temperature of the working fluid before it enters the evaporator, and thereby minimizes the heat transfer across a finite temperature difference.
3. Results showed that, for both configurations, the thermal and exergy efficiencies increase and the system total exergy loss decrease with the increase in the evaporator pressure for the analyzed cases. These results are consistent, since a decrease of the total system exergy loss corresponds to an increase in the system exergy efficiency. The reason for this behavior is attributed to the fact that with increasing evaporator pressure the temperature of the organic fluid is closer to the temperature of the hot gas entering the evaporator, thereby, facilitating heat addition across a lower temperature difference.

4. The effect of the hot gas inlet temperature on the system performance was examined. The smaller the difference between the evaporator temperature and the hot gas temperature, the better the exergy efficiency and smaller the exergy loss.
5. The results obtained for both configurations were represented using the exergy-wheel diagram. The visual analysis given in the exergy-wheel diagram gives a clear picture of the exergy flow and exergy destruction associated with different ORC components.
6. Finally, it can be concluded that the methodology proposed by Nikulshin et al. [2002, 2006] was successfully adapted to analyze the performance of ORC and this approach can be adapted to evaluate complex, energy-intensive system configurations.



## CHAPTER 7

### CONCLUSIONS

This dissertation presented an analysis of the performance of basic and regenerative ORC to produce power from waste heat. The analysis was based on the first and second laws of thermodynamics, and parameters such as thermal and second law efficiencies, irreversibility were evaluated. It was shown that the examined ORC could be used to generate power using low temperature waste heat. Organic fluids do not need to be superheated to increase the cycle thermal efficiency, since it remains approximately constant when the inlet temperature of the turbine is increased. However, using the second law analysis it was shown how superheating organic fluids increases the irreversibility. Therefore, organic fluids must be operated at saturated conditions to reduce the total irreversibility of the system.

For the different scenarios analyzed in this investigation, ORC using R113 shows the best thermal efficiency while those using Propane show the worst efficiency. However, it is important to point out that different organic fluids show better performance at different working temperature ranges.

It can also be concluded that the thermal efficiency of ORC increases when the condenser temperature is decreased. Therefore, using ORC in locations with low ambient temperatures will be more effective. The effect of the type of fluid was also investigated and evaluated. In general, organic dry fluids (R113, R123, R245ca, R245fa, and

Isobutane) show better performance than wet fluids (R134a and Propone). This is due to the fact that the dry fluids do not condensate after passing through the turbine as wet fluids do.

The influence of the boiling point temperature on the system thermal efficiency was determined. The fluid that shows the best thermal efficiency is the one that has the highest boiling point among the selected fluids (R113,  $T_{bp} = 47.59^{\circ}\text{C}$ ), while the fluid with the worst thermal efficiency has the lowest boiling point temperature (Propane,  $T_{bp} = -42.09^{\circ}\text{C}$ ). Therefore, it can be concluded that the higher the boiling point temperature of the organic fluid, the better the thermal efficiency that will be achieved by the ORC.

The regenerative ORC not only has higher first and second law efficiencies than basic ORC but lower irreversibility, and lower heat required to produce the same power. Dry organic fluids do not need to be superheated since the cycle thermal efficiency remains approximately constant when the inlet temperature of the turbine is increased. Moreover, second law analysis showed that superheating organic fluids increases the irreversibility and decreases the second law efficiency. Therefore, organic fluids should be operated at saturated conditions to reduce the total irreversibility of the system.

Two exergy evaluation techniques were applied to ORCs. From the topological method it was found that ORC thermal efficiency remains constant for both basic and regenerative configurations with the increase in the hot gas stream temperature. However, it was demonstrated that regenerative ORC produces better thermal efficiencies than basic ORC using a different approach. The exergy efficiency decreases while the system exergy loss increases with the increase in the hot gas temperature. An increase in

the system exergy efficiency leads to a decrease in the exergy efficiency. This approach also shows how the difference between the evaporator temperature and the hot gas temperature affect the system performance. The smaller the temperature difference, the better the exergy efficiency of the system.

## LIST OF REFERENCES

- Andersen, W. C., Bruno, T.J. "Rapid Screening of Fluids for Chemical Stability in Organic Rankine Cycle Applications", *Industrial and Engineering Chemistry Research*, 44, 15, 2005, pp. 5560-5566
- Angelino, G., Colonna di Paliano, P., "Multicomponent Working fluids for Organic Rankine Cycles (ORCs)", *Energy – The International Journal*, 23, 6, 1998, pp. 449-463.
- Angelino, G., Gaia, M., Macchi, E., "A Review of Italian Activity in the Field of Organic Rankine Cycles", *Proceedings of the Intl.VDI Seminar (Verein Deutsche Ingenieure)*, Bulletin 539, VDI-Düsseldorf, 1984, pp. 465-482.
- Armstead H. C. H. *Geothermal Energy*, 1978, E. & F. N. Spon Limited, London.
- Balli, O., Aras, H., and Hepbasli, A. " Exergo-economic Analysis of a Combined Heat and Power (CHP) System." *International Journal of Energy Research*, (article in press), DOI: 10.1002/er.1353, 2006.
- Bejan, A., "Advanced Engineering Thermodynamics", Wiley 3rd edition, 2006
- Bejan, A., Dan, N., Cacuci, D. G., and Schütz, W. "Exergy Analysis of Energy Conversion during the Thermal Interaction between Hot Particles and Water." *Energy*, 23, 11, 1998, pp. 913-928.
- Bejan, A., Tsatsaronis, G., and Moran, M. *Thermal Design and Optimization*, New York, USA: John Wiley & Sons; 1996.
- Bejan, A., "Second Law Analysis of Heat Transfer." *Energy*, 5, 1980, pp. 721-732.
- Bejan, A. "Entropy Generation Minimization: The New Thermodynamics of Finite-Size Devices and Finite-Time Processes." *Applied Physics*, 79, 3, 1996, pp. 1191-1218.
- Bejan, A. " Models of Power Plants that Generate Minimum Entropy while Operating at Maximum Power." *American Journal of Physics*, 64, 8, 1996, pp. 1054-1059.

Bejan, A. "Thermodynamic Optimization Alternatives: Minimization of Physical Size Subject to Fixed Power." *Int. J. Energy Research*, 23, 1999, pp. 1111-1121.

Bejan, A. "The Fundamentals of Exergy Analysis, Entropy Generation Minimization and the Generation of Flow Architecture." *International Journal of Energy Research*, 26, 2002, pp. 545-565.

Bejan, A., *Advanced Engineering Thermodynamics*, 3<sup>rd</sup> ed., John Wiley & Sons Inc., New Jersey, USA. 2006.

Branco, J. A. F., Pinho, C. T., Figueiredo, R. A. "First and Second-Law Efficiencies in a New Thermodynamical Diagram." *Journal of Non-Equilibrium Thermodynamics*, 27, 2002, pp. 239-256.

Brzustowski, T. A "Toward Second-Law Taxonomy of Combustion Processes." *Energy*, 5, 1980, pp. 743-755.

Caton, J. A. "On the Destruction of Availability (Exergy) due to Combustion Processes-With Specific Application to Internal-Combustion Engines." *Energy*, 25, 2000, pp. 1097-1117.

Cong, C.E., Velautham, S., Darus, A. M. "Sustainable Power: Solar Thermal Driven Organic Rankine Cycle." *Proceedings of the International Conferences on Recent Advances in Mechanical and Materials Engineering*, Paper No. 91, May 2005, pp. 424-429, Kuala Lumpur, Malaysia.

Chinese ,D., Meneghetti, A., Nardin, G., "Diffused introduction of Organic Rankine Cycle for biomass-based power generation in an industrial district: a systems analysis.", *International Journal of Energy Research* , 28, 11, 2004, pp. 1003 -1021

Cycle Tempo, "A program for thermodynamic modeling and optimization of energy conversion systems" Department of Process and Energy Technology, Faculty of Mechanical Engineering and Marine Technology, Delft University of Technology, 1998.

Defibuagh, D.R., Gillis, K.A., Moldover, M.R., Schmidt, J.W., and Weber, L.A. "Thermodynamic Properties of CHF(2)-CF(2)-CH(2)F, 1,1,2,2,3-pentafluoropropane." *International Journal of Refrigeration*, 19, 4, 1996, pp. 285-294.

Defibuagh, D.R. and Moldover, M.R. "Compressed and Saturated Liquid Densities for 18 Halogenated Organic Compounds." *Journal of Chemical Engineering*, 42, 1, 1997, pp. 160-168.

Dickson, M.H., Fanelli, M. *Fuel and Energy Abstracts*, 36, 5, September 1995 , pp. 347-347.

- Doldersum, A. "Exergy Analysis Proves Viability for Process Modifications." *Energy Conversion and Management*, 39, 1998, pp. 1781-1789.
- Drescher, U., Bruggemann, D. "Fluid Selection for the Organic Rankine Cycle (ORC) in Biomass Power and Heat Plants", *Applied Thermal Engineering*, 27, 2007, pp. 223-228.
- Dunbar, W. R. and Lior, N. M. "Sources of Combustion Irreversibility." *Combustion Science and Technology*, 103, 1994, pp. 41-61.
- Gurgenci, H. "Performance of Power Plants with Organic Rankine Cycles under Part-Load and Off-Design Conditions." *Solar Energy*, 36, 1, 1986, pp. 45-52.
- Huber, M.L. and Ely, J.F. "A Predictive Extended Corresponding States Model for Pure and Mixed Refrigerants including an Equation of State for R134a." *International Journal of Refrigeration*, 17, 1994, pp. 8-31.
- Hung, T.C., Shai, T.Y., and Wang, S.K. "A Review of Organic Rankine Cycles (ORCs) for the Recovery of Low-grade Waste Heat." *Energy*, 22, 7, 1997, pp. 661-667.
- Hung, T.C. "Waste Heat Recovery of Organic Rankine Cycle using Dry Fluids." *Energy Conversion & Management*, 42, 2001, pp. 539-553.
- Hung, T.C. "Waste Heat Recovery of Organic Rankine Cycle Using Dry Fluids." *Energy Conversion & Management*, 42, 2001, pp. 539-553.
- Larjola, J. "Electricity from Waste Heat Using the Organic Rankine Cycle (ORC)." *International Journal of Production Economics*, 41, 1991, pp. 227-235.
- Larjola, J., Sarkomaa, P., and Suistoranta, S. "New Technology ORC-Plant for Heat Recovery of Diesel Engines." *17<sup>th</sup> International Congress on Combustion Engines*, June 8-11, 1987, Paper D-12, Warsaw (CIMAC'87).
- Lee, K.M., Kuo, S.F., Chien, M.L., and Shih, Y.S. "Parameters Analysis on Organic Rankine Cycle Energy Recovery System." *Energy Conversion and Management*, 28, 2, 1988, pp. 129-136.
- Lee, M.J., Tien, D.L., and Shao, C.T. "Thermophysical Capability of Ozone Safe Working Fluids for an Organic Rankine Cycle System." *Heat Recovery System & CHP*, 13, 1993, pp. 409-418.
- Liu, B.T, Chien, K.H, Wang, C.C. "Effect of Working fluids on Organic Rankine Cycle for Waste Heat Recovery." *Energy*, 29, 2004, pp. 1207-1217.
- Mago, P.J., Chamra, L.M., and Somayaji, C. "Analysis and Optimization of Organic Rankine Cycles." *IMEchE Journal of Power and Energy*, 221, 3, May 2007, pp. 255-263.

Mago, P.J., Chamra, L. M., Srinivasan, K., and Somayaji, C. “An Examination of Regenerative Organic Rankine Cycles Using Dry Fluids, (article in press).” *Applied Thermal Engineering*, doi:10.1016/j.applthermaleng.2007.06.025, 2008.

Maizza, V., and Maizza, A. “Unconventional working fluids in organic rankine-cycles for waste energy recovery systems.” *Applied Thermal Engineering*, 21, 3, 2001, pp. 381-390.

Maizza, V., and Maizza, A. “Working Fluids in Non-steady Flows for Waste Energy Recovery Systems.” *Applied Thermal Engineering*, 16, 7, 1996, pp. 579-590.

Moran M.J. “Availability analysis— A Guide to Efficient Energy Use. corrected ed.” *The American Society of Mechanical Engineers*: New York, 1989.

Moran, M., and Shapiro, H. *Fundamentals of Engineering Thermodynamics*, 5th Edition. New York, USA: John Wiley & Sons; 2003.

Niggeman, R.E., Greenlee, W.J., and Lacey, P. “Fluid Selection and Optimization of an Organic Rankine cycle Waste Heat Power Conversion System.” *ASME 78-WA*, January 6, 1978.

Nikulshin, V., Bailey, M, Nikulshina.V. “Thermodynamic Analysis of Air Refrigerator on Exergy Graph.” *Thermal Science*, 10, 2006, pp. 99-110.

Nikulshin, V., Wu.C, Nikulshina.V. “ Exergy Efficiency Calculations of Exergy Intensive Systems by Graphs.” *Int. J. Applied Thermodynamics*, Vol. 5, June 2002, pp. 67-74.

Ozgener, L., Hepbasli, A., Dincer, I. “ Exergy Analysis of Two Geothermal District Heating Systems for Building Applications.” *Energy Conversion and Management*, 48, 2007, pp. 1185–1192.

REFerence fluid PROPERTIES (REFPROP), National Institute of Standards and Technology (NIST), Version 7.0.

Rosen, M. A. “Clarifying Thermodynamic Efficiencies and Losses via Exergy.” *Energy*, 2, 2002, pp. 3-5.

Rosen, M. A., Dincer, I. “Exergy Analysis of Waste Emissions.” *International Journal of Energy Research*, 23, 1999, pp. 1153-1163.

Rosen, M. A. and Dincer, I. “A Study of Industrial Steam Process Heating Through Exergy Analysis.” *International Journal of Energy Research*, 28, 2004, pp. 917-930.

Somayaji, C., Mago, P. J., and Chamra, L. M., "Second Law Analysis and Optimization of Organic Rankine Cycles." *ASME Power Conference*, Paper No. PWR2006-88061, Atlanta, GA, May 2-4, 2006.

Somayaji, C., Mago, P. J., and Chamra, L. M., "Second Law Analysis and Optimization of Organic Rankine Cycles." *Proceedings of IMECE2006 ASME International Mechanical Engineering Congress and Exposition*, November 5-10, 2006, Chicago, Illinois, USA

Somayaji, C., Mago, P. J., and Chamra, L. M., Srinivasan, K. K. "An Examination of Exergy Destruction in Organic Rankine cycles" *International Journal of Energy Research*, Published online in Wiley InterScience (www.interscience.wiley.com) DOI: 10.1002/er.1406, 2008.

Spurrier, B., "A Development of Exergy Based Bond Graph System Variables", 1990

Srinivasan, K. K. Mago, P. J. Zdaniuk, G. J. Chamra, L. M., and Midkiff, K. C. "Improving the Efficiency of the Advanced Injection Low Pilot Ignited Natural Gas Engine using Organic Rankine Cycles." *ASME Energy Sustainability Conference*, Long beach CA, Jun 24-29, 2007.

Stegou-Sagia, A, and Paigniannis, N. "Evaluation of mixtures efficiency in refrigerating systems." *Energy Conversion and Management*, 46, 2005, pp. 2787–2802.

Tillner-Roth, R. and Baehr, H.D. An International Standard Formulation of the Thermodynamic Properties of 1,1,1,2-tetrafluoroethane (HFC-134a) Covering Temperatures from 170 K to 455 K at Pressures up to 70 MPa. *Journal of Physical Chemistry*, Ref. Data 23, 1994, , pp. 657-729.

Twidell, J.W., Weir, A.D. *Renewable Energy Resources*, 1986, E. & F. N. Spon, London.

Verkhiver, G. P. and Kosoy, B. V. "On the Exergy Analysis of Power Plants." *Energy Conversion and Management*, 42, 2002, pp. 2053-2059.

Verschoor, M.J.E. and Brouwer, E.P. "Description of the SMR cycle, which combines fluid elements of steam and organic rankine cycle." *Energy*, 4, 20, 1995, pp. 295-304.

Vijayaraghavan, S., and Goswami, D.Y. "Organic Working Fluids for a Combined Power and Cooling Cycle." *ASME Journal of Energy Resources Technology*, 127, 2005, pp. 125-130.

Wall, G. "Exergy Tools." *Proceedings of the Institution of Mechanical Engineers. Journal of Power and Energy* , 217, 2003, pp. 125-136.



Yamamoto, T., Furuhashi, T., Arai, N., and Mori, K. "Design and Testing of the Organic Rankine Cycle." *Energy*, 26, 3, 2001, pp. 239-251.

Younglove, B.A. and McLinden, M.O. "An International Standard Equation-of-State Formulation of the Thermodynamic Properties of Refrigerant 123 (2,2-dichloro-1,1,1-trifluoroethane)." *Journal of Physical Chemistry, Ref. Data* 23, 1994, pp. 731-779.